

Fig. 3-4-3 Distribution of Embedded Type Manganese Nodules

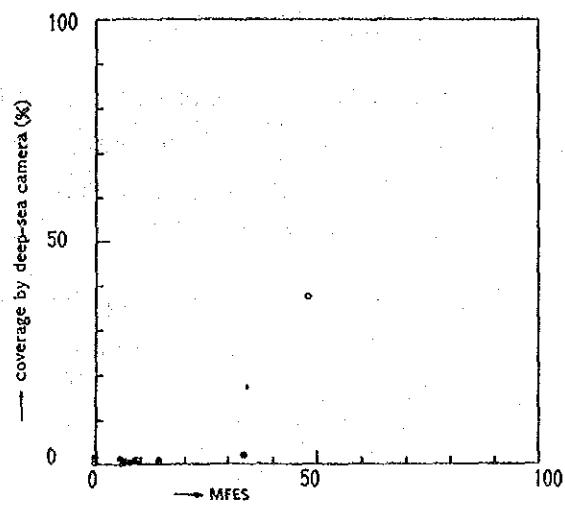
3) Estimation of Manganese Nodules by Means of MFES

The estimated abundance of manganese nodules by means of MFES is shown in Annexed figure 6. Data processing is described in proceeding paragraph. On the figure, the area of type d_2 and d_s where Quasi-anomaries are probably observed and the area of type d_1 where unreliable data are probably obtained are distinguished from others with horizontal lines.

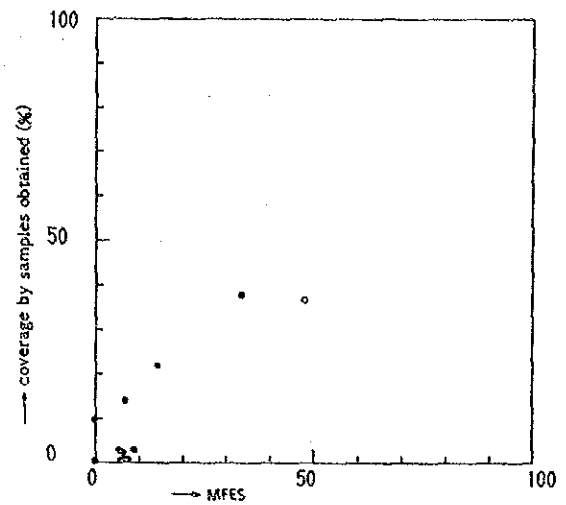
Characteristics of the provinces are as follows.

(1) Plain (northern part of the surveyed area)

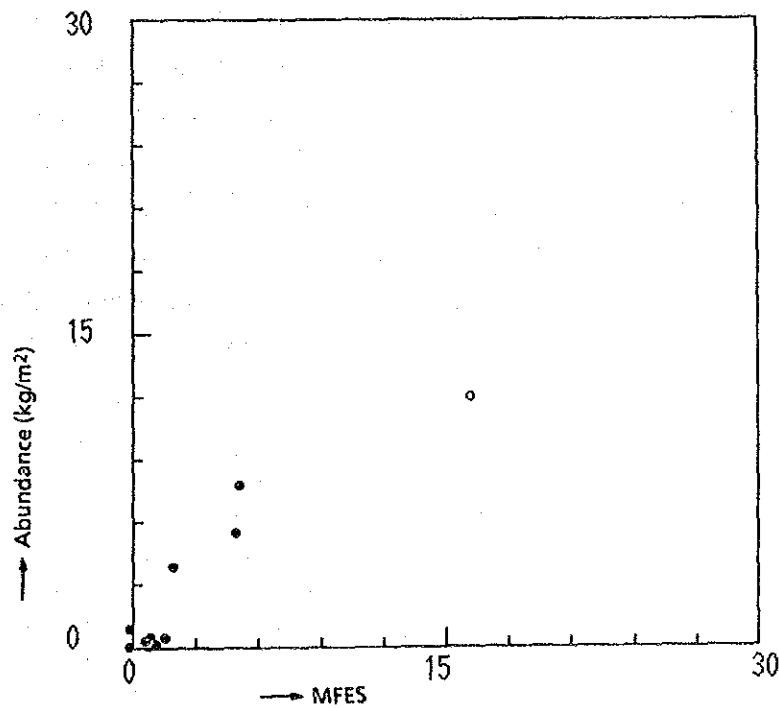
The type b is mainly distributed and the type d_1 is observed everywhere. The topography is relatively flat and upper transparent layer spreads, so that the abundance of manganese nodules in this province is generally low. Especially, the vast part from north to east, where the type b and type bc are distributed, the thickness of transparent layer is more than 100m, and the values of MFES indicate almost 0 kg/m². This vast sterile part tents to farther north. A few points where the abundance indicate more than 10 kg/m² are observed near the sea knolls; however, these are extremely small in scale.



(1)



(2)



$r = 0.93$
 $a = 0.81$
 $b = 0.06$
 $Y = a \cdot X + b$
 $N = 17$

- : exposed type
- : embedded type

(3)

Fig. 3-4-4 Influence of Embedded Type Manganese Nodules on MFES Measurement

(2) Quasi-plain (south-eastern part of the surveyed area)

The type d_2 is predominant in the central part and type d_1 , d_s are scattered in there. MFES shows generally high, but this is presumed Quasi-anomaly. The type b having predominant transparent layer is distributed both east and west sides of type d_2 and these types forms a low abundance zone.

Especially, the eastern part of the zone is like sterile and spreads to the vast sterile part of the plain. In the same way as in the plain, a few points where the abundance indicate more than 10 kg/m^2 are observed; however, these are small in scale.

(3) Mountainous (the central part of the surveyed area)

The type d_1 due to sea mounts and sea knolls are distributed like much islands, and the type d_2 and d_s are around the outskirts of them. In these area, MFES indicates high values, but these are also presumed Quasi-anomalies. Especially, in the vast zone of type d_2 center: $2^\circ 30' \text{ S}, 171^\circ \text{ W}$), the topography is plain and the high MFES values are observed; however, this zone is considered as similar to barren zone. The types containing transparent layer are distributed as they fill between the sea knolls. The high abundance zone is not recognized in there. As above mentioned, the opaque layer zone accounts for the many part in the surveyed area. The zone of MFES high value is almost included in there, so that it is highly probable that Quasi-anomalies are observed in this zone. The promising high abundance zone of manganese nodules is not observed even in the point where the transparent layer exists upper part. (It is possible to estimate the abundance of manganese nodules by MFES)

3-5 Bearing Situation of Manganese Nodules

Sampling manganese nodules by means of FG and SC was practiced. The sampled manganese nodules were measured and observed in many different ways on board, while on shore, chemical and mineral analysis was performed on some representative samples.

1) Classification of Types and Properties

Analyzed herein the bearing situation of manganese nodules in the view of its morphology, granular size and external appearance in order to explain the characteristic of the distribution. Manganese nodules are classified mainly by those morphology as shown in Fig. 3-5-1. General characteristics are as follows and physical properties are summarised in Table 3-5-1. The weight ratio of sampled nodules in each type is shown in Fig. 3-5-2.

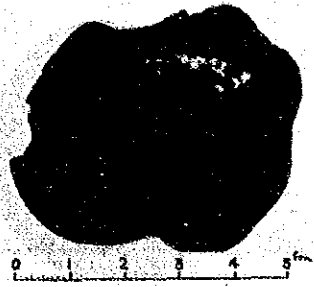
(1) Morphology

The types of manganese nodules can be divided into 8 as below;

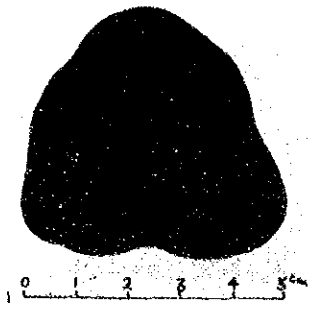
- 1 Spheroidal type: The shape of this type is nearly perfect sphere.
- 2 Ellipsoidal type: This type has a hamburger like external form and a crushed spheroidal form.
- 3 Ellipsoidal fat type: This type is more irregular and larger than ellipsoidal type.
- 4 Pebble thin type: This type is like small pebbles on the sea shore or like a "go" stone with a relatively smooth surface without irregularity.
- 5 Pebble type: This type looks like gravel on shore and on the river bed. (its diameter is around 2-4cm)
- 6 Massive type: This type has irregular and rather angular shape, (including various shapes like spheroidal, ellipsoidal or plate).
- 7 Plate type: This type has a thin and round shape like a tile or a rice cake.
- 8 Other type: The manganese nodule which can not be classified into above 7 types.

Table 3-5-1 Physical Properties Associated with Morphology of Manganese Nodules

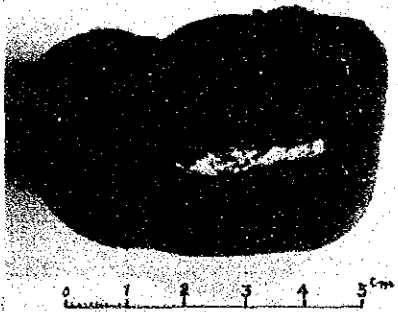
		Spheroidal	Ellipsoidal	Ellipsoidal fat	Pebble thin	Pebble	Massive	Platy	Other
		50 %	50 %	50 %	50 %	50 %	50 %	50 %	50 %
Size (cm)	0 ~ 2								
	2 ~ 4								
	4 ~ 6								
	6 ~ 8								
	8 ~ 16								
	16 ~								
Surface texture	Top	Smooth							
		やや滑らか							
		やや粗							
		Rough							
	Bottom	Smooth							
		Smooth > Rough							
		Smooth < Rough							
		Rough							
Single/Poly	単体								
	Single > Poly								
	Single = Poly								
	Single < Poly								
	Poly type								
Crack	Many								
	Medium								
	Rare								
Fissure	Many								
	Medium								
	Rare								
Moisture content (%)	Mean	27.81	30.58	26.89	26.88	24.57	27.59	22.90	28.88
	Standard deviation	2.18	0.00	3.16	0.58	3.12	1.93	0.69	1.63
	Maximum	31.72	30.77	32.21	27.92	30.00	30.73	23.81	30.30
	Minimum	15.38	30.43	20.00	26.59	19.29	23.91	22.40	16.67
Specific gravity (wet)	Mean	2.02	2.01	2.03	2.03	2.06	2.01	1.93	1.98
	Standard deviation	0.03	0.00	0.07	0.07	0.05	0.04	0.02	0.06
	Maximum	2.08	2.03	2.14	2.06	2.11	2.10	1.94	2.04
	Minimum	1.88	2.00	1.86	1.90	1.90	1.87	1.90	1.70



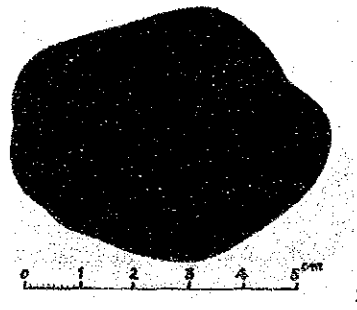
87S0270FG01 (Section)
Massive



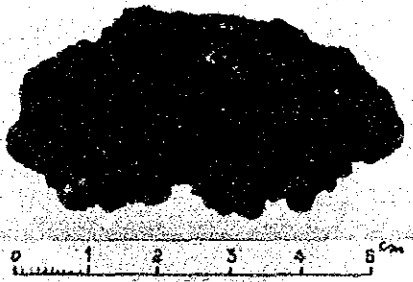
(Upper surface)



87S0570FG09 (Section)
Massive



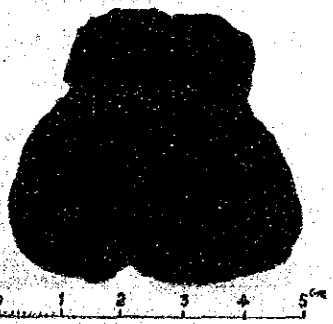
(Upper surface)



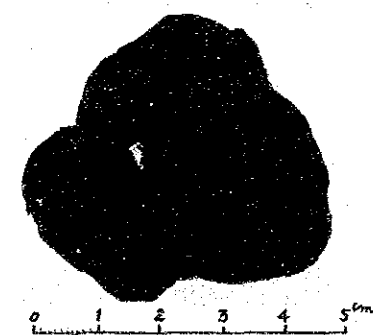
87S0470FG12 (Section)
Other



(Upper surface)

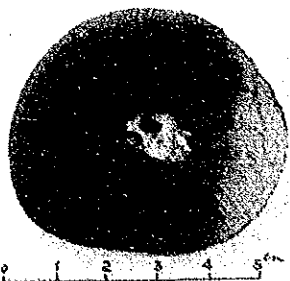


87S0470FG19 (Section)
Polygonal and Spheroidal

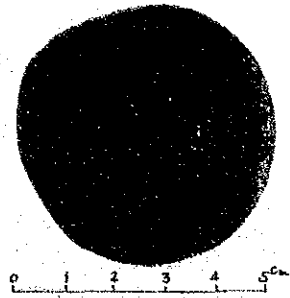


(Upper surface)

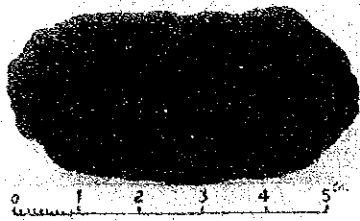
Fig. 3-5-1 Morphology of Manganese Nodules (1)



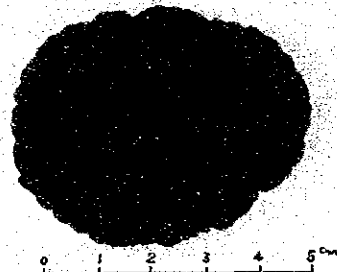
87 S 0 5 7 0 F G 2 4 (Section)
Spheroidal



(Upper surface)



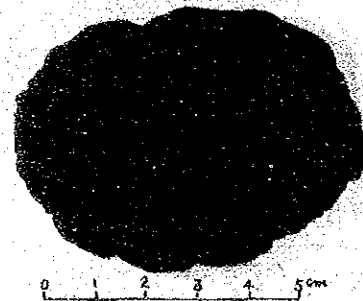
87 S 0 3 6 9 F G 0 6 (Section)
Ellipthoidal



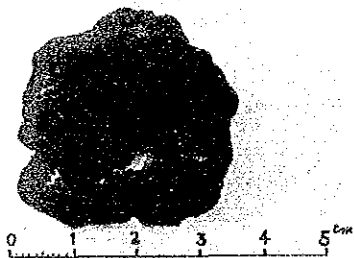
(Upper surface)



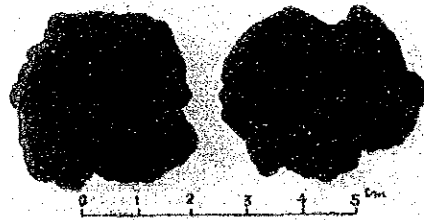
87 S 0 2 7 0 F G 0 4 (Section)
Ellipthoidal Fat



(Upper surface)



87 S 0 5 7 0 F G 0 4 (Section)
Pebble



(Upper surface)

Fig. 3-5-1 Morphology of Manganese Nodules (2)

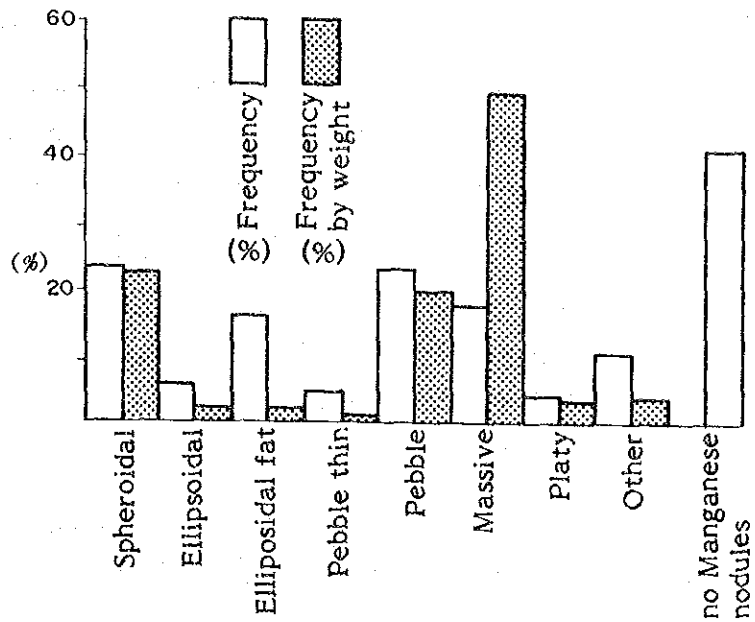


Fig. 3-5-2 Morphology and Sampling Weight of Manganese Nodules

1 Spheroidal type

The diameter is mainly between 1 - 5cm and is about 8cm at maximum. Manganese nodules more than 2cm in diameter have various surface such as slightly smooth or rough. Smooth surface is more common. On the other hand, manganese nodules less than 2cm in diameter have round shaped projections and are mainly like a confetto with rough surface.

2 Ellipsoidal type

The surface is rough with tiny concaves and convexes. This type is mainly manganese nodules with small cracks. This type is rarely observed in this surveyed area.

3 Ellipsoidal fat type

This type is one of the variations of the spheroidal type and larger than ellipsoidal type. In this surveyed area, single type manganese nodules with rough surface and small or medium size less than 4cm in diameter, are mainly observed. The combined type is also observed rarely.

4 Pebble thin type

This type usually shows a thin and round or over shape like a small stone or a "go" stone. There is no concave and convex on the surface. Manganese nodules of this type are mainly small with slightly rough surface.

5 Pebble type

The diameter is mainly between 2 - 4cm. The surface is more smooth than the other types. The combined type manganese nodules are abundant compared with the other spheroidal types.

6 Massive type

The diameter is mainly between 4 - 6cm. The large size one has hardly any angular shape and shows "potato" shape. The surface is slightly rough.

7 Plate type

The diameter varies enormously. The surface shows mainly rough and the manganese nodules after contains rock fragments.

8 Other type

In this surveyed area, the manganese nodules classified into this type are mainly so small that these shapes are difficult to be determined. The stick type one will be grouped in this type.

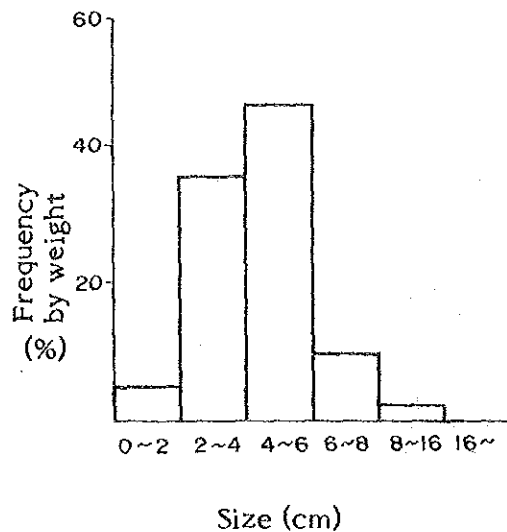


Fig. 3-5-3 Size and Sampling Weight of Manganese Nodules

(2) Size distribution

The size distribution of manganese nodules is shown in Fig. 3-5-3. This figure indicate that medium size manganese nodules with 2 - 6cm in diameter are most common in this area.

(3) Characteristics of external appearance

The characteristics of external appearance are shown in Table 3-5-1. The surface of the manganese nodules vary from relatively rough (r-type) to smooth (s-type). Most of the manganese nodules in the northern part of the surveyed area are classified into "r-type", having rough surface. Most of the manganese nodules in the southern part of the surveyed area are classified into "s-type", having relatively smooth surface. On the other hand, in the central part of the surveyed area, those type is between "r-type" and "s-type". It is to be noticed that cracks or fragmentations of nodules are rather obscure; however, the manganese nodules considered to be the fragmentation-growth type are often observed. Combined forms are found in consideration quantities in some places.

2) Abundance and Occurrence

(1) Morphology distribution of manganese nodules

The morphology distribution of manganese nodules was classified into 4 zones having a different character as follows and it is shown in Fig. 3-5-4.

(a) zone where spheroidal type is superior

(b) zone where pebble, pebble thin and plate types are superior

(c) zone where the main type of manganese nodules is ellipsoidal and more than 20% in the whole

(d) zone where massive type is superior

The distribution of (a) and (b) is wide, while that of (c) and (d) generally restricted.

(2) Size distribution of manganese nodules

The size distribution of manganese nodules is shown in Fig. 3-5-5. In the high abundance zone, the manganese nodules of medium or large size more than 4cm in diameter, are relatively abundant. The distribution of the same size zone corresponds with the topographic structure.

(3) Granular size and morphology

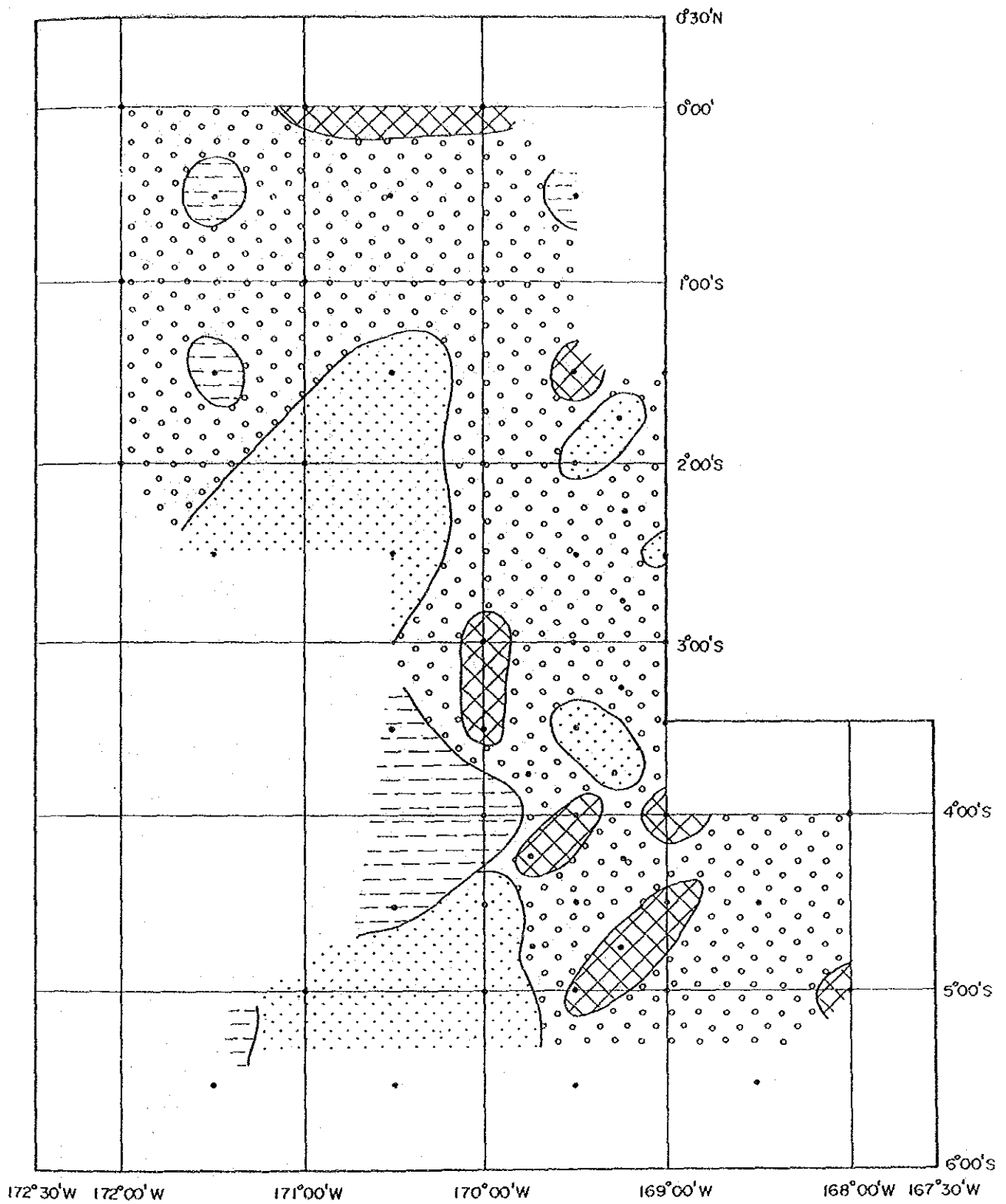
The morphological appearance ratio of manganese nodules by respective granular size is shown in Fig. 3-5-6. The larger the granular size of manganese nodules becomes, the amount of the spheroidal type decreases and those of the massive type and the plate type increases. Generally speaking, many of large manganese modules are combined type, and many of small ones contain rock fragments as cores.

(4) Local topography and morphology

The morphology distribution of manganese nodules is shown in Fig. 3-5-4, and the relationship between local topography and morphology is shown in Fig. 3-5-7. The morphology distribution of manganese nodules is concordant with topography. (a) in paragraph (1) spreads over the plain, the quasi-plain and partially on the seamounts. Samely (b) lies mainly in the mountainous, the quasi-plain and partially on the sea knoll, the platform and the channel. (c) lies on the flat in the plain and the quasi-plain, and (d) spreads on the flat and the platform and the sea knoll in the plain and the quasi-plain.

(5) SBP type and morphology

The relation between SBP type and morphology, the relation between upper transparent layer thickness and morphology are shown respectively in Fig. 3-5-8 and Fig. 3-5-9. These figures indicate that the distribution ratios of the spheroidal, ellipsoidal fat and massive types are high, but that of the pebble type is low in types a, b and e₁ with clear transparent layers. On the other hand, the distribution ratios of the pebble, massive and plate types are high, but that of the ellipsoidal is low and the ellipsoidal type is not exist in types c, d₁ and d₂ which have no transparent layers. The thickness of the upper transparent layer indicates these relations more clearly. That is to say, the distribution ratios of the massive and pebble types are high at where the thickness of the upper transparent layer is between 0 - 10m. Especially, the plate type is observed only where the upper transparent layer is not exist. The distribution ratio of the spheroidal type is high where the thickness of the uppertransparent layer is between 20 - 40m. The distribution ratio of the ellipsoidal fat type is high, and the pebble type or the plate type is not exist where the thickness of the upper transparent layer is between 50 - 60m. The distribution ratio of the other type is high where the thickness of the upper transparent layer is more than 70m.



Legend


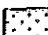
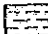


-  Main is spheroidal.
 -  Main is pebble, pebble thin and platy.
 -  Main is ellipsoidal, and sub is over 20% of pebble, massive and platy.
-  Main is massive.
 -  Sampling station.

Fig. 3-5-4 Morphology Distribution of Manganese Nodules

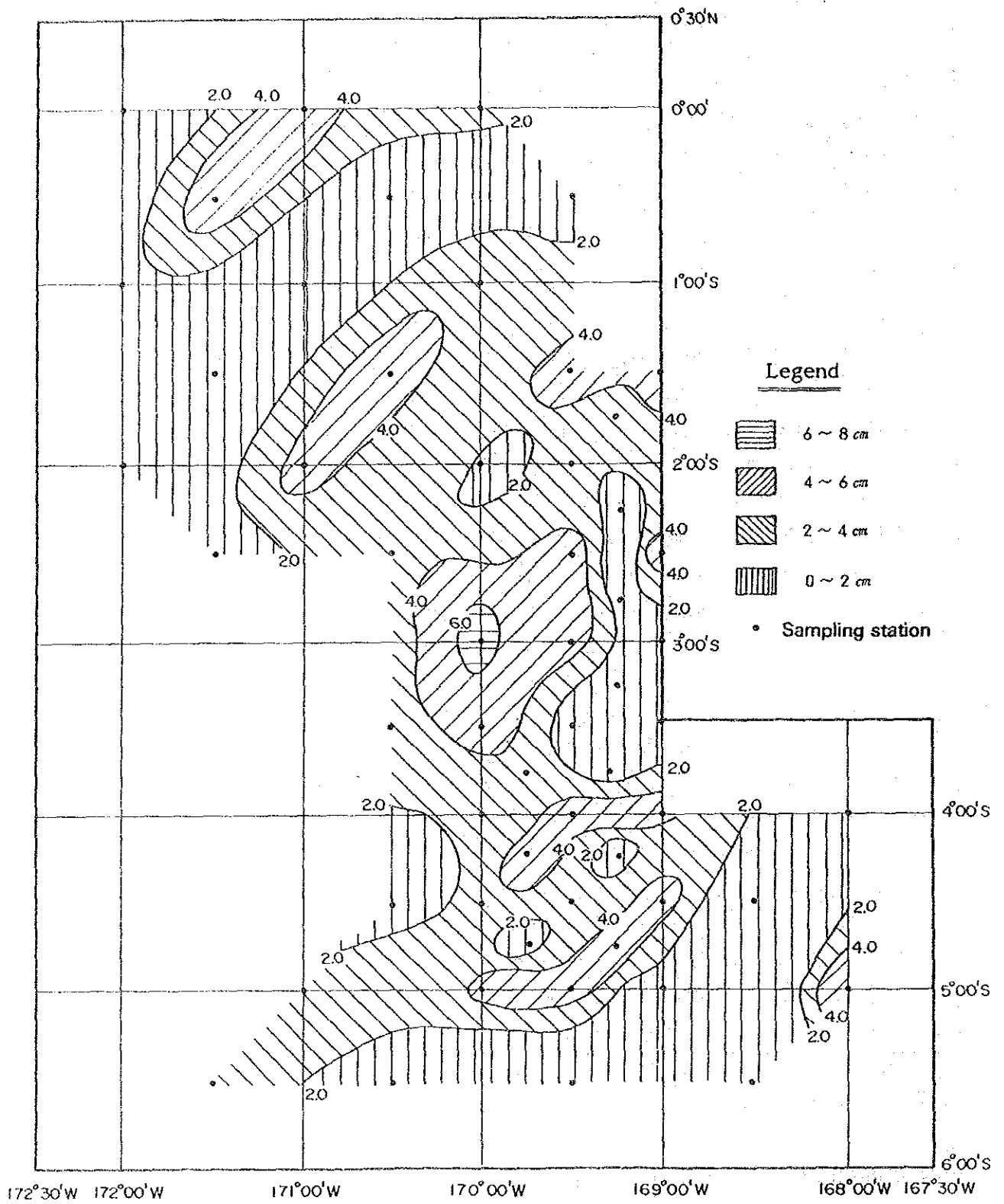


Fig. 3-5-5 Size Distribution of Manganese Nodules

(6) Bottom materials and morphology

The relation between bottom sediments and morphology is shown in Fig. 3-5-10. The distribution ratios of the massive and pebble types are high, and every types such as spheroidal, ellipsoidal, etc are observed in brown clays, siliceous clays and calcareous clays. While, in foraminifera ooze, the spheroidal type and the pebble type account for nearly each half of whole, and only the ellipsoidal fat type occurs in a small amount.

(7) Abundance of the manganese nodules

The abundance map of the manganese nodules is shown in Annexed Figure 7.

The areas where the abundance of manganese nodules indicate more than

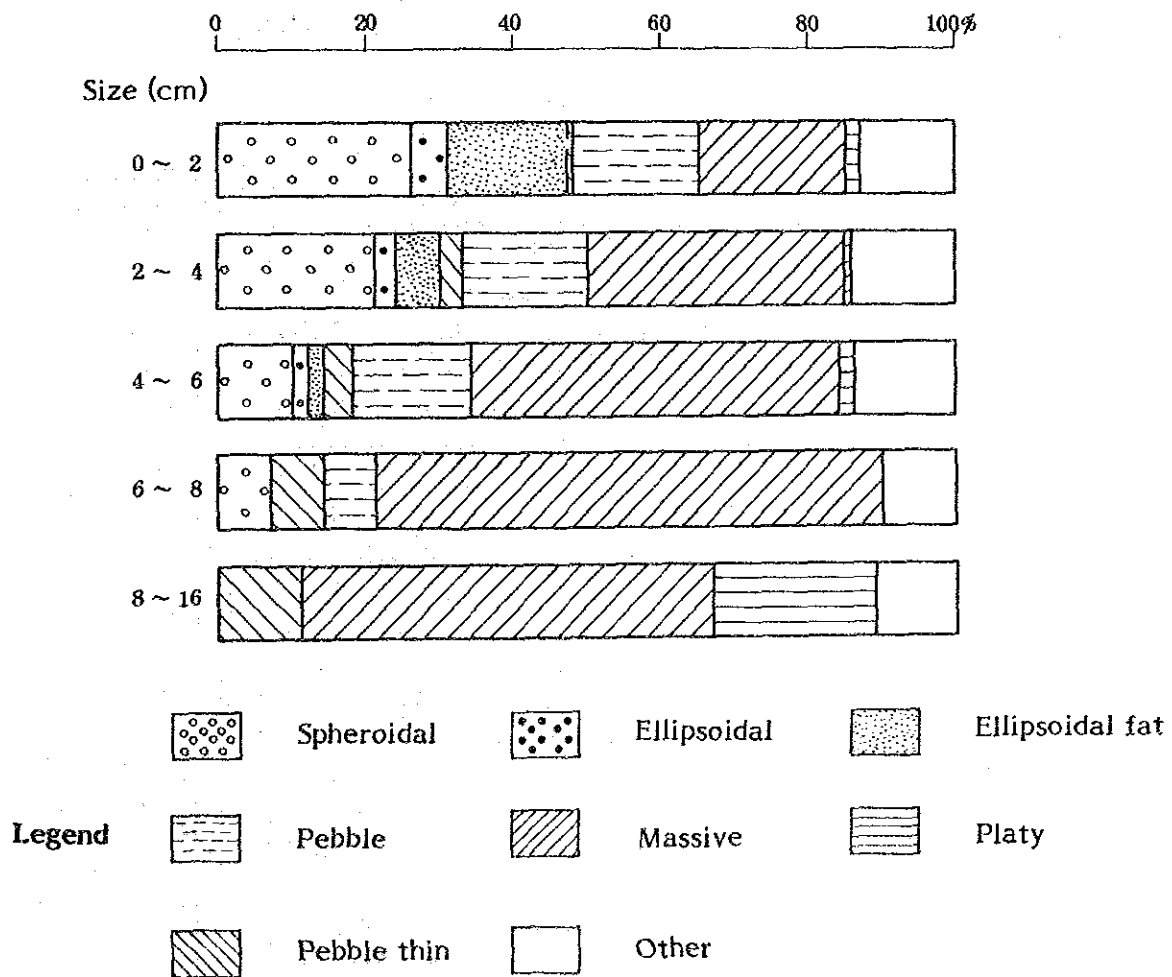


Fig. 3-5-6 Relation between Size and Morphology

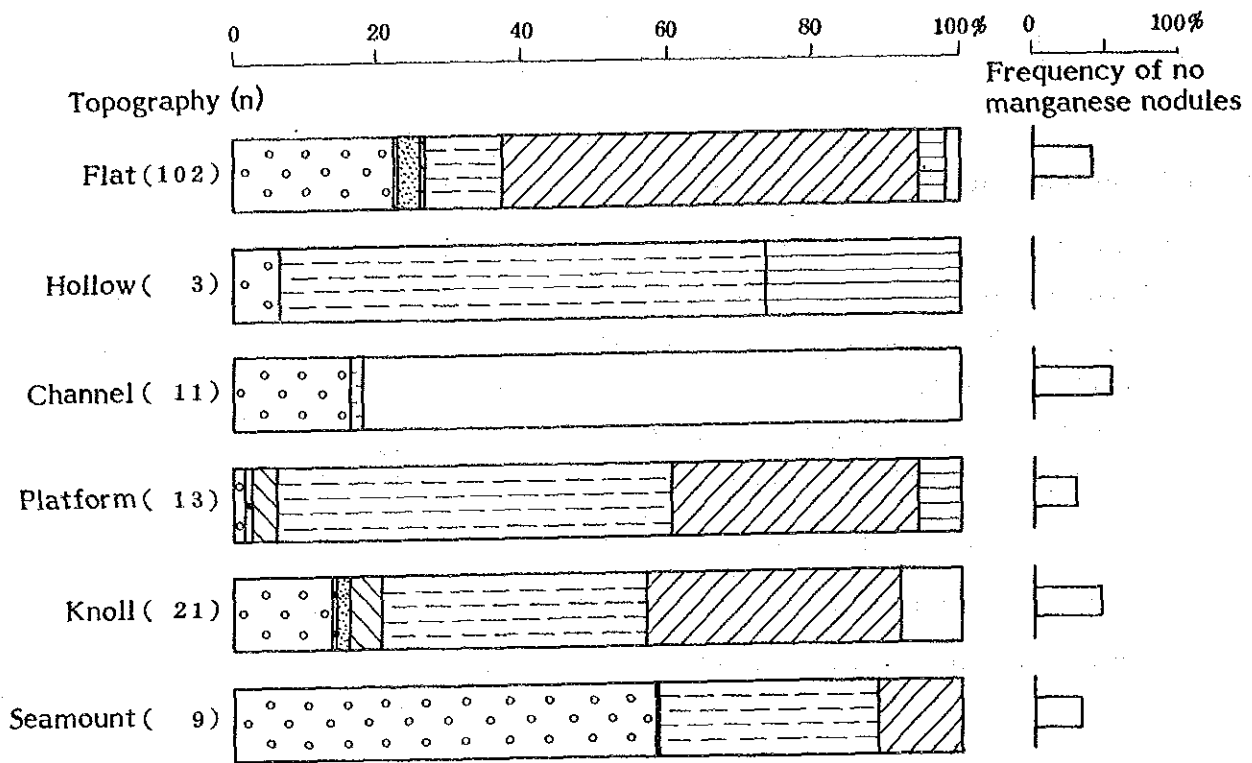


Fig. 3-5-7 Relation between Local Topography and Morphology

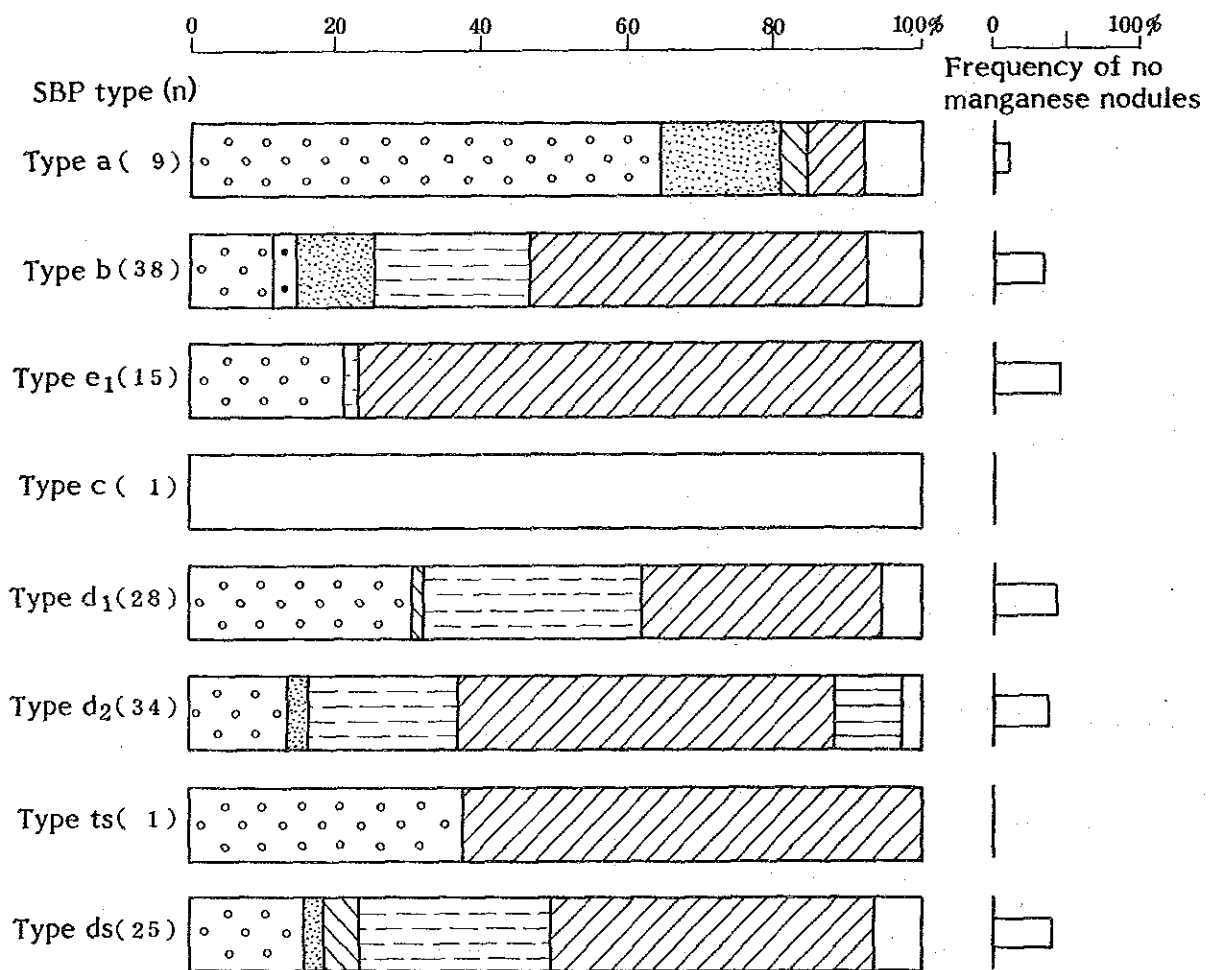


Fig. 3-5-8 Relation between SBP Type and Morphology

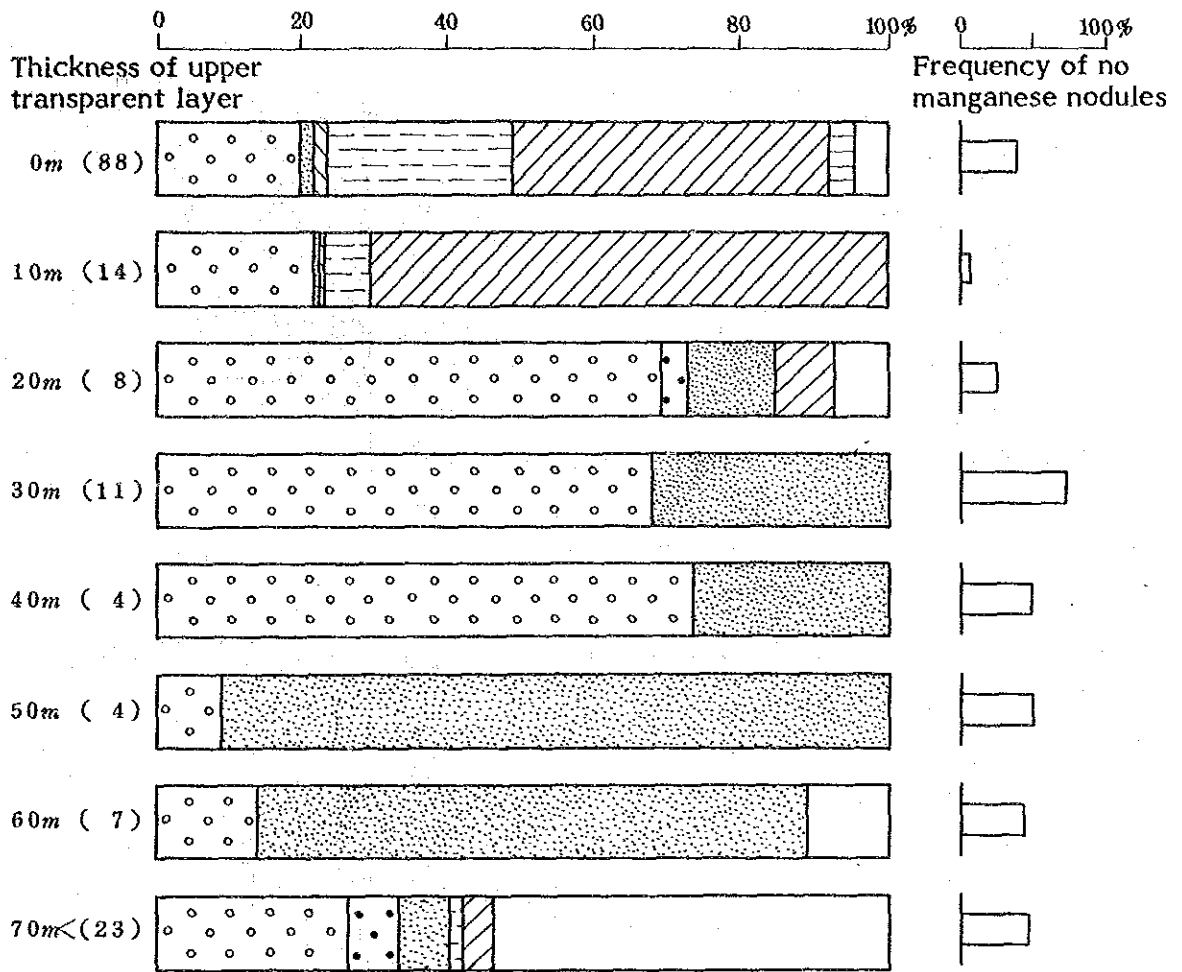


Fig. 3-5-9 Relation between Upper Transparent Layer Thickness and Morphology

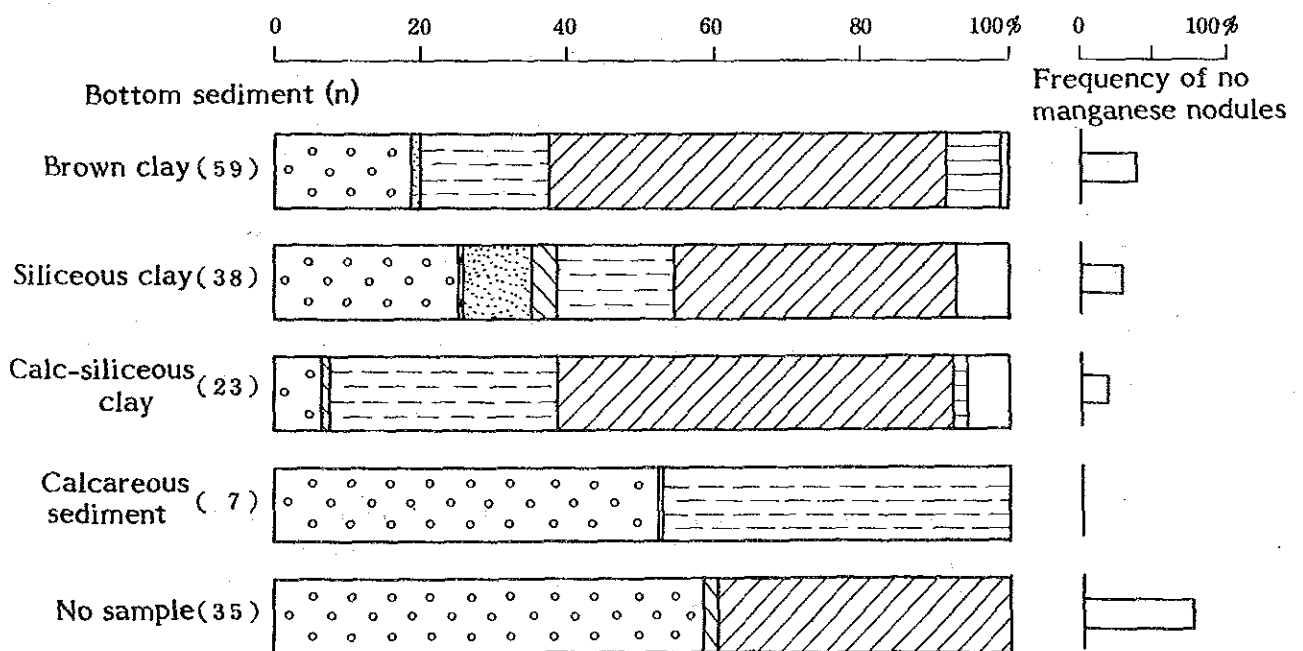


Fig. 3-5-10 Relation between Bottom Sediments and Morphology

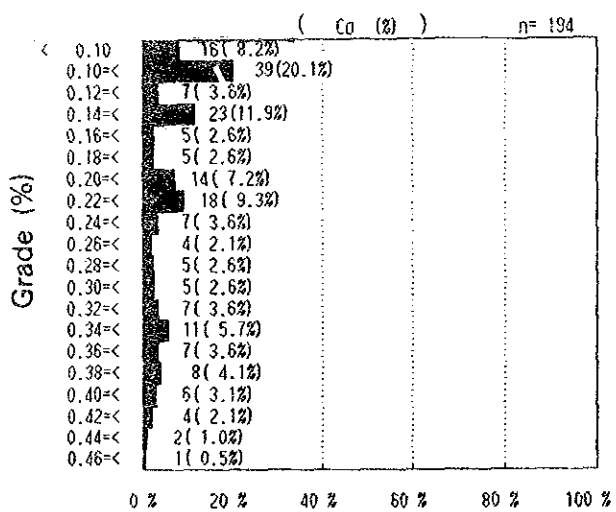
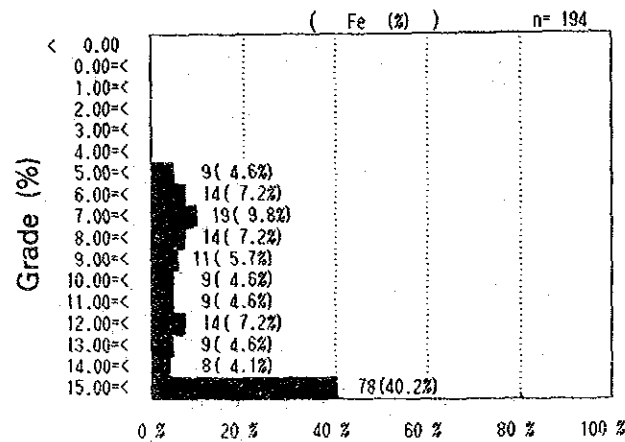
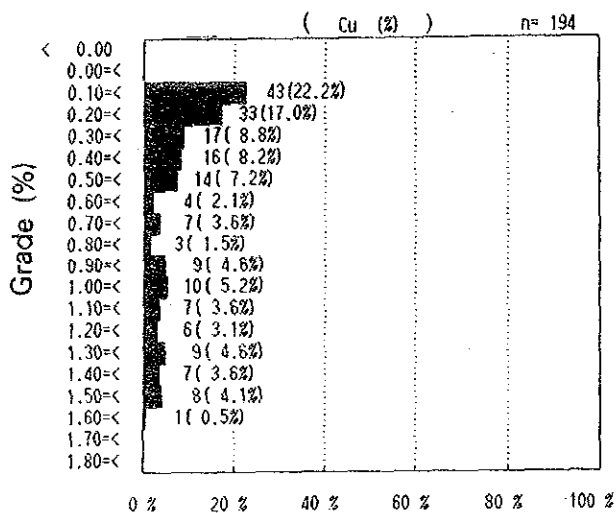
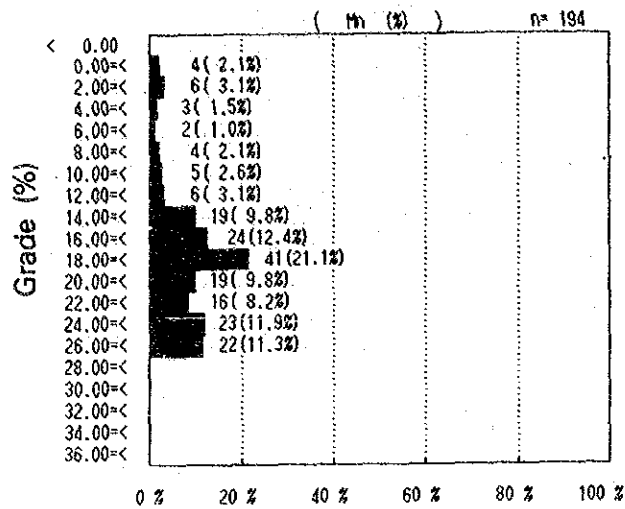
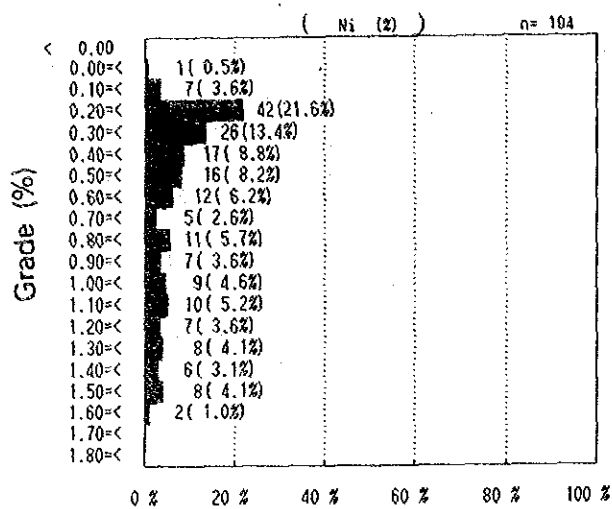
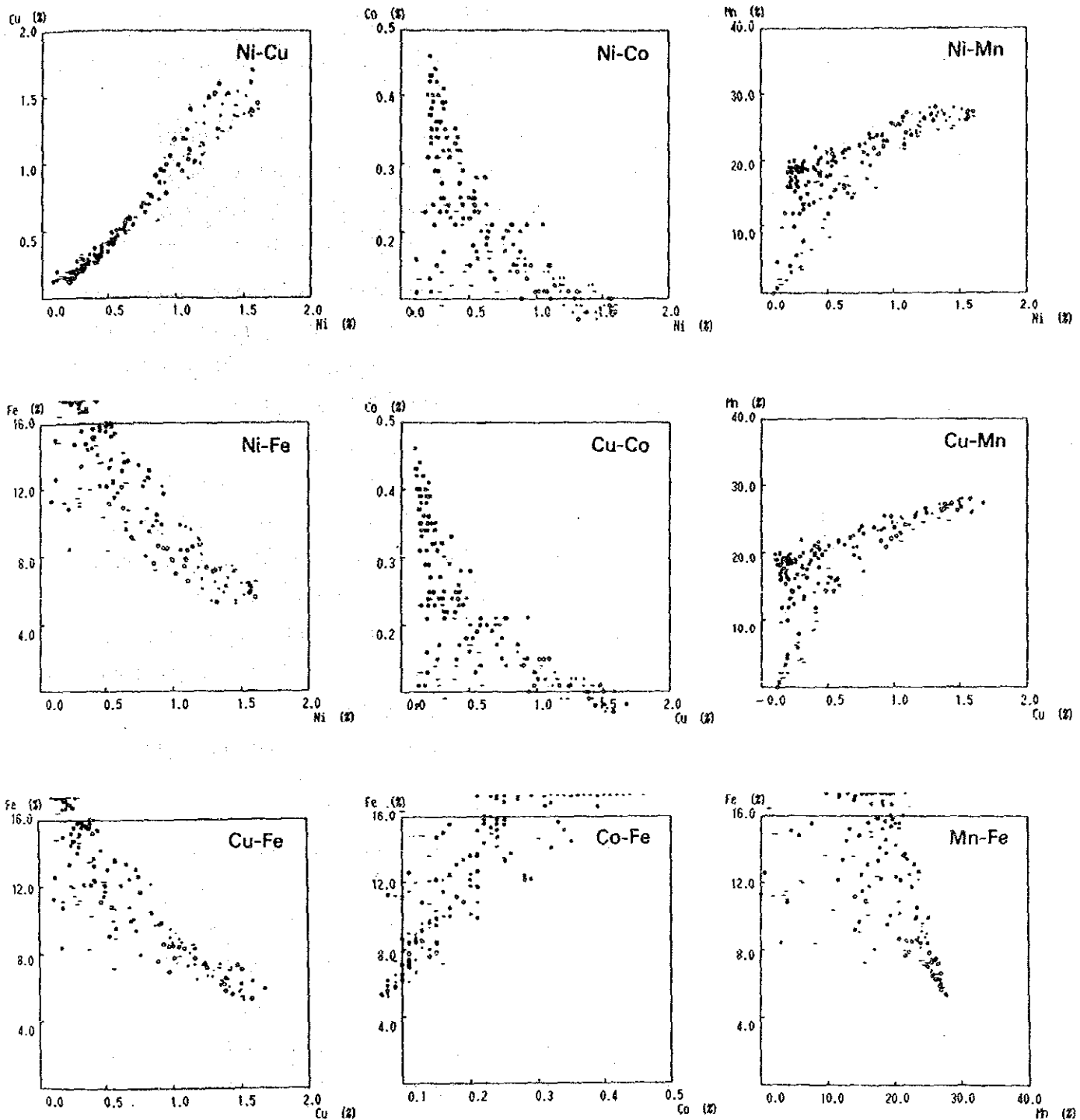


Fig. 3-5-11 Frequency Distribution of Five Principal Chemical Components



Legend

• Spheroidal	◆ Ellipsoidal	○ Ellipsoidal fat	● Pebble thin
● Pebble	■ Massive	— Platy	— Other (n=194)

Fig. 3-5-12 Scatter Distribution Diagram among Respective Components

10.0 kg/m² in the surveyed area are following five.

- 1 the sea area around 169° 30' W and enclosed with 4° 00' S and 5° 00' S.
(about 40miles x 60miles)
- 2 the sea area centering around 1° 30' S: 170° 30' W. (1 station only)
- 3 the sea area centering around 2° 30' S: 169° 00' W. (1 station only)
- 4 the sea area centering around 5° 00' S: 168° 00' W. (1 station only)
- 5 the sea area centering around 5° 00' S: 170° 00' W. (1 station only)

Among these sea areas, the considerable continuity of manganese nodules is recognized only in the area of 1. In the other areas, distribution of the manganese nodules scattered each other. The surveyed area is recognized the area where the continuity of the high abundance zone is worse.

3) Chemical Properties

Fluorescent X-ray analysis for 5 components (Ni, Cu, Co, Mn and Fe) of each granular size was done on board. Analysis of auxiliary components of representative samples selected from the foresaid samples was done on shore. Some manganese nodules were divided into several pieces considering their section structure and each of these pieces was analyzed by fluorescent X-ray method. The chemical properties of manganese nodules will be described according to these results. Statistical consequences derived from small number of samples should be treated carefully.

Table 3-5-2 Chemical Properties of Manganese Nodules

	Statistics (%)				Correlation coefficient				
	Average	Standard deviation	Maximum	Minimum	Fe	Mn	Co	Cu	Ni
Ni	0.66	0.43	1.61	0.09	-0.87	0.76	-0.71	0.98	1.00
Cu	0.60	0.46	1.68	0.11	-0.88	0.74	-0.74	1.00	
Co	0.22	0.11	0.46	0.07	0.89	-0.15	1.00		
Mn	18.74	6.24	27.98	0.00	-0.43	1.00			
Fe	13.13	4.96	21.21	5.21	1.00				

(n = 194)

(1) 5 principal components and their distribution

Fig. 3-5-11 shows the frequency distribution of the 5 principal components of manganese nodules in the surveyed area. Fig. 3-5-12 and Tab. 3-5-2 show a scatter diagram of each component and statistics of the average grade of manganese nodules respectively. The average values of Ni, Cu and Co are 0.66%, 0.60% and 0.22% respectively. The average values of Ni and Cu are rather low in comparison with the others. The average values of Mn and Fe are 18.76% and 13.13%. These average values above-mentioned are the reflection of the grade of massive and pebble type nodules collected with high amount. Annexed Fig. 8 - 10 shows grade distribution of Ni, Cu and Co. This figure shows that the grades of Ni and Cu are higher than its average grade in the flat area of the northern part of the surveyed sea area. The grade of Co, on the other hand, is high in the sea area of $4^{\circ} 00' S - 5^{\circ} 00' S$ where is correspondent with the high abundance zone of nodules. It shows that the grades are high also in the northern part sea having shallow depth where is represented by seamount and sea knoll. The grade distributions of each element are shown in Annexed Fig. 8-12.

General outlines as for the grades of Ni, Cu, Co, Mn and Fe in the surveyed area are summarized as follows. It has a tendency that the grades of Ni and Cu are low and is high in Co.

1 Ni

The grade of Ni is 1.61% in maximum, 0.09% in minimum and 0.66% in average respectively. The distribution of Ni grade shown in Annexed Fig. 8, denotes slightly higher in the northern part of the area. And the area having over 0.5% of Ni covers almost all of the surveyed area in the north of $3^{\circ} 00' S$. On the contrary, in the south of $3^{\circ} 00' S$, the area having more than 0.5% of Ni is limited and scattered. In general, the distribution of manganese nodule has a tendency to decrease in the sea area where the grade of Ni is high.

2 Cu

The grade of Cu is 1.68% in maximum, 0.11% in minimum and 0.60% in average respectively. The distribution of Cu grade shown in Annexed Fig. 9, having similar tendency to that of Ni, denotes slightly higher in the north of $3^{\circ} 00' S$ and lower in the south of $3^{\circ} 00' S$. A correlation coefficient between Ni and Cu is high, namely it is 0.93, as shown in Tab. 3-5-2.

Table 3-5-3 Morphology and Chemical Properties of Manganese Nodules

Morphology	n	Ni (%)				Cu (%)				Co (%)			
		Average	Standard deviation	Maximum	Minimum	Average	Standard deviation	Maximum	Minimum	Average	Standard deviation	Maximum	Minimum
Spheroidal	28	1.18	0.36	1.56	0.26	1.13	0.38	1.52	0.19	0.14	0.08	0.39	0.07
Ellipsoidal	4	0.94	0.23	1.15	0.63	0.96	0.35	1.30	0.48	0.15	0.05	0.21	0.10
Ellipsoidal fat	19	1.08	0.32	1.60	0.53	1.11	0.35	1.58	0.42	0.13	0.04	0.24	0.07
Pebble thin	7	0.76	0.11	0.88	0.59	0.68	0.15	0.91	0.48	0.19	0.04	0.24	0.14
Pebble	42	0.44	0.25	1.14	0.09	0.37	0.25	1.24	0.12	0.23	0.07	0.39	0.08
Massive	65	0.46	0.32	1.57	0.21	0.37	0.35	1.68	0.11	0.30	0.10	0.46	0.08
Platy	3	0.31	0.29	0.65	0.14	0.27	0.20	0.50	0.14	0.13	0.04	0.17	0.10
Other	26	0.64	0.44	1.61	0.16	0.56	0.42	1.42	0.14	0.16	0.08	0.40	0.09

Morphology	n	Mn (%)				Fe (%)				※ Cu/Ni ratio	※ Mn/Fe ratio
		Average	Standard deviation	Maximum	Minimum	Average	Standard deviation	Maximum	Minimum		
Spheroidal	28	24.89	2.95	27.98	16.42	8.71	4.46	21.14	5.21	0.94	3.42
Ellipsoidal	4	23.75	2.18	26.58	21.72	10.07	4.39	16.49	7.01	1.00	2.67
Ellipsoidal fat	19	23.62	3.83	27.86	14.13	8.01	2.32	15.18	5.30	1.02	3.23
Pebble thin	7	20.12	2.58	23.28	16.27	10.97	2.00	14.14	7.97	0.89	1.88
Pebble	42	15.30	6.21	26.44	0.00	15.19	3.39	20.60	7.38	0.83	1.09
Massive	65	18.84	3.40	27.13	3.09	16.17	4.31	21.21	5.90	0.73	1.33
Platy	3	6.91	9.19	17.51	1.21	14.50	2.05	16.37	12.31	0.95	0.54
Other	26	14.11	7.40	26.40	1.86	11.59	4.00	19.97	6.53	0.85	1.46

3 Co

The grade of Co is 0.46% in maximum, 0.07% in minimum and 0.11% in average respectively. Annexed Fig. 10 shows the equal-grade chart of Co. Distribution of Co is spreading over the surveyed area excepting that the high abundance zone of above 0.25% Co is concentrated in the zone between 4° 00' S and 5° 00' S. The area having high grade of Co corresponds to the area having high abundance of manganese nodules, and is contrast to the distributions of Ni and Cu.

4 Mn and Fe

The grade of Mn is 27.98%, in maximum 1.12% in minimum and 18.74% in average. The grade of Fe is 21.21% in maximum, 5.21% in minimum and 13.13% in average. The grade of Mn which shows strong correspondency with the grade of Ni and Cu is high in the northern part of the surveyed sea. On the other hand, the grade of Fe which shows strong correlation with Co is high in the central area along 169° 30' W and surrounded with 4° 00' S and 5° 00' S. (Annexed Fig. 11 & 12).

(2) Grade characteristics

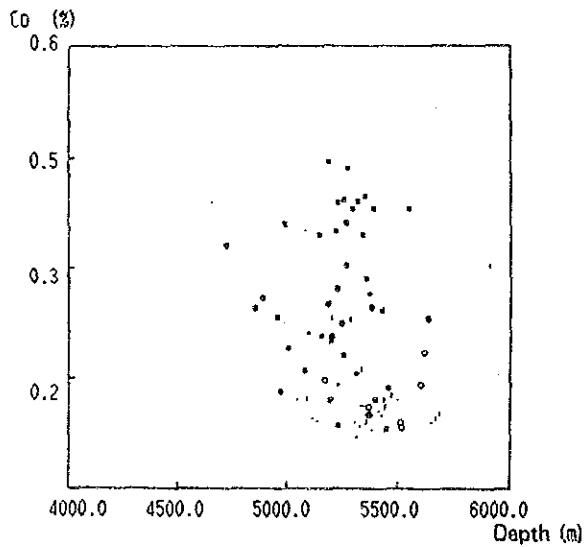
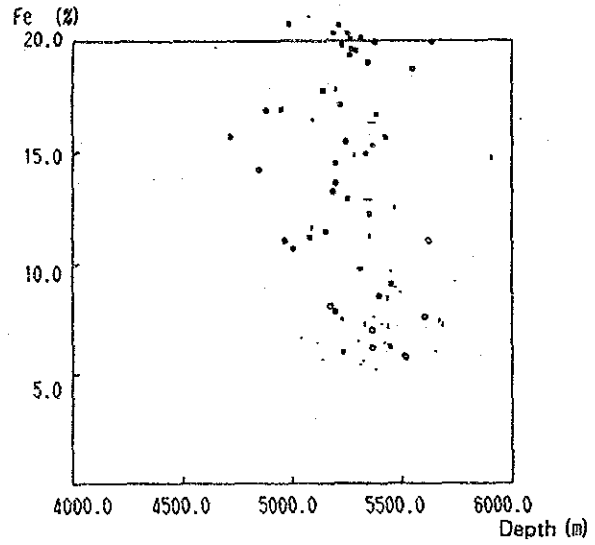
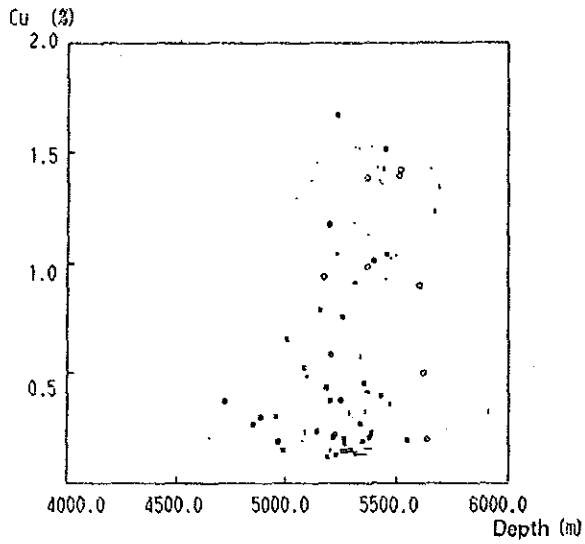
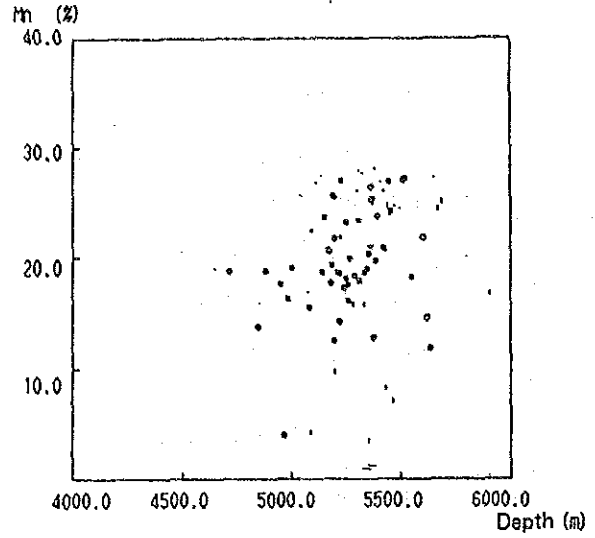
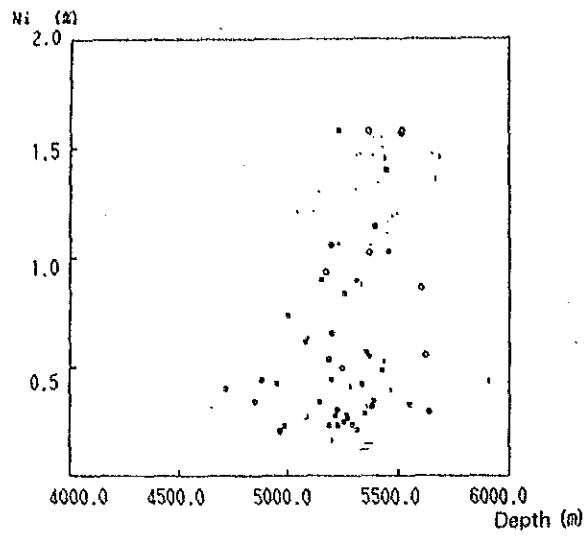
1 Relative correlation among each element

Tab. 3-5-2 shows the correlation coefficient of five elements. It is evident that the correlations are positive among Ni-Cu-Mn system and between Co-Fe system. It is also evident that the correlation is negative between the former and the latter system. Fig. 3-5-13 shows relation between the grade of five main elements and water depth. It is not recognized that there is clear correlation between water depth and each element. Nevertheless, the grades of Ni and Cu increase gradually in proportion to the water depth but the grade of Cu decreases under 2,000m level. The grades of Co and Fe decrease in proportion to the water depth but the grades do not change under 5,100m level.

2 Grade difference according to the morphology of manganese nodules.

Tab. 3-5-3 shows the grade properties classified by the shape of manganese nodules. The contents are summarized in the following four points.

- (a) Spheroidal, ellipsoidal and ellipsoidal fat types show a similar tendency of grades. Ni, Cu and Mn are relatively high, and Co and Fe are low. The Cu/Ni ratio and Mn/Fe ratio are high.
- (b) Pebble and fat type nodules have similar tendency, namely Ni, Cu and Mn are low, whereas Co and Fe are high. The Cu/Ni and Mn/Fe ratio are low. These are the reverse tendency of (a).
- (c) Pebble thin type nodule has a tendency between (a) and (b), namely Ni, Cu, Co, Mn and Fe are high. Also the Cu/Ni and Mn/Fe ratio are low.
- (d) The plate type nodule has low grade in all elements. This is considered as a influence of rocks included as a core.



Legend

- Spheroidal
- ◆ Ellipsoidal
- Ellipsoidal fat
- Pebble thin
- Pebble
- Massive
- Platy
- | Other

Fig. 3-5-13 Relation between Each Five Principal Chemical Components and the Water Depth

3 Grade difference according to the grain size of manganese nodules (Tab. 3-5-4).

An evident tendency is observed that the grade of Ni and Cu and the ratio of Cu/Ni and Mn/Fe are getting higher and the grade of Co is getting lower as the granular size is becomes smaller. It is observed that the grade of Fe is high in the medium size nodules (4 - 6cm).

4 Grade difference according to topography

Tab. 3-5-5 shows the grade properties classified by typography. The contents are summarized in the following three points.

- (a) The tendency of grades are similar in the flat area and in the seamount. The grades of Ni, Cu and Mn are low and the grade of Co and Fe are high.

Table 3-5-4 Size and Chemical Properties of Manganese Nodules

Size (cm)	n	Ni (%)				Cu (%)				Co (%)			
		Average	Standard deviation	Maximum	Minimum	Average	Standard deviation	Maximum	Minimum	Average	Standard deviation	Maximum	Minimum
0-2	52	0.91	0.52	1.61	0.09	0.82	0.50	1.59	0.12	0.15	0.07	0.36	0.07
2-4	60	0.64	0.42	1.57	0.12	0.60	0.48	1.68	0.11	0.21	0.10	0.43	0.07
4-6	47	0.50	0.28	1.29	0.14	0.43	0.34	1.51	0.12	0.25	0.11	0.44	0.10
6-8	29	0.54	0.32	1.24	0.21	0.49	0.40	1.48	0.11	0.28	0.12	0.46	0.10
8-16	6	0.61	0.32	0.93	0.15	0.55	0.32	0.98	0.16	0.19	0.11	0.40	0.10

Size (cm)	n	Mn (%)				Fe (%)				Cu/Ni ratio	Mn/Fe ratio
		Average	Standard deviation	Maximum	Minimum	Average	Standard deviation	Maximum	Minimum		
0-2	52	19.36	7.85	27.98	0.00	10.40	4.43	19.96	5.21	0.90	2.43
2-4	60	18.77	6.34	27.87	0.64	13.43	5.09	21.14	5.30	0.85	1.81
4-6	47	17.70	5.13	26.75	2.00	14.89	4.42	21.21	7.01	0.78	1.34
6-8	29	19.74	3.62	27.03	9.65	14.62	4.70	20.85	6.56	0.79	1.59
8-16	6	16.41	7.72	21.91	1.21	12.83	4.46	19.97	8.48	0.89	1.48

Table 3-5-5 Sea Floor Topography and Chemical Properties of Manganese Nodules

Topography	n	Ni (%)				Cu (%)				Co (%)			
		Average	Standard deviation	Maximum	Minimum	Average	Standard deviation	Maximum	Minimum	Average	Standard deviation	Maximum	Minimum
Flat	45	0.39	0.31	1.57	0.12	0.30	0.32	1.66	0.13	0.31	0.10	0.43	0.07
Channel	3	0.78	0.34	1.46	0.43	0.70	0.37	1.43	0.32	0.14	0.04	0.30	0.09
Platform	8	0.47	0.20	1.21	0.28	0.38	0.23	1.37	0.20	0.24	0.06	0.30	0.10
Knoll	11	0.75	0.24	1.30	0.40	0.71	0.29	1.45	0.31	0.18	0.04	0.23	0.09
Seamount	5	0.26	0.04	0.40	0.21	0.20	0.02	0.37	0.19	0.29	0.10	0.39	0.13

Topography	n	Mn (%)				Fe (%)			
		Average	Standard deviation	Maximum	Minimum	Average	Standard deviation	Maximum	Minimum
Flat	45	17.87	4.92	27.98	0.83	17.12	3.97	20.75	5.21
Channel	3	17.27	4.96	27.18	15.07	9.40	1.94	14.65	6.03
Platform	8	17.20	2.08	26.71	15.40	15.69	3.74	19.31	6.40
Knoll	11	20.94	4.42	27.32	12.37	12.07	2.57	16.49	5.66
Seamount	5	13.69	6.07	18.90	3.90	17.69	4.36	21.11	11.05

(b) The tendency of grades are similar in the channel and the sea knoll. The grade of Ni, Cu and Mn are high and the grades of Co and Fe are low. These are the reverse tendency of (a).

(c) The tendency of grades in platforms has an intermediate type between (a) and (b). The grade of Co is high, the grades of Ni, Cu and Fe are low.

5 Grade difference according to bottom materials.

Tab. 3-5-6 shows the grade properties classified by bottom materials. The grades of Ni, Cu and Mn are high, while the grades of Co and Fe are low in manganese nodules existing in siliceous clay area. On the other hand, in contrast with this, the grade of Ni and Cu are low, and the grade of Co and Fe are high in manganese nodules existing in foraminifera ooze area. The

Table 3-5-6 Bottom Sediments and Chemical Properties of Manganese Nodules

Sediment	n	Ni (%)				Cu (%)				Co (%)			
		Average	Standard deviation	Maximum	Minimum	Average	Standard deviation	Maximum	Minimum	Average	Standard deviation	Maximum	Minimum
Brown clay	23	0.34	0.26	1.57	0.12	0.24	0.23	1.51	0.13	0.32	0.11	0.43	0.08
Siliceous clay	20	0.72	0.36	1.57	0.29	0.66	0.41	1.52	0.20	0.23	0.10	0.38	0.07
Calc-siliceous clay	19	0.48	0.28	1.57	0.21	0.40	0.31	1.66	0.15	0.25	0.09	0.38	0.08
Calcareous sediment	4	0.28	0.03	0.53	0.26	0.20	0.01	0.43	0.19	0.36	0.02	0.39	0.25

Sediment	n	Mn (%)				Fe (%)			
		Average	Standard deviation	Maximum	Minimum	Average	Standard deviation	Maximum	Minimum
Brown clay	23	16.30	5.91	26.93	0.83	17.81	3.44	20.32	5.81
Siliceous clay	20	21.72	3.00	27.98	11.70	12.44	3.74	19.91	5.21
Calc-siliceous clay	19	17.04	5.28	27.32	3.90	15.08	3.82	20.75	5.66
Calcareous sediment	4	17.53	1.00	18.90	16.83	20.60	0.80	21.11	13.22

tendencies of grades in the area of brown clay and calcareous-siliceous clay have intermediate type of both, but the manganese nodules in brown clay area have similar tendency of foraminifera ooze, while calcareous-siliceous has similar pattern to siliceous clay.

(2) Auxiliary components

Total analysis and minor element analysis were executed on 4 samples selected from samples used for the 5 principal components analysis on board, considering their shapes, sea bottom topography and areas, in order to investigate the auxiliary component properties of manganese nodules. Tab. 3-5-7 shows both the total and small quantity analysis values along with the 5 principal components values analyzed on board. The TiO_2 , CaO, Pb and Sr components of manganese nodules in the surveyed areas have a higher grade than the average grade (*1) in the Clarion-Clipperton Prime area by Mckelvey et al (1979). On

(*1) 7.81% Si, 0.61% Ti, 2.84% Al, 1.80% Mg, 1.47% Ca, 0.32% Ba, 1.87% Na, 0.82% K, 0.23% P, 0.048% Pb, 0.066% Mo, 0.048% V, 0.016% B, 0.13% Zn, 0.01% Y.

the contrary, Al_2O_3 , MgO , BaO , Na_2O , K_2O , P_2O_5 , Mo , V and Zn have a lower grade than the average grade in the Clarion-Clipperton Prime area. Total analysis and minor element analysis based on morphological classification show almost same values and do not indicate extreme differences.

(3) Chemical properties variation in the section of manganese nodules.

It is useful to investigate the chemical properties (distribution of metal elements) of the sectional surface of the manganese nodules in order to understand the grade variation according to the above-mentioned factors (shape, granular size, topography and bottom materials etc.) and to elucidate for solution to historical process, especially its relation to sedimentation, of the growth of manganese nodules. (A. Nishimura 1986). Total three representative samples, one sample for spheroidal type and two samples for massive type nodules were selected. Fluorescent X-ray analysis on these samples were carried out. The samples, for analysis, separated into groups of several layers by the naked eyes, were collected by hand picking method using a small chisel. Fig. 3-5-14 shows the sampling positions. Table 3-5-8 and Fig. 3-5-15 show the results of analysis.

The contents are summarized as follows:

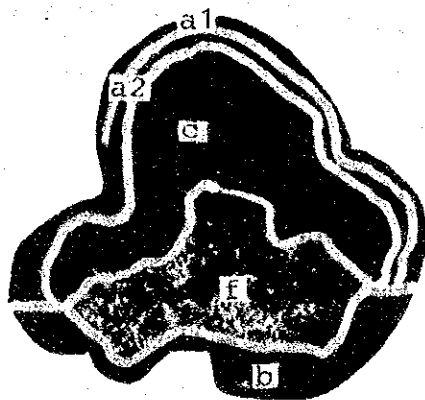
- (a) The grades show almost the same values both upper side and lower side. Fig. 3-5-15 shows that the grades are symmetrical graph about the core.
- (b) The grades of Ni variation is not constant.
- (c) Although the Co grade variation is not so remarkable but the tendency of the increase of Co toward the inner side can be observed.

Table 3-5-7 Total and Minor Element Analysis of Manganese Nodules

Sampling No.		87S0369FG04	87S0370FG05	87S0570FG19	87S0668FG01
Topography		(Mount) platform	(Mount) Seaknoll	(Quasi) Flat	(Quasi) Flat
Depth (m)		4959	5288	5229	5356
Morphology		Pebble	Massive	Spheroidal	Pebble thin
Size (cm)		2-4	4-6	4-6	2-4
Analysis (%)	Ni	0.50	0.37	0.23	0.62
	Cu	0.34	0.32	0.13	0.51
	Co	0.22	0.22	0.37	0.28
	Mn	17.42	12.90	18.14	21.10
	Fe	15.86	14.36	19.83	12.08
Major elements (%)	SiO ₂	16.58	19.81	11.56	16.61
	TiO ₂	2.08	1.83	2.39	1.44
	Al ₂ O ₃	4.06	6.13	3.18	6.58
	Fe ₂ O ₃	21.96	19.84	24.51	15.64
	FeO	<0.01	<0.01	<0.01	<0.01
	MnO ₂	25.64	23.79	28.69	30.78
	MgO	2.40	1.94	1.75	2.86
	CaO	2.70	2.23	2.82	2.64
	BaO	0.16	0.17	0.19	0.16
	Na ₂ O	2.16	2.64	2.01	2.30
	K ₂ O	0.74	1.37	0.64	0.99
	P ₂ O ₅	0.81	0.55	0.66	0.58
	Ig-loss	19.21	17.83	20.09	17.89
Minor elements (%)	Pb	0.074	0.078	0.116	0.062
	Sr	0.122	0.098	0.136	0.088
	Mo	0.019	0.016	0.027	0.025
	V	0.019	0.020	0.025	0.022
	As	0.013	0.011	0.016	0.010
	B	0.017	0.015	0.018	0.012
	Zn	0.071	0.096	0.060	0.079
	Y	0.012	0.010	0.013	0.010
	Pt	<0.0001	<0.0001	<0.0001	<0.0001

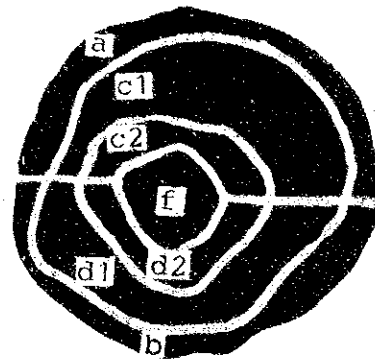
Table 3-5-8 Chemical Compositional Difference between Outer and Inner Part of Manganese Nodules

Sample No.	Size (cm)	Morphology	Analysed position	XRF Analyses (%)					Cu/Ni	Mn/Fe	
				Ni	Cu	Co	Mn	Fe			
878 0271FG03	6-8	Massive	Upper	Out. 1	0.79	0.55	0.19	22.61	13.80	0.70	1.64
				Out. 2	0.83	0.59	0.22	22.65	11.38	0.71	1.69
				In.	0.35	0.32	0.32	19.81	15.38	0.91	1.29
			Core	0.41	0.62	0.06	2.12	7.68	1.51	0.28	
			Lower	Out.	0.56	0.41	0.22	20.83	16.56	0.73	1.26
878 0670FG08	6-8	Spheroidal	Upper	Out.	0.21	0.13	0.39	18.03	22.02	0.62	0.82
				In. 1	0.31	0.16	0.46	20.83	17.65	0.52	1.18
				In. 2	0.35	0.15	0.50	21.37	14.05	0.43	1.52
			Core	0.39	0.17	0.41	19.23	12.24	0.44	1.57	
			Lower	In. 2	0.34	0.15	0.50	21.35	13.76	0.44	1.55
				In. 1	0.29	0.16	0.44	20.13	17.94	0.55	1.12
				Out.	0.23	0.15	0.40	18.06	21.33	0.65	0.85
Out. 1	0.60	0.49		0.18	22.13	15.38	0.82	1.44			
878 0171FG03	4-6	Massive	Upper	Out. 2	0.69	0.64	0.19	21.79	14.84	0.93	1.47
				In. 1	0.98	0.86	0.17	23.48	11.80	0.88	1.99
				In. 2	0.75	0.68	0.22	21.18	11.89	0.91	1.78
				Core	0.53	0.54	0.14	9.86	7.51	1.02	1.31
			Lower	In. 2	0.53	0.51	0.25	19.50	12.91	0.96	1.51
				In. 1	1.08	0.94	0.19	23.69	10.75	0.87	2.20
				Out. 2	0.74	0.66	0.19	22.79	14.46	0.89	1.58
				Out. 1	0.60	0.48	0.18	22.18	15.57	0.80	1.42



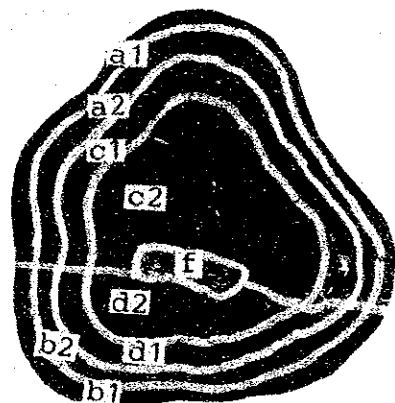
0 1 2 3 4 5cm

87S0271FG03 (6-8cm)
Massive



0 1 2 3 4 5cm

87S0670FG08 (6-8cm)
Spheroidal



0 1 2 3 4 5cm

87S0171FG03 (4-6cm)
Massive

Outer Crust
a: (Upper)

Outer Crust 1
b1: (Lower)

Inner Crust 2
c2: (Upper)

Outer Crust 1
a1: (Upper)

Outer Crust 2
b2: (Lower)

Inner Crust 1
d1: (Lower)

Outer Crust 2
a2: (Upper)

Inner Crust
c: (Upper)

Inner Crust 2
d2: (Lower)

Outer Crust
b: (Lower)

Inner Crust 1
c1: (Upper)

f: Core

Fig. 3-5-14 Photos of Manganese Nodules for Section Analysis

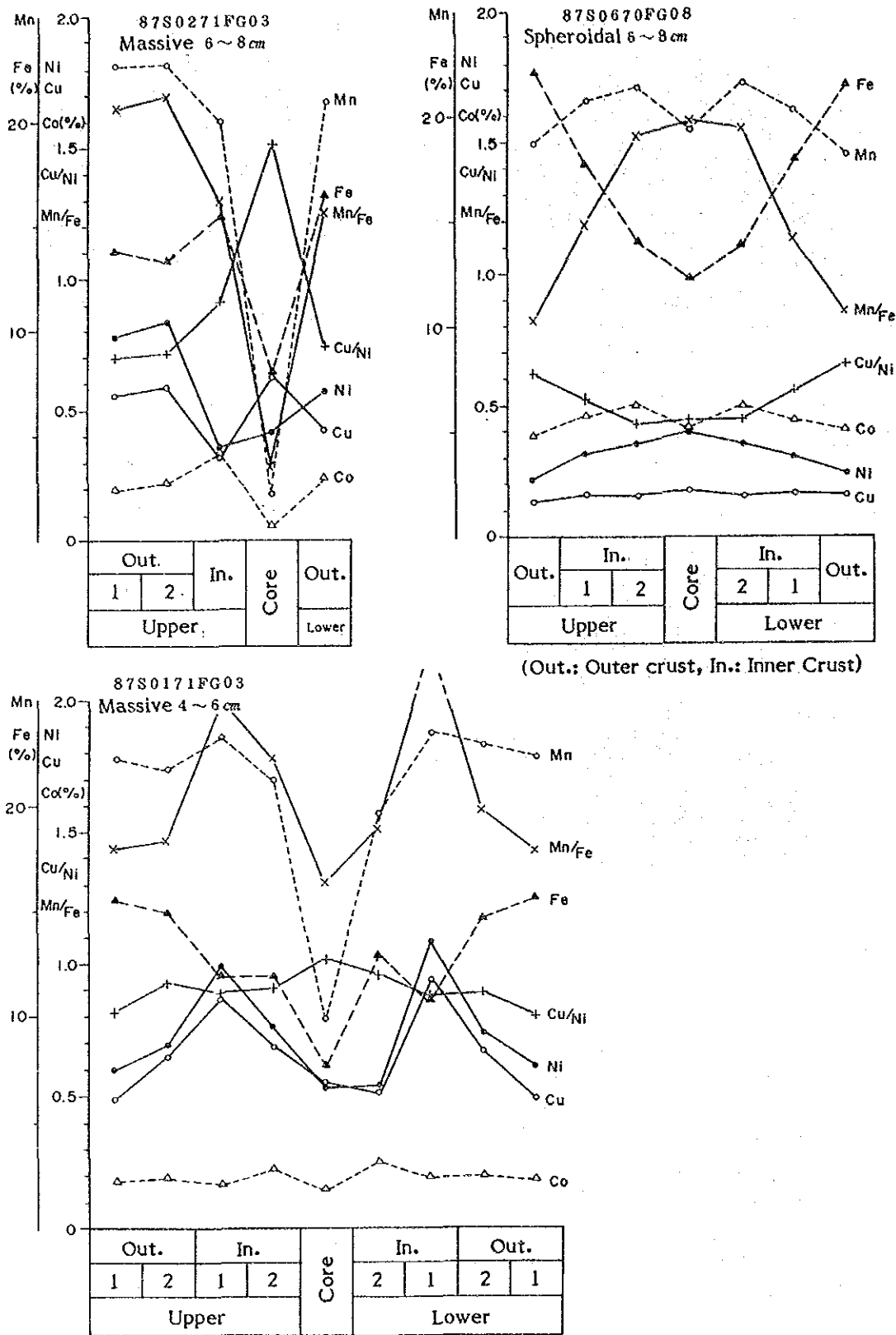


Fig. 3-5-15 Grade of Respective Section of Manganese Nodules (on Board Analysis)

4) Mineral Properties

Concerning the representative samples, X-ray diffraction analysis and observation of polished thin sections by microscope were done in order to investigate the mineral composition and inner structure of manganese nodules.

(1) X-ray diffraction analysis

Manganese nodules were roughly divided into the outer crust, inner crust and core; moreover each of the samples shown in Fig. 3-5-16 was divided into several smaller parts on which X-ray diffraction analysis was executed. The results of analysis are in Tab. 3-5-9 and the X-ray diffraction patterns are in Fig. 3-5-17. Detected minerals are 10\AA manganite, $\delta\text{-MnO}_2$ manganese mineral, quartz, plagioclase, montmorillonite, phillipsite, harmotome, carbonate apatite etc. The characteristic are follows: The main manganese mineral composing manganese nodules (87S0570FG19) is $\delta\text{-MnO}_2$, on the contrary, 870171FG03 is 10\AA manganite. (Provided that $\delta\text{-MnO}_2$ is detected only in the core of sample 87S0171FG03.) Although manganese minerals composing nodules are different each other, both of sample have high peak of diffraction lines in the outer crust than in the inner crust. The core parts are composed of plagioclase, montmorillonite, phillipsite, harmotome and carbonate apatite, and manganese minerals are hardly detected.

(2) Observation by microscope

Polished thin sections were prepared for the spheroidal type of manganese nodules and observation was done by a reflecting microscope and a polarizing microscope. Spheroidal type (87S0570FG19, Fig. 3-5-18)

- Observation by naked eyes:

The external appearance is almost spheroidal having a diameter of 5.5cm. The symmetrical concentrically circled structure is growing around the core composing basalt fragment and having a diameter of 2cm.

- Observation by microscope:

The core is composed of "dolerite" having medium size and perfect crystalline. Main minerals are plagioclase, clinopyroxene, small size opaque mineral considered to be illumenite, and clay minerals scattered in the spaces of main minerals. Manganese oxide has a stratiform texture composed of uniform $\delta\text{-MnO}_2$ and thin layer of 10\AA manganite (over 0.04mm) is rarely existing among

them. The growth pattern shows that a dense stratiform texture having monotonous regularity and branch shaped ripple-like texture form bedding repeatedly one after the other. The growth patterns are different between that of the core to the surface and that of the core to the bottom. The former has more regular pattern, the latter has clear branch shaped texture having disordered pattern.

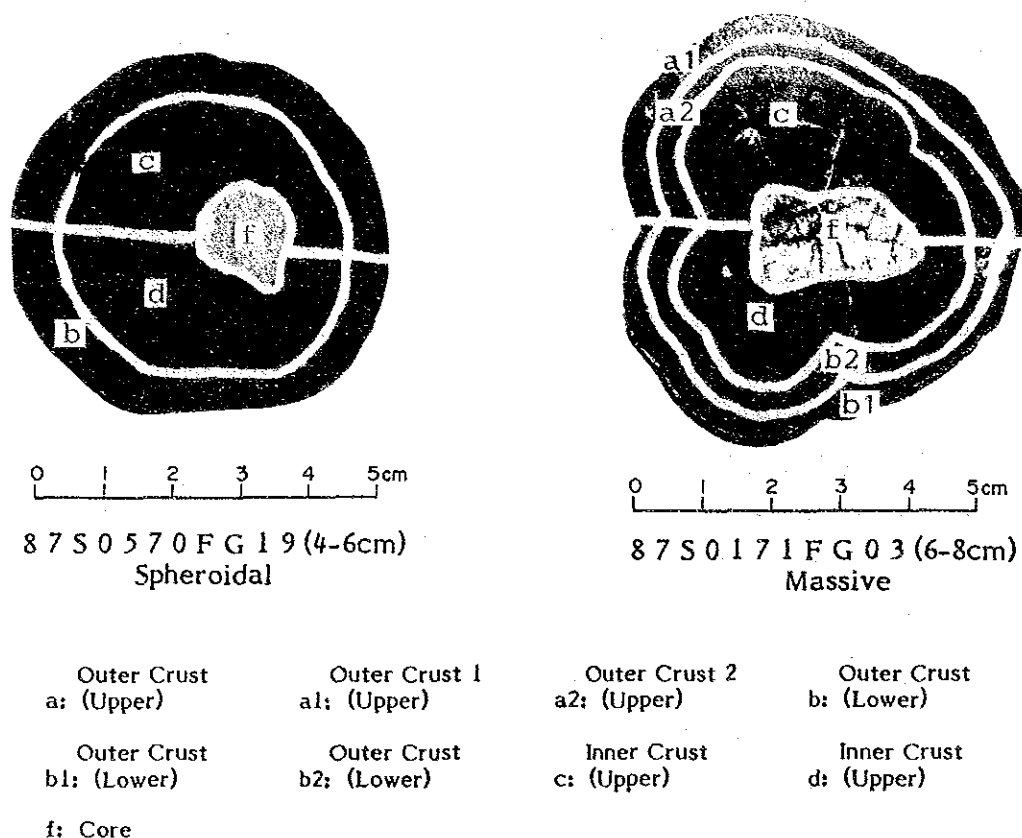
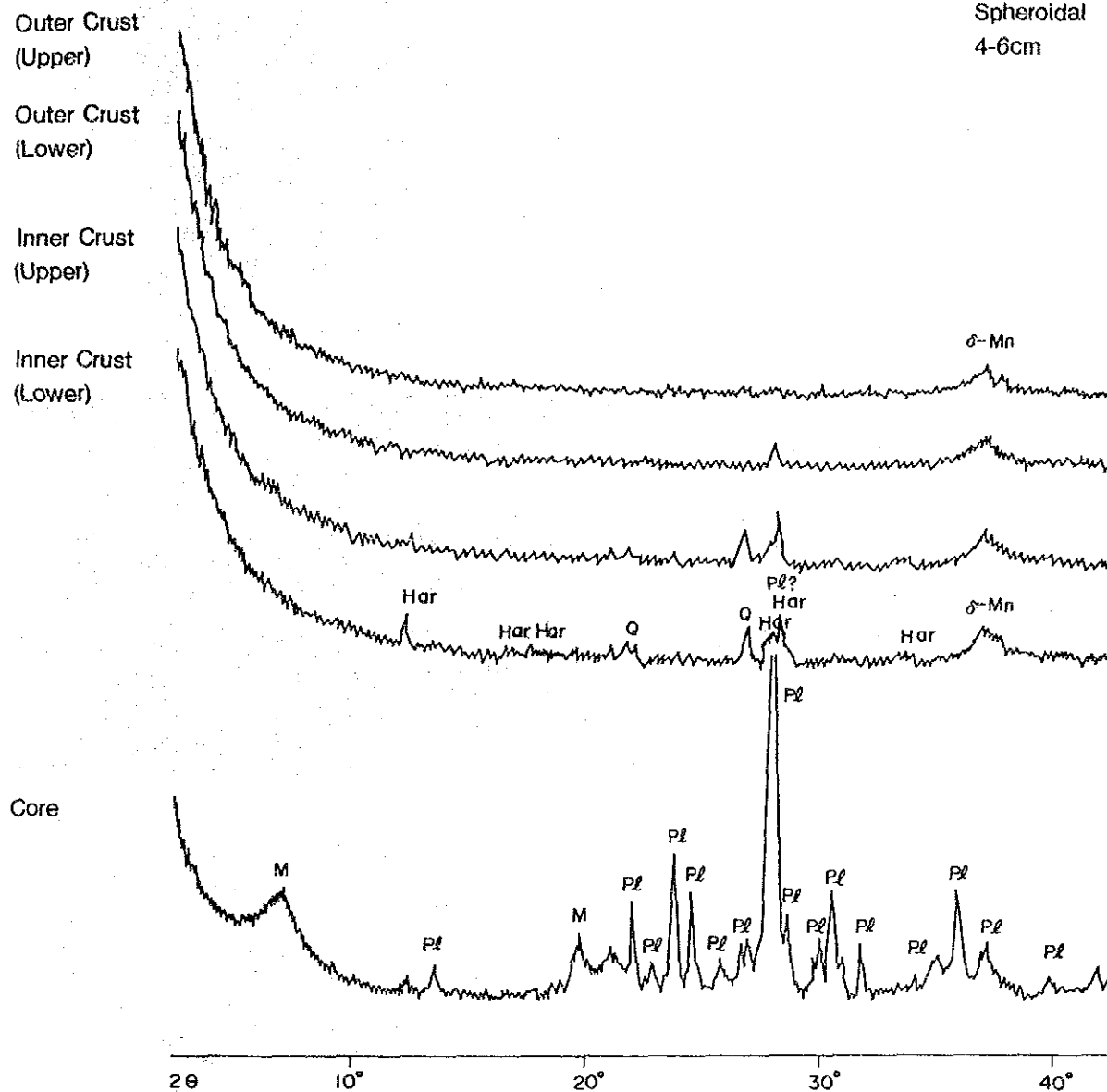


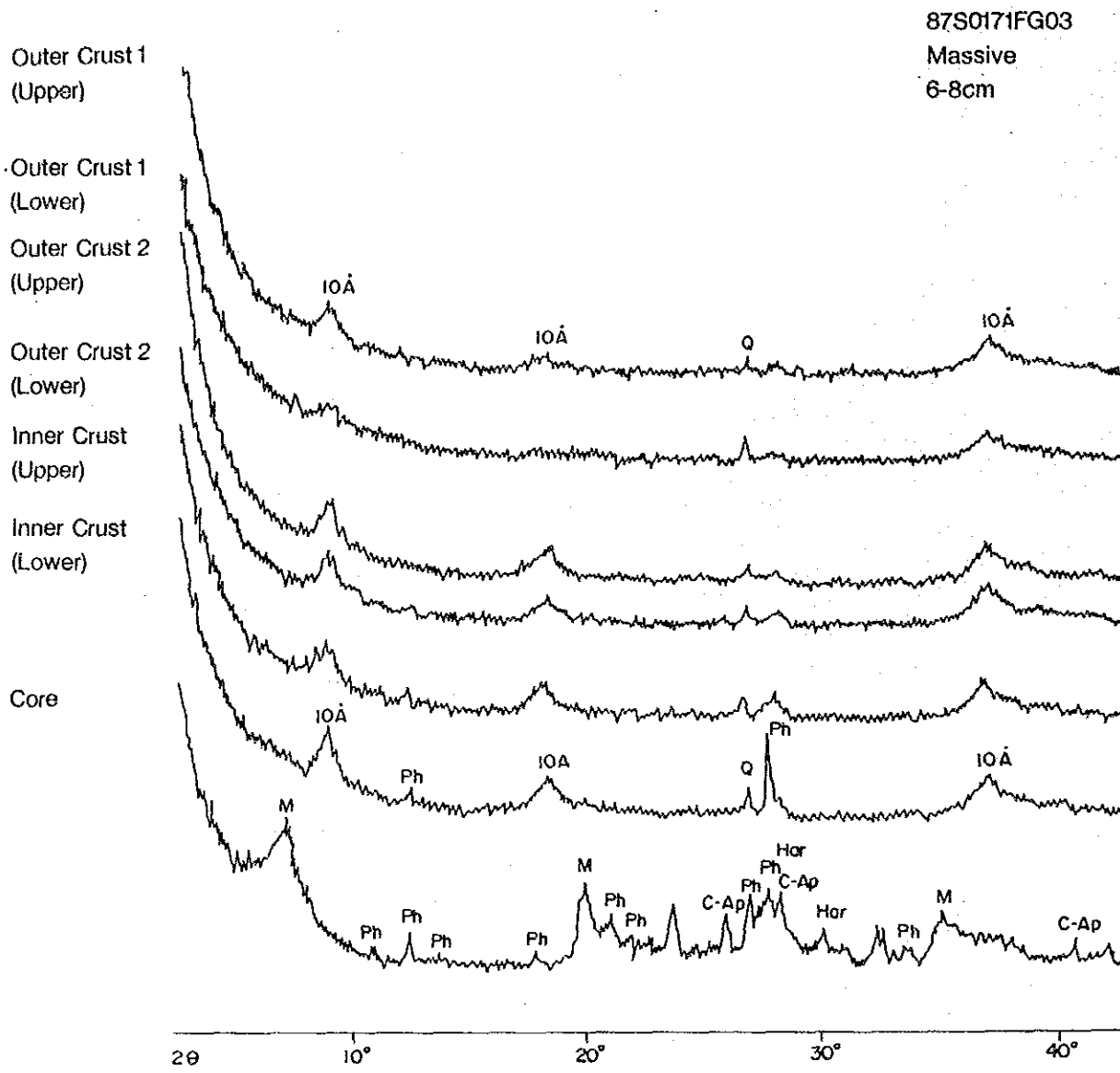
Fig. 3-5-16 Photos of Manganese Nodules for X-ray Analysis

87S0570FG19
Spheroidal
4-6cm



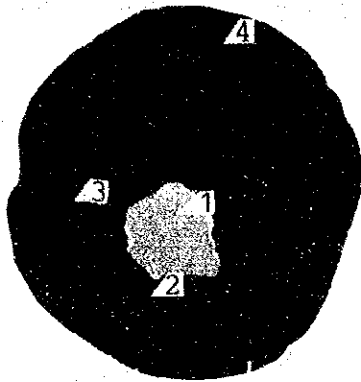
Legend δ -Mn : δ -MnO₂ Q : Quartz Pl : Plagioclase
M : Montmorillonite Har : Harmotome

Fig. 3-5-17 X-ray Diffraction Patterns of Manganese Nodules (1)



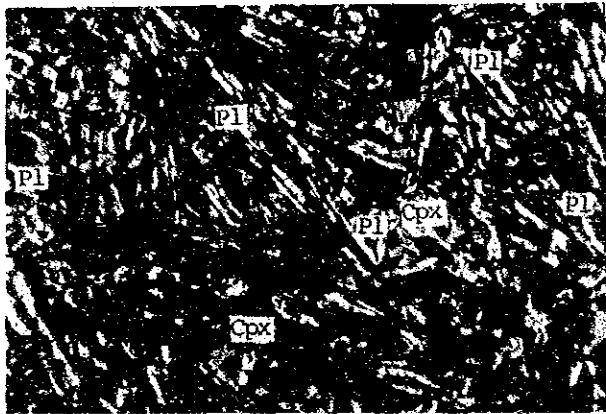
Legend IOA : 10A Manganite δ -Mn : δ -MnO₂ Q : Quartz PI : Plagioclase M : Montmorillonite
Ph : Phillipsite Har : Hornotome C-AP : Carbonate-apatite

Fig. 3-5-17 X-ray Diffraction Patterns of Manganese Nodules (2)



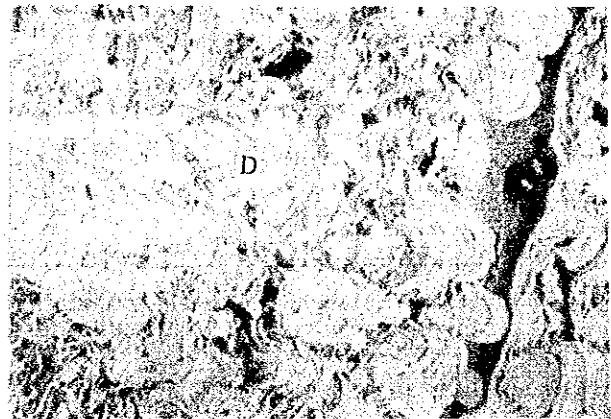
87S0570FG19
spheroidal

1. Section
Number of this photo shows micro-photo's position.
2. 1-4 Microscopic photo
Pl: plagioclase
Cpx: Clinopyroxene
D: δ -MnO₂
T: 10Å Manganite



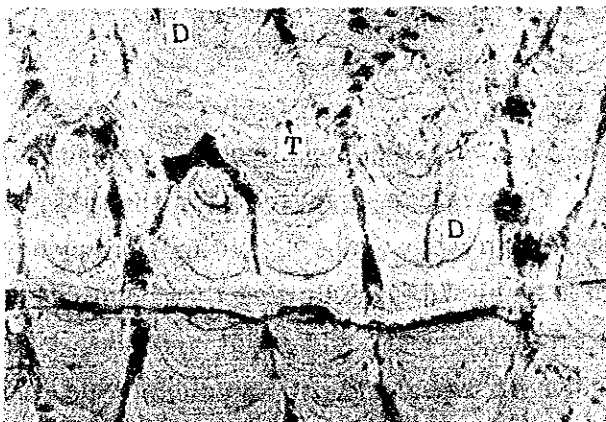
2-1 (Core)

Polarized light



2-2 (Inner part)

reflected light



2-3 (Inner part)

reflected light



2-4 (Outer part)

reflected light

Fig. 3-5-18 Macro-photo and Microscopic Photos of Polished Thin Sections of Manganese Nodules

Table 3-5-9 Result of X-ray Diffraction Analysis of Manganese Nodules

Sample No.	Size (cm)	Morphology	Analysed position	10Å	δ-Mn	Q	Pl	Mo	Ph	Har	C-Ap		
87S0570FG19	4-6	Spheroidal	Out.	Upper		±							
				Lower		±		±					
			In.	Upper		±	±	±			±		
				Lower		±	±	±			±		
			Core					+++	+				
87S0171FG03	6-8	Massive	Out.	1	Upper	±		±					
					Lower	±		±					
				2	Upper	±		±					
					Lower	±		±	±				
			In.	Upper	±		±	±					
				Lower	±		±				+		
			Core			±				+	±	+	+

10Å: 10Å manganite δ-Mn: δ-MnO₂ Q: Quartz
 Pl: Plagioclase Mo: Montmorillonite Ph: Phillipsite Har: Harmotome
 C-Ap: Carbonate-Apatite

+++, ++, +, ± indicate intensity of diffraction peaks,
 (+++: high, ++: moderate, +: weak, ±: very weak)

5) Sea Bottom Situation and Abundance

(1) Morphology and abundance of manganese nodules

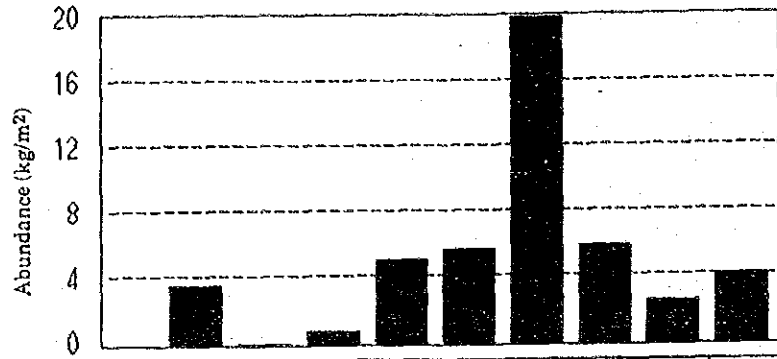
Fig. 3-5-19 shows the average abundance and the appearance frequency of abundance of respective morphology. The average abundance for the massive type is 19.8kg/m² and this is extremely high value. The appearance frequency of over 10kg/m² for the massive type is highly 76%. Following this, pebble type is 5.96kg/m² and spheroidal type is 3.73kg/m² (Ellipsoidal flat and plate type are excluded because of small number of samples). Both pebble type and spheroidal type have excellent appearance ratio 0 - 2.5kg/m². All of the abundance of ellipsoidal are included in 0 - 2.5kg/m².

(2) Sea floor topography and abundance

The correlation between the sea bottom topography and the abundance of manganese nodules of all sampling points, is shown in Fig. 3-5-20. The surveyed area are divided, from macroscopic point of view, into 3 parts as shown in Fig. 3-5-20. This figure shows the average abundance in plains and in mountainous area north of 3° S are 2.77kg/m² and 2.17kg/m² respectively, and the appearance ratio of more than 10kg/m² are low as 11.9% and 6.7% respectively. On the other hand, the occurrence ratio more than 5.40kg/m² and 10kg/m² is 22.4% in quasi-plains. This is higher than two area above mentioned. But according to the frequency diagram the appearance frequency of 0 - 2.5kg/m² is excellent in quasi-plains north of 3°S similarly in plain and in mountainous. Comparing the weight coefficient, the order are plains (18.6kg/m²), mountainous (23.9kg/m²), quasi-plains (28.8kg/m²) in ascending. This also shows that the diameter of manganese nodules become large in accordance with southward. It is a distinguished feature that the embedded type of manganese nodules exist abundantly in plains and mountainous of two northern area. The average embedded ratio (*1) are 80.9% and 61.1% respectively. On the other hand, the embedded ratio is equal to zero in quasi-plains of southern part where nodules are exposing type mostly. It is considered that there is relevant relation to the upper transparent layers thickness increasing toward north. The statistical results of the sea floor topography observed microscopically are shown in Fig. 3-5-21. Number of sampling points for flat is prominent. While that for the other area is very low, so the correlation between the topography and the abundance cannot be discussed with the same accuracy. But as for tendency, it is divided into two groups. One is the group of the deep water depth such as plains, platter and channel and the other is the group of the shallow water depth such as platform, sea knoll and seamount. The average abundance and the occurrence ratio more than 10kg/m² are low in the former group. The frequency diagram shows 0 - 2.5kg/m² are excellent. On the other hand, the latter group has maximum frequency in the zone of 0 - 2.5kg/m², but the average abundance and the occurrence ratio more than 10kg/m² is high as compared with the former group. The weight coefficient are 22.2kg/m² and

*1 The degree of manganese nodules embedded (%)

= (1 - coverage by deep sea camera/coverage by obtained samples) x 100



LEGEND

Morphology

- Sp Spheroidal
- E Ellipsoidal
- Ef Ellipsoidal fat
- Pt Pebble thin
- P Pebble
- M Massive
- Pl Platy
- Ot Other

Abundance

- 1 0.0 - 2.5 kg/m²
- 2 2.5 - 5.0
- 3 5.0 - 7.5
- 4 7.5 - 10.0
- 5 10.0 <

Morphology	Sp	E	Ef	Pt	P	M	Pl	Ot	Total
Average Abundance (kg/m ²)	3.73	0.07	0.84	5.20	5.96	19.81	6.09	2.63	4.20
Appearance ratio (%) of $\geq 10\text{kg/m}^2$	13.6	0.0	0.0	0.0	41.2	76.0	33.0	9.0	17.6
Standard deviation	6.28	0.07	1.77	4.10	7.17	11.83	5.88	4.46	8.48
Number of Samples	22	6	13	2	17	21	3	11	159

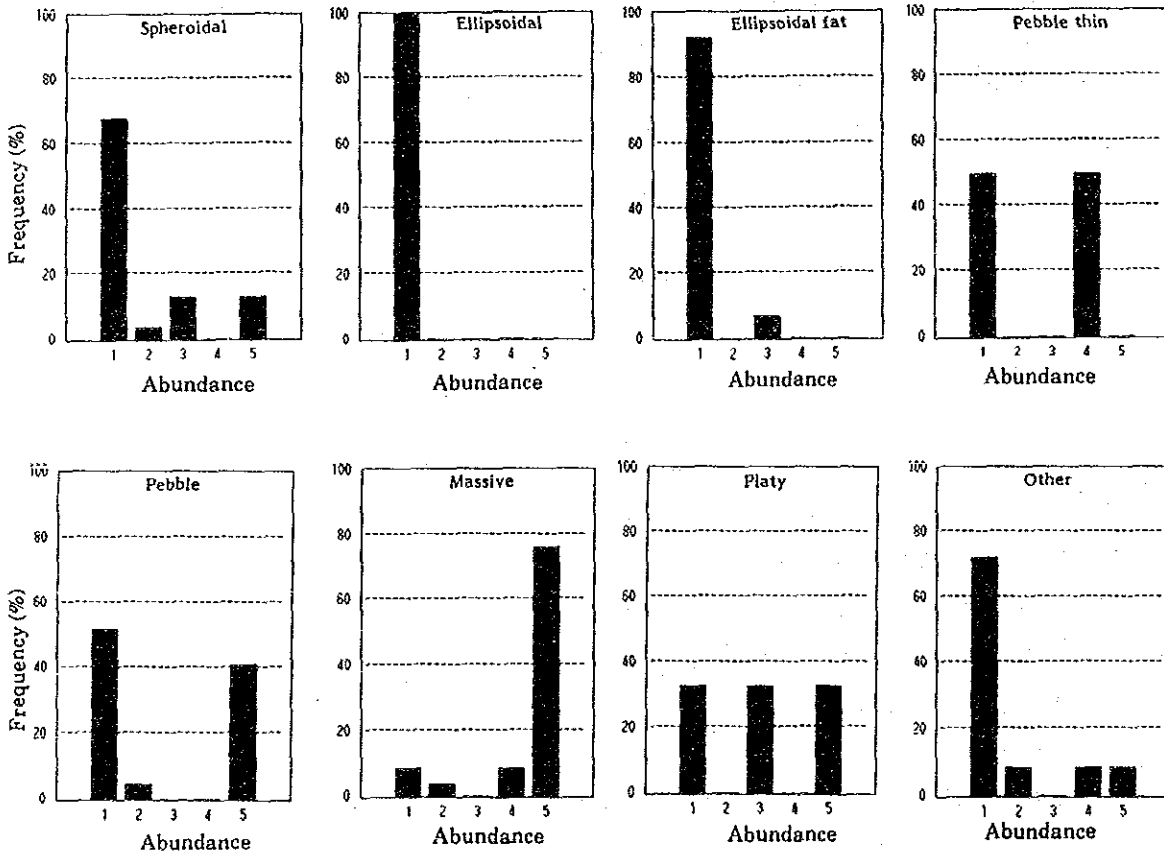
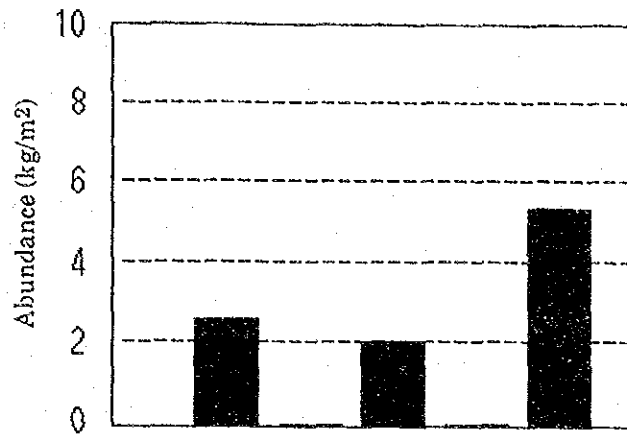


Fig. 3-5-19 Relation between Morphology and Abundance of Manganese Nodules



Topography	Plain	Mountainous	Quasi Plain
Average Abundance (kg/m ²)	2.77	2.17	5.40
Appearance ratio of $\geq 10\text{kg/m}^2$	11.9	6.7	22.4
Weight Coefficient (kg/m ²)	18.6	23.9	28.8
Embedded ratio (%)	80.9	61.1	0.0
Number of Samples	42	30	98

LEGEND

Abundance

- 1 0.0 - 2.5 kg/m²
- 2 2.5 - 5.0
- 3 5.0 - 7.5
- 4 7.5 - 10.0
- 5 10.0 <

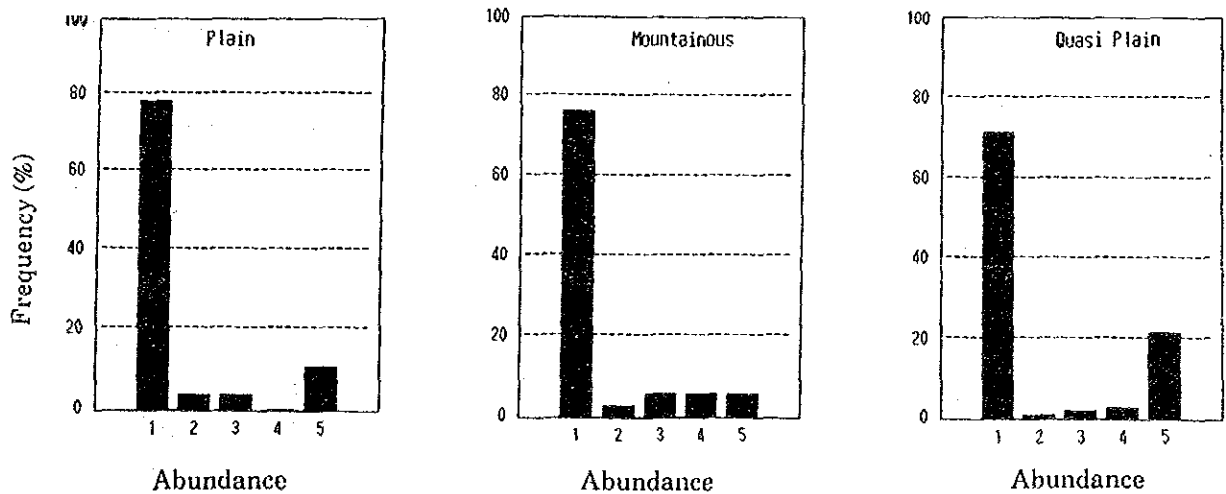


Fig. 3-5-20 Relation between Macroscopic Topography and Abundance of Manganese Nodules

24.4kg/m² in the seamount and sea knoll respectively, but that of channel is 32.0kg/m².

(3) SBP type and abundance

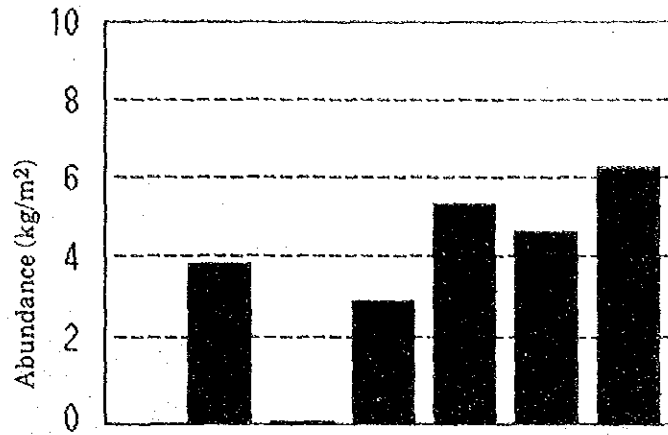
The relationship between the SBP type and the abundance of manganese nodules is shown in Fig. 3-5-22.

1 The type having upper transparent layers. (type a, b, bc, e₁)

Type a, b, bc and e₁ show low abundance as 0 - 2kg/m². The frequency distribution diagram shows inclination toward 0 - 2.5kg/m² and the appearance ratio more than 10kg/m² is zero. The abundance are very low in type b and type bc having transparent layers. It is presumed as a barren zone. Type e₁ have comparative high occurrence ratio more than 10kg/m² and have two peaks of 10kg/m² and 0 - 2.5kg/m². As a result, the average occurrence is slightly high (5.39kg/m²) although the dispersion is large.

2 The type having upper opaque layers (type d₁, d₂ ds)

Though the average abundance are comparatively high as 4.76 - 6.26kg/m², the frequency distribution have two peaks of 0 - 2.5kg/m² and over 10kg/m² with wide dispersion. These are considered that the area showing opaque layer are complex in general and the distribution of manganese nodules are not uniform but are full of variety. Also type e₁ above mentioned has the similar tendency. These are considered as following, type e₁ is discovered in composing the transition zone and the area is close to opaque group in topography as a consequence.



Topography	fl	ho	ch	ph	kn	mt
Average Abundance (kg/m ²)	3.95	0.01	3.01	5.45	4.78	6.33
Appearance ratio of $\geq 10\text{kg/m}^2$	13.9	0.0	8.3	26.7	26.1	33.3
Weight Coefficient (kg/m ²)	25.1	—	32.0	25.8	24.4	22.2
Embeded ratio (%)	11.9	—	0.0	1.9	66.6	23.5
Number of Samples	108	3	12	15	23	9

LEGEND

Topography

- fl flat
- ho hollow
- ch channel
- ph plat-form
- kn sea knoll
- mt sea mount

Abundance

- 1 0.0 - 2.5 kg/m²
- 2 2.5 - 5.0
- 3 5.0 - 7.5
- 4 7.5 - 10.0
- 5 10.0 <

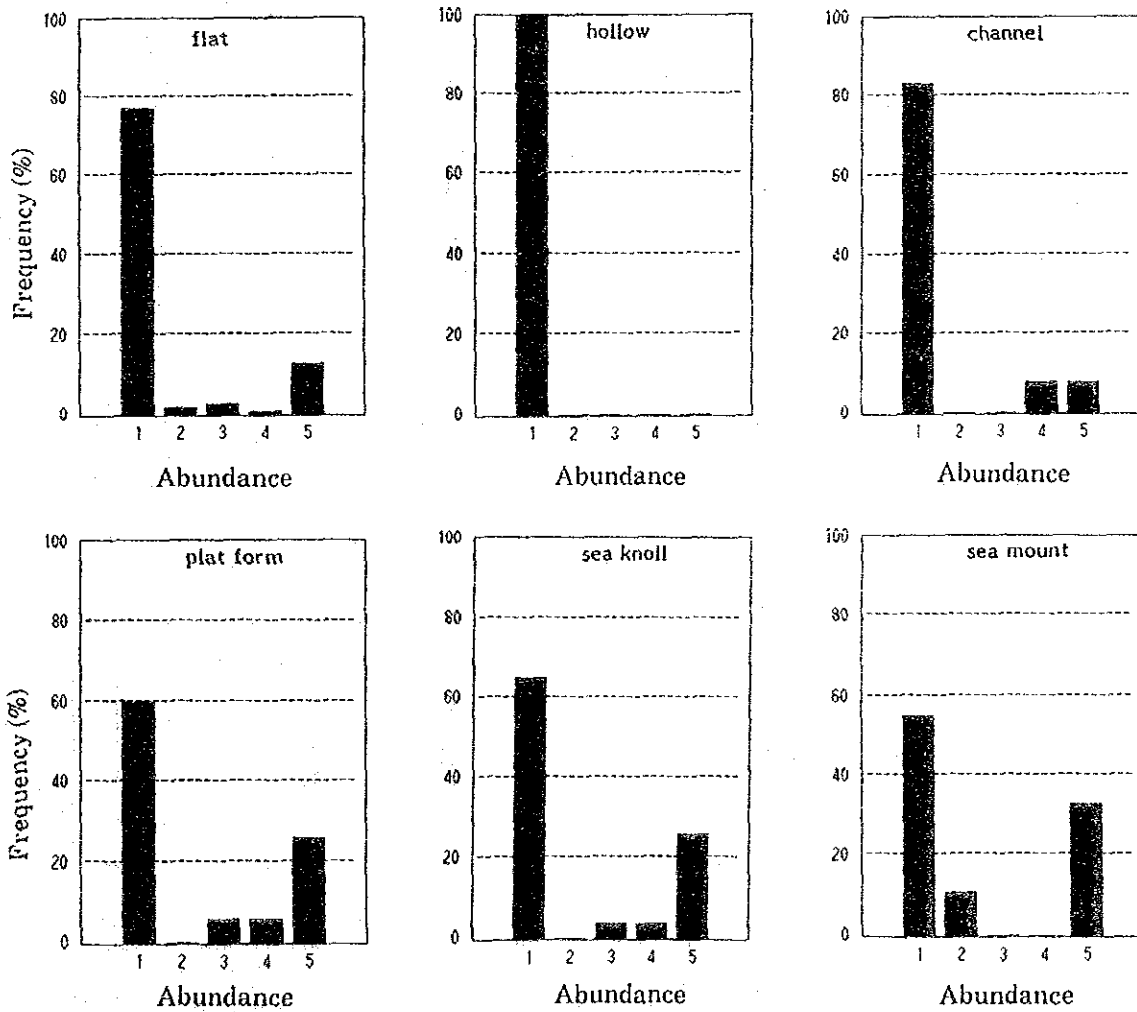
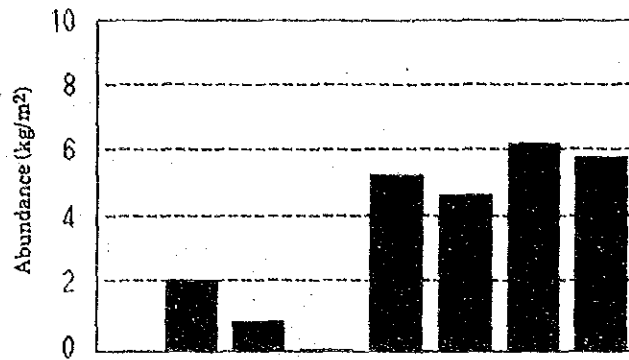


Fig. 3-5-21 Relation between Microscopic Topography and Abundance of Manganese Nodules



SBP Type	a	b	bc	e1	d1	d2	ds
Average Abundance (kg/m ²)	2.20	0.92	0.00	5.39	4.76	6.26	5.83
Standard deviation	2.56	3.24	0.00	12.87	8.36	10.25	7.81
Number of Samples	9	40	8	16	30	35	29

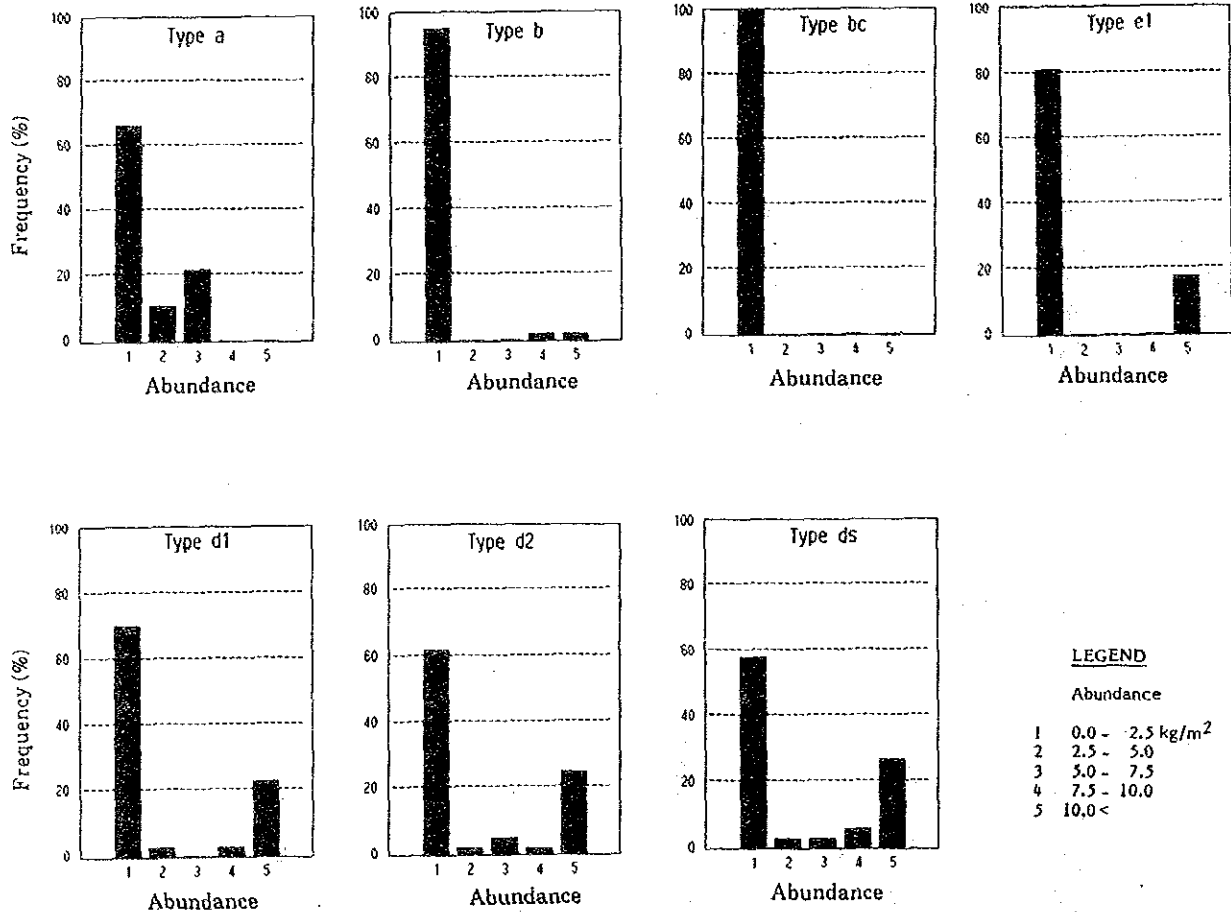


Fig. 3-5-22 Relation between SBP Type and Abundance of Manganese Nodules

(4) Upper transparent layers and abundance

The relation between upper transparent layers of SBP and abundance of manganese nodules is shown Fig. 3-5-23. The figure shows the abundance is maximum in 10m transparent layer thickness and the average abundance is about 10kg/m². After that, the abundance show 5.22kg/m², 2.5kg/m² in 0m, 20m transparent layer respectively. But the abundance is extremely low, less than 1kg/m², and the appearance ratio of over 10kg/m² is zero. That is to say, the abundance have a tendency toward lower in accordance with increase thickness expecting that of 0 m.

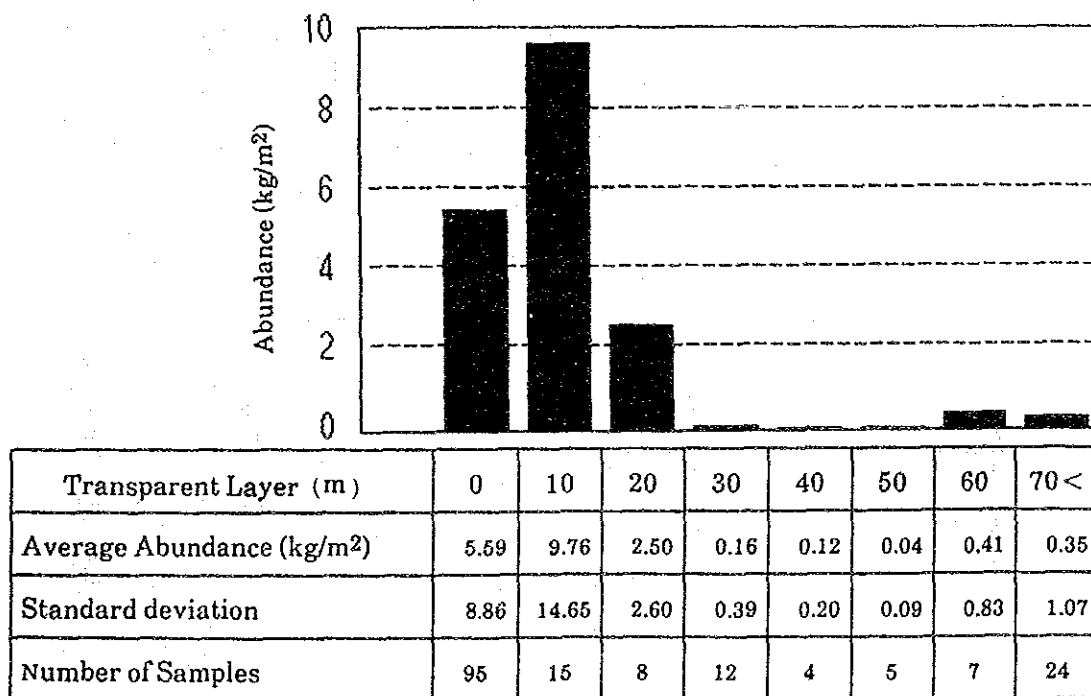


Fig. 3-5-23 Relation between Upper Transparent Layer Thickness and Abundance of Manganese Nodules

(5) Bottom materials and abundance

Fig. 3-5-24 shows the relation between bottom materials and abundance of manganese nodules. Abundance for calcareous-siliceous clay is the highest and is 10.28kg/m² in average. Two peaks are observed, namely in 0 - 2.5kg/m² and in 12.5 - 15.0kg/m², in the frequency diagram and the appearance ratio over 10kg/m² is getting 50% or more. The average abundances of brown clay and

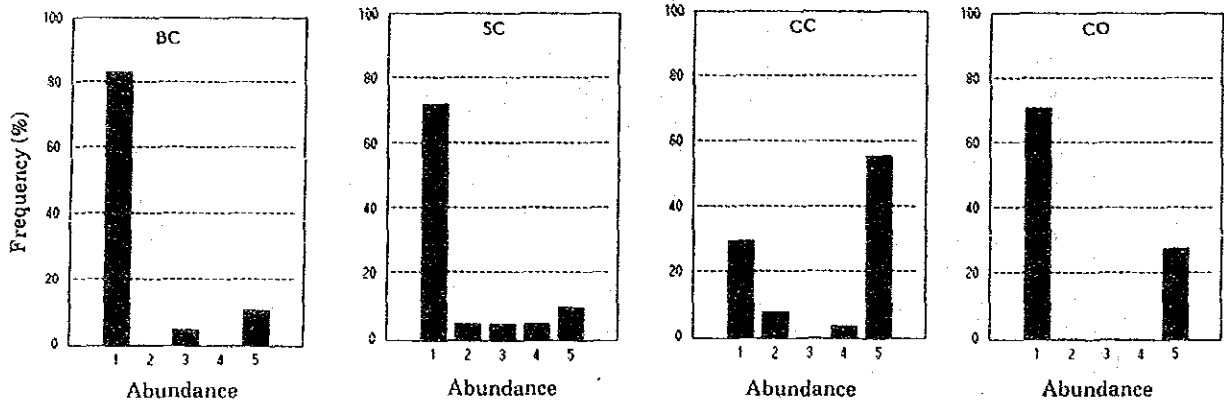
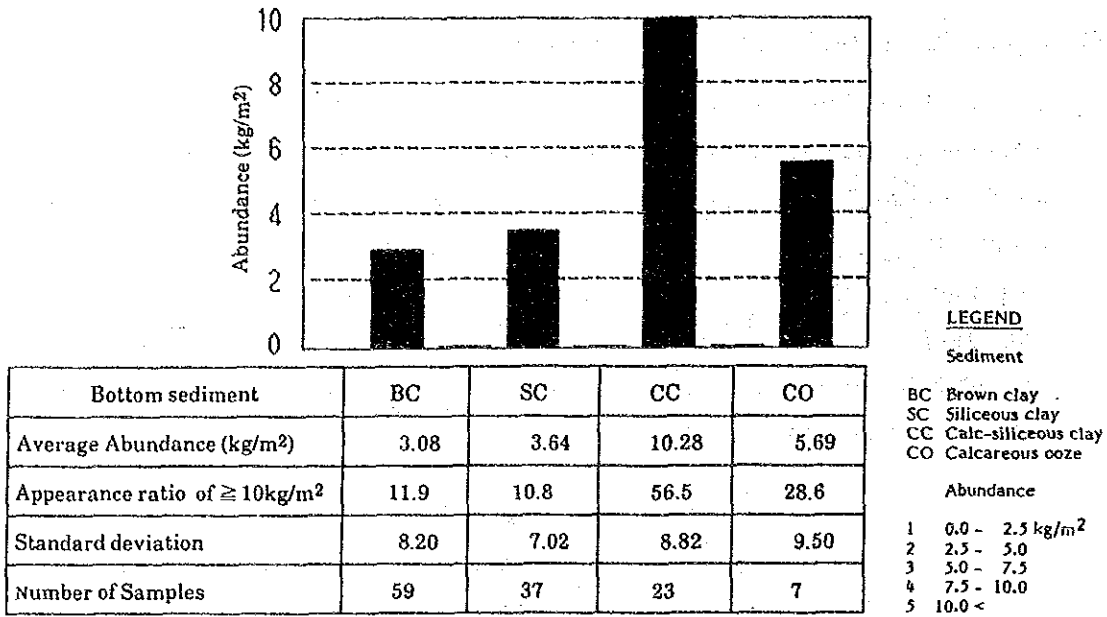


Fig. 3-5-24 Relation between Bottom Sediments and Manganese Nodules

calcareous-siliceous clay zone are low as 5kg/m^2 or less. The frequency diagram also shows the inclination toward $0 - 2.5\text{kg/m}^2$. Calcareous ooze, number of sampling points is few, so any conclusion cannot be done, but the tendency is shown similar to that of brown clay etc.

6) Observation Results by CDC

CDC-survey was executed in about 50 hours, from 7th Oct. to 9th Oct., end of 1st survey for sampling. During this term, 59.5 miles of length along two survey lines was surveyed and 32 observation points were taken by photograph, 161 pieces of sea

Table 3-5-10 Coverage and Abundance of Manganese Nodules at Each Station of CDC-Survey

Survey line 01			Survey line 02		
Station	Coverage ratio	Abundance	Station	Coverage ratio	Abundance
01-01	76.1	26.05	02-01	0	0
02	0.7	0.27	02	0	0
03	30.2	7.34	03	5.5	1.06
04	65.9	19.75	04	0	0
05	2.6	1.22	05	0	0
06	61.9	18.57	06	5.7	1.26
07	7.4	1.15	07	25.2	4.30
08	34.5	8.38	08	23.3	4.99
09	36.6	10.14	09	13.0	2.82
10	14.5	3.16	10	26.7	4.98
11	0.7	0.16	11	10.3	1.30
12	0	0	12	0.6	0.20
13	0	0	13	0	0
14	0	0	14	0	0
15	0	0			
16	13.5	2.33			
17	13.1	2.94			
18	28.8	3.85			
Average	21.5 %	5.85 kg/m ²	Average	7.9 %	1.14 kg/m ²

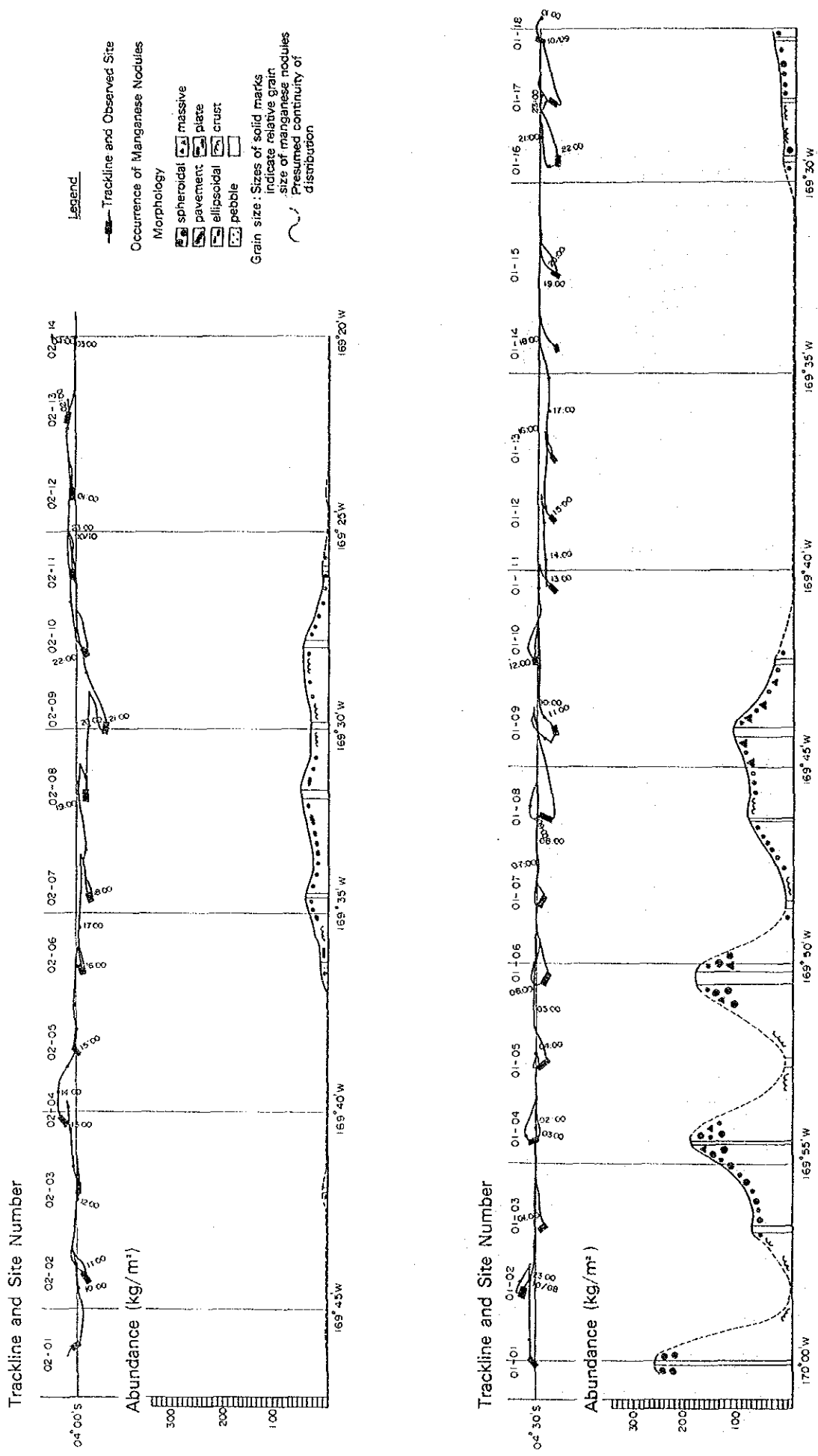


Fig. 3-5-25 Modified Occurrence of Manganese Nodules obtained by CDC survey

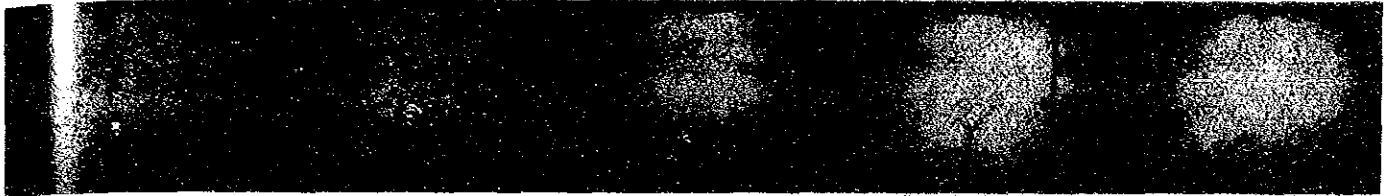
0101



20.4 (6.25) 25.9 (79.1) 25.5 (77.6) 30.0 (83.0) 28.4 (78.2)

Continuous distribution of spheroidal nodules with about 5 cm diameter.

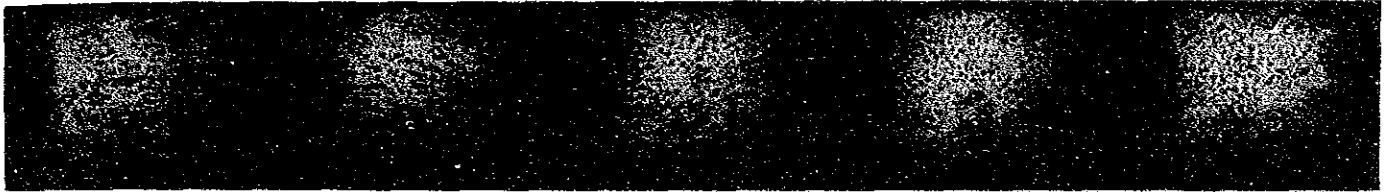
020



4.8 (28.6) 8.2 (41.9) 4.6 (27.2) 1.9 (12.8) 2.2 (15.7)

Pebbly nodules prominent. Mud-mound formed by benthic animals.

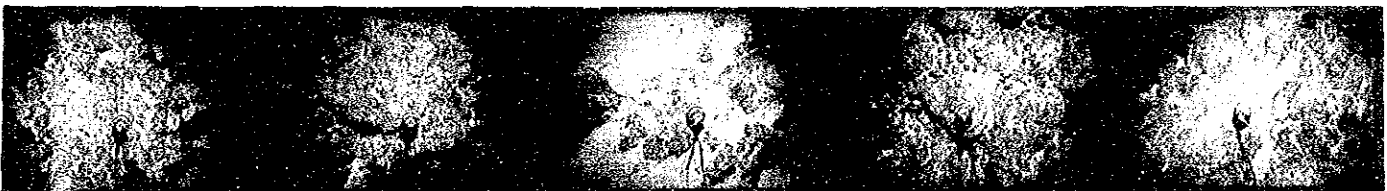
0109



6.8 (28.2) 11.0 (39.8) 11.9 (39.1) 10.8 (38.1) 10.2 (38.0)

Massive nodules with pebbly nodules mixture. Size is about 4 cm diameter

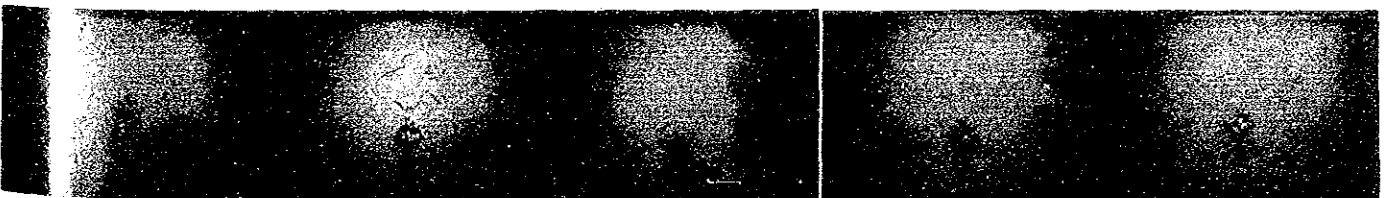
0214



-- -- -- -- --

Bed-rock exposure coated by thin crust.

011

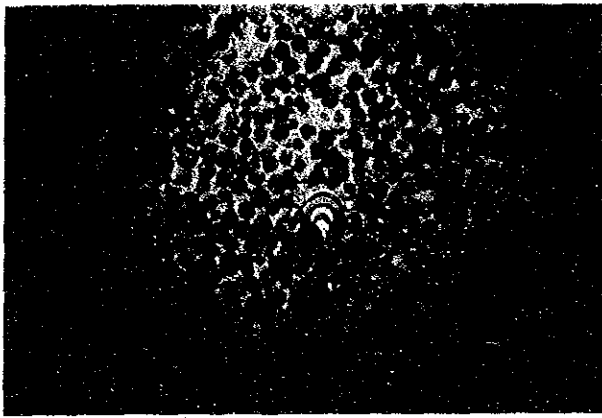


0.0 (0.0) 0.0 (0.0) 0.0 (0.0) 0.0 (0.0) 0.0 (0.0)

No nodules. Trace of benthic animals.

{ Numbers at leftside-up: Station number, at bottom left: abundance, and bottom right: coverage. }

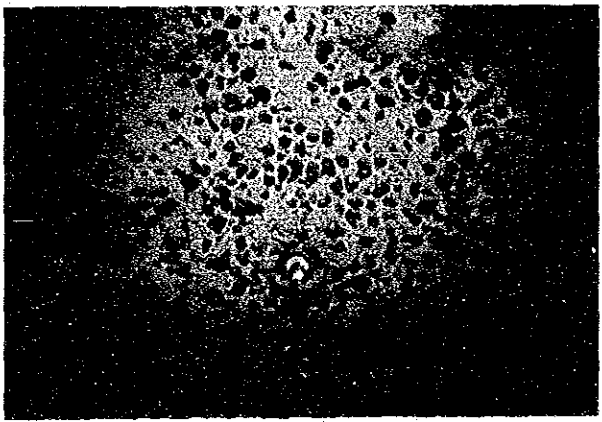
Fig. 3-5-26 Examples of Continuous Photos by CDC Survey



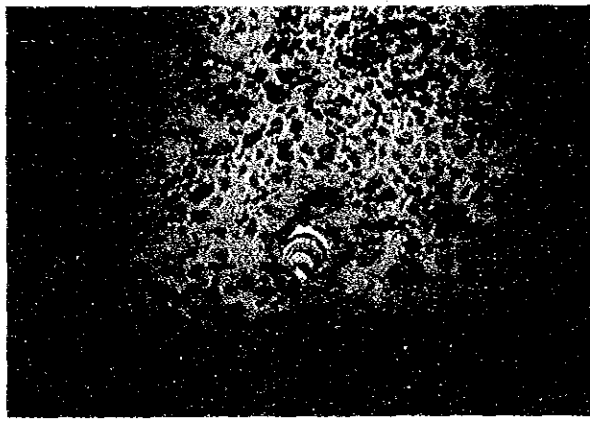
87SCDC0101
Spheroidal. Abundance: 30.0 Kg/m²



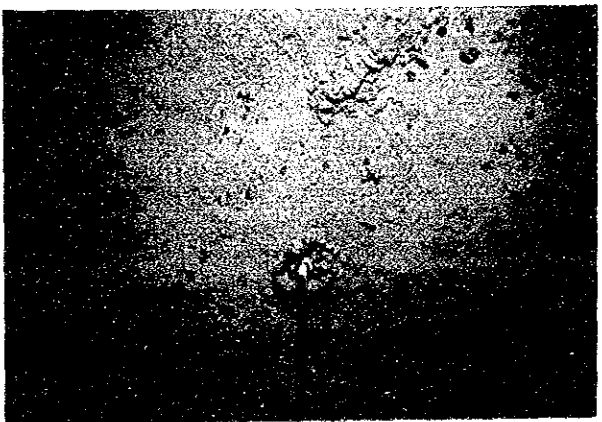
87SCDC0204
Mud.
Mud-mound formed by benthos



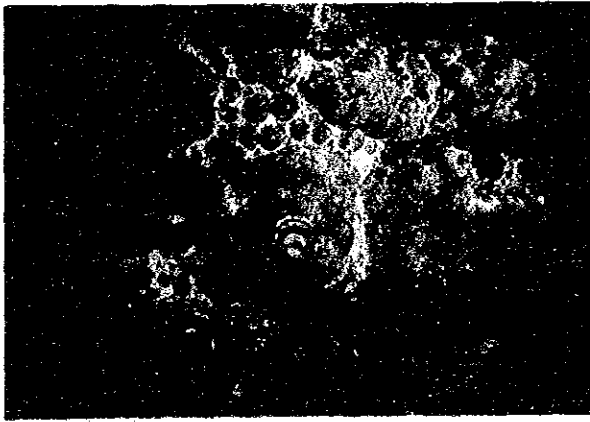
87SCDC0109
Pebble and Spheroidal
Abundance: 6.8 Kg/m²



87SCDC0207
Pebble. Abundance: 8.2 Kg/m²



87SCDC0111
Pebble. Abundance: 2.2 Kg/m²



87SCDC0214
Crust. Mud at hollows

Fig. 3-5-27 Examples of Photos by CDC Survey

bottom photo were obtained as a consequence.

(1) The observation result

Tab. 3-5-10 shows coverage (%) and abundance (%) calculated from sea bottom photo at all observation points. Fig. 3-5-25 shows the outline of abundance, morphology, particle size and presumptive continuity of distribution along each survey line. Fig. 3-5-26 and Fig. 3-4-27 show more detail conditions in representative observation points.

1 No. 1 survey line

The $169^{\circ} 24' W$ line divides high abundance zone in westward from low abundance zone in eastward. In westward, the manganese nodules are mainly spheroidal and massive type and pebble type is subsidiary. The diameter of nodules are 3 - 5cm. The growth of crust covered bedrock is observed in several points of west side (observation point 01 - 02, 5,547m water depth), but the nodules is changed to spheroidal and pebble (point 01 - 03, water depth 5,750m). Although westward is generally flacking in continuity, has high partial coverage as 35 - 76%, and is recognized having high abundance in comparatively deep point as 5,300 - 6,100m water depth. On the other hand, in eastward, the mud layer is observed, but the distribution of manganese nodules is not observed. The depth of water is 4,700 - 5,600m and the growth of crust covered rock is observed according as decreasing of water depth. The some traces indicating the movement of the life of sea-bottom are found in the mud prominent area. In No.1 survey line, the reversed phenomenon was observed between the results of FG sampling and the abundance by CDC photograph. This is mystereous phenomenon contrary to our previous expectation.

2 No. 2 survey line

The $169^{\circ} 32' W$ line divides the mud prominent zone in westward from the manganese nodules abundant zone. In westward, the several traces indicating the movement of the life of sea-bottom is observed in the mud prominent area. The manganese nodules are little observed except a small quantity of small-size pebble type. On the other hand in eastward, most of manganese nodules are 1 - 2cm diameter and the coverage is low as 10 - 25%, therefore abundance is also low in general. The manganese nodules are not found in the observation points at eastend (02 - 13, 02 - 14), because the

Table 3-5-11 Comparison of Abundance Obtained by FG Sampling and CDC Survey

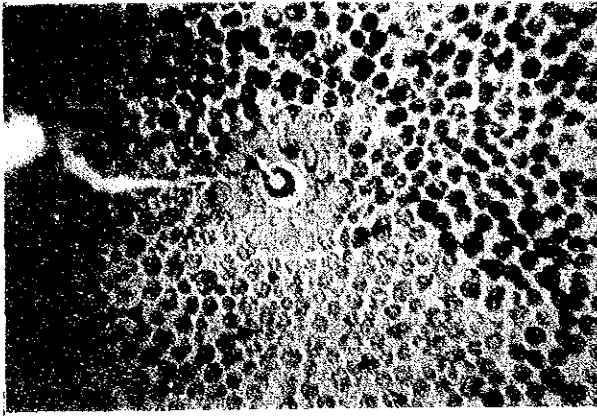
(kg/m²)

FG Sampling			CDC Survey		
Station	Sampling points	Average	Average	Observed points	Station
87440	0.00	3.92	26.05	20.25	01-01
	11.76			25.88	
	0.00			25.54	
				30.03	
				28.44	
87424	13.86	17.83	2.33	2.23	01-16
	25.90			4.82	
	13.74			3.88	
				0.70	
				0	
87425	29.81	11.43	2.82	3.23	02-09
	4.49			0	
	0			5.11	
				0.73	
				2.21	

area is changed from mud zone to rock zone, through the foot and the slope of sea-knoll. Accordingly, No.2 survey line is lacking in continuity of manganese nodules, and only low abundance zone is found.

(2) Comparison these results and those from FG Sampling

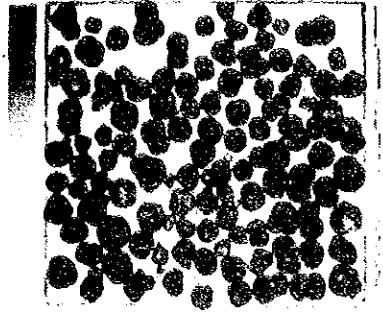
The comparison was made on the abundance got in this survey with the results obtained by FG sampling. This report picked up three observation points of CDC survey corresponding to the extent formed by three points (FG triangle having 2.1 mile long sides and 1.4 miles short side). Tab. 3-5-11 shows the result. This result shows that the value of abundance is reversed in No.1 surveying line as mentioned above and this is different from prospective view. In No.2 surveying line, the result of CDC survey correspond with the prospective value obtained by MFES, although a little difference is observed. Fig. 3-5-28 shows the representative photo of see bottom and on board FG sampling.



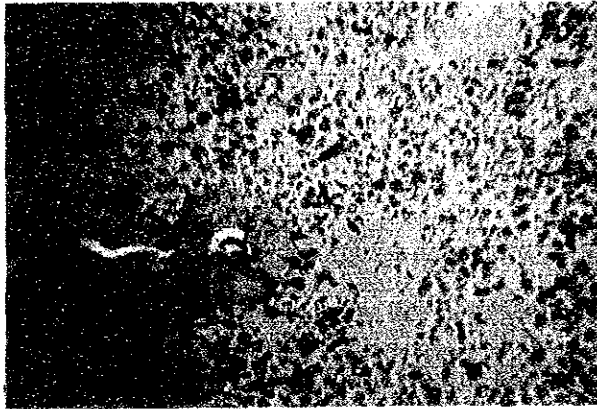
87S0570FG05 (Sea Bottom)

(Spheroidal. Coverage: 58.6%, Abundance: 25.90 kg/m²)

87S0570FG05 9.13



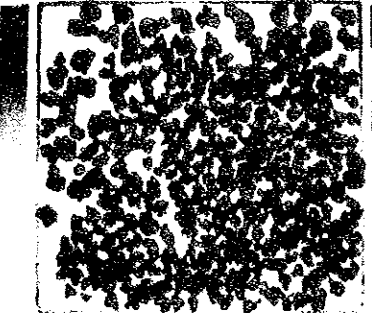
(Collected)



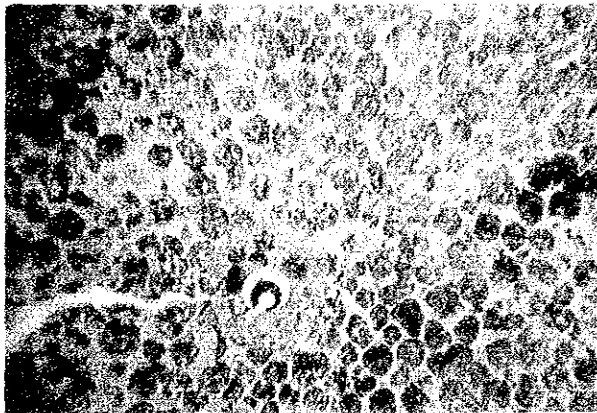
87S0570FG08 (Sea Bottom)

(Pebble. Coverage: 31.0%, Abundance: 13.80 kg/m²)

87S0570FG08 10.4



(Collected)



87S0570FG19 (Sea Bottom)

(Massive. Coverage: 71.3%, Abundance: 39.95 kg/m²)

87S0570FG19 10.6



(Collected)

Fig. 3-5-28. Comparison between Sea Bottom Picture and Collected Samples

7) Distribution of Metal Quantity

Considering manganese nodules as a useful ore reserve, it is necessary to consider not only the quantity of the manganese nodules per unit area, that is, coverage, but also the metal quantity included in the manganese nodules (specially Ni, Cu and Co). For Ni, Cu and Co, the metal quantity per unit area is calculated for each sampling point as in the following formulas with metal content value, and the results are described in Annexed Fig. 13 ~ 15.

- o Ni metal quantity per unit area = abundance x (1-water content ratio) x Ni grade
- o Cu = abundance x (1-water content ratio) x Cu grade.
- o Co = abundance x (1-water content ratio) x Co grade.

In this case, a cut-off value is not adopted to both of grade and abundance. The characteristics of distribution of metal quantity in the surveyed area is, as described below, the abundance of Ni, Cu and Co coincides with the distribution of abundance of manganese nodules.

(1) Ni (Annexed Fig. 13)

The sea area having Ni metal content more than 20g/m² are the following five.

- 1 The area encircled 1° 00' S, 3° 00' S, 169° 00' W and 171° 00' W.
- 2 The area between 4° 00' and 5° 00' S, and around 169° 30' W longitude line.
- 3 The area with 0° 00' S: 171° 00' W as the centre.
- 4 The area with 1° 00' S: 172° 00' W as the centre.
- 5 The area with 5° 00' S: 168° 00' W as the centre.

The total area is about 40,500km² containing more than 20g/m² of Ni in this sea area. The average abundance is 32.1g/m².

(2) Cu (Annexed Fig. 14)

The sea area having more than 20g/m² of Cu metal contents correspond with the abundance area of Ni as above-mentioned. The total area is about 34,500km² containing more than 20g/m² of Cu. The average abundance is 30.9g/m².

(3) Co (Annexed Fig. 15)

1 The area between $4^{\circ} 00' S$ and $5^{\circ} 00' S$, and around $169^{\circ} 30' W$ longitude line.

2 The area with $3^{\circ} 00' S$: $169^{\circ} 00' W$ as the centre.

3 The area with $5^{\circ} 00' S$: $168^{\circ} 00' W$ as the centre.

The total area is about $11,700\text{km}^2$ containing more than $20\text{g}/\text{m}^2$ of Co in this sea area. The average abundance is $40.8\text{g}/\text{m}^2$.

3-6 Conclusion and Problems

The following three points are the characteristics of the manganese nodules bearing in this sea area.

- (1) The continuity of distribution is extremely bad.
- (2) The abundance is high in the depth of 5,000 - 5,200m, on the contrary it suddenly decrease in the depth of more than 5,400m.
- (3) The occurrence and the type of manganese nodules are different in the northern part and in the southern part of the sea area. The so-called "rough" types are abundant in northern part and the so-called "smooth" type are abundant in southern part. These characteristics are accepted as the phenomena reflecting the situation of the sea floor topography and the condition of sedimentation in this sea area. In regard to (1), the primary factor is the sea floor topography which has a plenty undulations through all area coexisting with trough, ridge, seamounts, atolls lot of sea knolls and hilly province. The sea floor topograph have rise and fall even in the deep-bottom area excluding the zone having sea knoll or hilly province, excepting the zone of slightly continuous transparent layer in the north end of surveyed area. This is considered as the reason of altering the abundance of manganese nodules largely even in the nallow area composed by three sampling points very near each other. This instability of the sea floor topograpy are reflected on the distribution of transparent layer and of SBP. In general, the rather thin transparent layer which is convenient for the growth of manganese nodules is restricted within narrow area, on the other hand, the d_1 , d_2 and d_s in SBP type are developed widely. In regard (2), it is considered that the CCD (Carbonate Compensation Depth) is about 5,200m in this sea area. In general, it is considered that the high abundance zone of manganese nodules is situated around lithocline level or below the CCD (Carbonate Compensation Depth) (D.S. Cronan 1984, et al). The phenomena of this sea area can be regarded as being in accord with those considerations. Although the topographic conditions are bad, the high abundance zones are observed in sea-knoll and hilly province, these results can be illustrated by the water depth close to CCD. On the contrary, the primary cause of inferiority of manganese nodules in this area depends largely on the water depth more than 5,400m at wide area, and the instability of topographical conditions. In regard

to the reason of (3), it is considered the biological productivity has the difference between south part and the north part. (Cronan, 1984) The northern half part of the area belongs to the extent of high productivity of $50\text{gc}/\text{cm}^2\cdot\text{y}$, but the productivity decreases toward south. On the other hand, it is assumed that the Antarctic bottom current coming from the south goes up to the north along southern part of the area to the elevation of the south fringe of Nova Canton Trough and turns to north-eastward. (Lonsdale and Smith, 1980). This streamline acts on decreasing of supply deposits on the sea bottom. Accordingly, the difference of the sedimentation velocity is made in the south and in the north divided by Nova Canton Trough as the barrier, this is appeared in the distribution of transparent layer and in the types of bottom materials. Also the following are considered, type "r" of manganese nodules being buried one are formed in the northern part having relatively large sedimentation velocity, on the contrary type "s" of nodules being exposed one are formed in the southern part. In practice, in addition to the location, the formation of nodules are will be affected by the topographical conditions, type "s" is formed in the shallower convexed place such as sea knoll and hilly province and type "r" is formed in concaved place. The similar distributions tendency of type "r" and type "s" are shown in the report Usui et al (1983). The characteristics of occurrence of manganese nodules are considered as the results of the combined effects of above-mentioned three factors.

Chapter 4. Results of the Survey • II (Cobalt Crust)

4-1 Seamount Topography

1) Classification of Seamounts and Topography

Seamounts are classified by their morphology as Table 4-1-1.

Table 4-1-1 Classification of Topographic Type of Seamount

Classification	Morphological characteristics
Single seamount guiyot	The summit is flat and horizontal.
Round top seamount	The summit is roundish.
Inclined top seamount	The summit is flat, but not level.
Peaked seamount	The summit is sharp.
Combined seamount	The seamount which has more than 2 above mentioned characteristics (including the originally complexed seamount).
Atoll	The summit reaches the surface of the sea and forms atoll.

The seamounts surveyed in this time are 2 atolls and 4 sharp ridges. Although one of these seamounts is topographically independent, it is described as a part of SA03 seamount. A seamount topography is roughly divided into "Top" and "Slope", which are subdivided as follows in order to facilitate the description;

Table 4-1-2 Classification of Topography of Seamount

	Classification	Topographical characteristics
The top	Central part	The area where the center of the summit is flat or gently inclined.
	Margine	The transitional zone from the central part of the top to the upper part of the slope.
The slope	Upper part	The area where the upper part of the slope is steep. (The water depth is shallower than 2,000m)

Middle part	The area between the upper and the lower part of the slope. The slope is medium. The water depth is between 2,000 and 3,000m.
Lower part	The area where the lower part of the slope is gentle. The water depth is more than 3,000m.

In the seamounts survey for cobalt crusts, the area of which water depth is less than 3,000m is the main target. Accordingly, the vessel navigated so that the echo survey (topographical measuring) may be carried out densely on the top and the upper - middle part of the slope, and roughly on the lower part of the slope. And for the safety of the navigation, the survey in the atoll was not carried out in the area shallower than 1,000m. Generally, the central part of the top is flat or gently inclined and has a distribution of granule sediment in a quite limited part according to the SBP record. On the other hand, its shallower part presents a highly undulating and complicated topography. In the convex part, rock is directly exposed, while, in the concave part, distribution of big pebble-small pebble is expected. The transformation of the cant of the slope is shown in the topographical map of the sea bottom and the table of the topographical characteristics. The upper part of the slope has the steepest cant which is inclined at an angle of 19° - 23° on average and its middle part still has considerable steep cant which is inclined at an angle of 15° - 22° on average, but in its lower part, its cant becomes considerably gentle and its inclined at an angle of 7° - 16° on average.

2) Topographical Features of Seamounts

Topographical characteristics of the seamounts SA01-SA05 are shown in the Table 4-1-3. Topographical plans and cross sections of seamounts are shown in Annexed Fig. 17(1)(2)(3)(4) and their bird's eye view is shown in Fig. 4-1-1. The topographical characteristics of seamounts are as follows.

(SA01 Seamount)

The water depth of the top shows a slightly deep figure of 1,640m. It is a peaked seamount, with a peak having an extent of 3x14km and a height of 3,600m. The seamount stretches long and narrow in the direction of NNE-SSW, its long axe lies in the direction of N10E (Ref. Annexed Fig. 17(1)). A peak type topography is not observed on the summit nor on the shoulder. The slightly convex area develops at

the upper and middle part of the slope. The cant of the slope is 13° on average and that of western part of the slope is $15^\circ - 18^\circ$, which is slightly steep. The acoustic transparent layer by means of SBP shows a maximum thickness of 70m at the plain stretching on the ridge of the summit.

(SA02 Seamount; Sydney Island or Manla atoll)

The dimensions of the atoll are 2×2 km. It forms a circular shape with a radius of 20km at the depth of 5,000m. The convexed parts are observed at an interval 400-500m on the slope deeper than 1,000m. The average cant of the slope is 15° and it become gentle, dropping down to 11° , at the lower part of slope, deeper than 3,500m. An acoustic transparent layer by means of SBP is rarely observed and it is to be judged that sediments are a little (Cf. Annexed Fig. 17(2)).

(SA03 Seamount; Pheonix Island)

It is a complex seamount found as a combination of an atoll and a seamount. The size of the atoll (Pheonix Island) located in the north-west is 2.5×2.5 km² and the extent of the top is 4×3 km² and the long axis direction is N50W. The cant of the slope is slightly steep, showing an angle of 15° . The seamount located in the south-west is a peak seamount of which water depth to the summit is 1,030m and the height is 4,170m. The direction of long axis is N60E. The cant of the upper part of the slope is steep and at an angle of 20° (Ref. Annexed Fig. 17(3)). The transparent layer by means of SBP is not observed at these seamounts and the sediments are a little.

(SA04 Seamount)

It is a seamount which was newly discovered in this survey. It is a peaked seamount of which water depth to the summit is 1,040m and the extent of the summit is 3×3 km² and the height is 4,360m. The direction of long axis is N70W having the topography as showing the gap from east to west. The cant of the slope is steep at an angle of $21^\circ - 24^\circ$ at the upper and middle part of the slope and it is gentle at angle of $10^\circ - 15^\circ$ at the lower part of the slope. The convexed area and the steep profile area is spreading. (Ref. Annexed Fig. 17(4))

(SA05 Seamount)

It is a seamount which was newly discovered in this survey. It is a peaked seamount of which water depth to the summit is 1,170m and the extent of the summit is 2×2 km and the height is 4,230m. The cant of the slope is steep at an angle of $21^\circ -$

Table 4-1-3 Topographic Feature of Individual Seamount (1)

Seamount	Macroscopic Topography	Microscopic Topography
SA01	<p>Location 5° 37' S, 170° 14' W</p> <p>Type Peaked seamount</p> <p>Scale*1 37 x 15 km</p> <p>Range of Water Depth 1,600 - 5,000m</p> <p>Size of Top 3 x 14 km*5</p> <p>Inclination of Slope</p> <p>Upper part*2 140 ± 60</p> <p>Middle part*3 130 ± 50</p> <p>Lower part*4 110 ± 50</p> <p>Others Direction of the major axis N10° E</p>	<p>SBP Data</p> <p>Many side-echo, acoustic transparent layer is observed on a part of the ridge. The maximum thickness 70m.</p> <p>Area (Water Depth)</p> <p>less than 3,000m 376km²</p> <p>less than 2,000m 23km²</p> <p>2,000 - 2,500m 155km²</p> <p>2,500 - 3,000m 198km²</p> <p>Others Western slope is steep, eastern slope is gentle.</p>
SA02	<p>Location 4° 27' S, 171° 15' W</p> <p>Type Atoll</p> <p>Scale*1 21 x 19 km</p> <p>Range of Water Depth 0 - 5,000m</p> <p>Size of Top 8 x 8 km*6</p> <p>Inclination of Slope</p> <p>Upper part*2 190 ± 60</p> <p>Middle part*3 150 ± 40</p> <p>Lower part*4 110 ± 50</p> <p>Others Nearly cone</p>	<p>SBP Data</p> <p>Acoustic transparent layer is not observed.</p> <p>Area (Water Depth)</p> <p>less than 3,000 311km²</p> <p>less than 2,000 105km²</p> <p>2,000 - 2,500m 86km²</p> <p>2,500 - 3,000m 120km²</p> <p>Others It cannot be surveyed between the top - 1,000m in water depth. Details are unknown. Atoll is confirmed. There is inner lake.</p>
Island east side of SA03	<p>Location 3° 43' S, 170° 43' W</p> <p>Type Atoll</p> <p>Scale*1 24 x 19 km</p> <p>Range of Water Depth 0 - 5,000m</p> <p>Size of Top 4 x 3 km*6</p> <p>Inclination of Slope</p> <p>Upper part*2 190 ± 30</p> <p>Middle part*3 140 ± 30</p> <p>Lower part*4 130 ± 30</p> <p>Others Direction of the major axis N50° W</p>	<p>SBP Data</p> <p>Many side-echo. Acoustic transparent layer is not observed.</p> <p>Area (Water Depth)</p> <p>less than 3,000 349km²</p> <p>less than 2,000 102km²</p> <p>2,000 - 2,500m 92km²</p> <p>2,500 - 3,000m 155km²</p> <p>Others It cannot be surveyed between the top - 1,000m in water depth. Details are unknown. Atoll is confirmed. There is inner lake.</p>

- *1 Contour line at 3,000m in water depth
- *2 1,000 - 2,000m in water depth
- *3 2,000 - 3,000m in water depth
- *4 3,000 - 4,500m in water depth
- *5 less than 2,000m in water depth
- *6 less than 1,000m in water depth

Table 4-1-3 Topographic Feature of Individual Seamount (2)

Seamount	Macroscopic Topography	Microscopic Topography
Seamount west side of SA03	<p>Location 30° 53' S, 170° 56' W</p> <p>Type Peaked seamount</p> <p>Scale*1 14 x 9 km</p> <p>Range of Water Depth 1,000 - 5,000m</p> <p>Size of Top 3 x 2 km*5</p> <p>Inclination of Slope</p> <p>Upper part*2 200° ± 30°</p> <p>Middle part*3 120° ± 30°</p> <p>Lower part*4 70° ± 20°</p> <p>Others Direction of the major axis N60° E</p>	<p>SBP Data</p> <p>Acoustic transparent layer is not observed.</p> <p>Area (Water Depth)</p> <p>less than 3,000m 112km²</p> <p>less than 2,000m 23km²</p> <p>2,000 - 2,500m 39km²</p> <p>2,500 - 3,000m 50km²</p> <p>Others The top shows peaked shape.</p>
SA04	<p>Location 00° 38' S, 171° 00' W</p> <p>Type Peaked seamount</p> <p>Scale*1 18 x 13 km</p> <p>Range of Water Depth 1,000 - 5,000m</p> <p>Size of Top 3 x 3 km*5</p> <p>Inclination of Slope</p> <p>Upper part*2 230° ± 70°</p> <p>Middle part*3 220° ± 70°</p> <p>Lower part*4 160° ± 70°</p> <p>Others Direction of the major axis N70° W</p>	<p>SBP Data</p> <p>Acoustic transparent layer is not observed.</p> <p>Area (Water Depth)</p> <p>less than 3,000m 150km²</p> <p>less than 2,000m 36km²</p> <p>2,000 - 2,500m 51km²</p> <p>2,500 - 3,000m 63km²</p> <p>Others The top shows peaked shape.</p>
SA05	<p>Location 00° 36' S, 170° 35' W</p> <p>Type Peaked seamount</p> <p>Scale*1 13 x 13 km</p> <p>Range of Water Depth 1,000 - 5,000m</p> <p>Size of Top 2 x 2 km*5</p> <p>Inclination of Slope</p> <p>Upper part*2 240° ± 60°</p> <p>Middle part*3 210° ± 40°</p> <p>Lower part*4 160° ± 40°</p> <p>Others Star shape. Its ridges spread into five directions.</p>	<p>SBP Data</p> <p>Acoustic transparent layer is not observed.</p> <p>Area (Water Depth)</p> <p>less than 3,000m 99km²</p> <p>less than 2,000m 20km²</p> <p>2,000 - 2,500m 27km²</p> <p>2,500 - 3,000m 52km²</p> <p>Others The top shows peaked shape.</p>

- *1 Contour line at 3,000m in water depth
- *2 1,000 - 2,000m in water depth
- *3 2,000 - 3,000m in water depth
- *4 3,000 - 4,500m in water depth
- *5 less than 2,000m in water depth
- *6 less than 1,000m in water depth

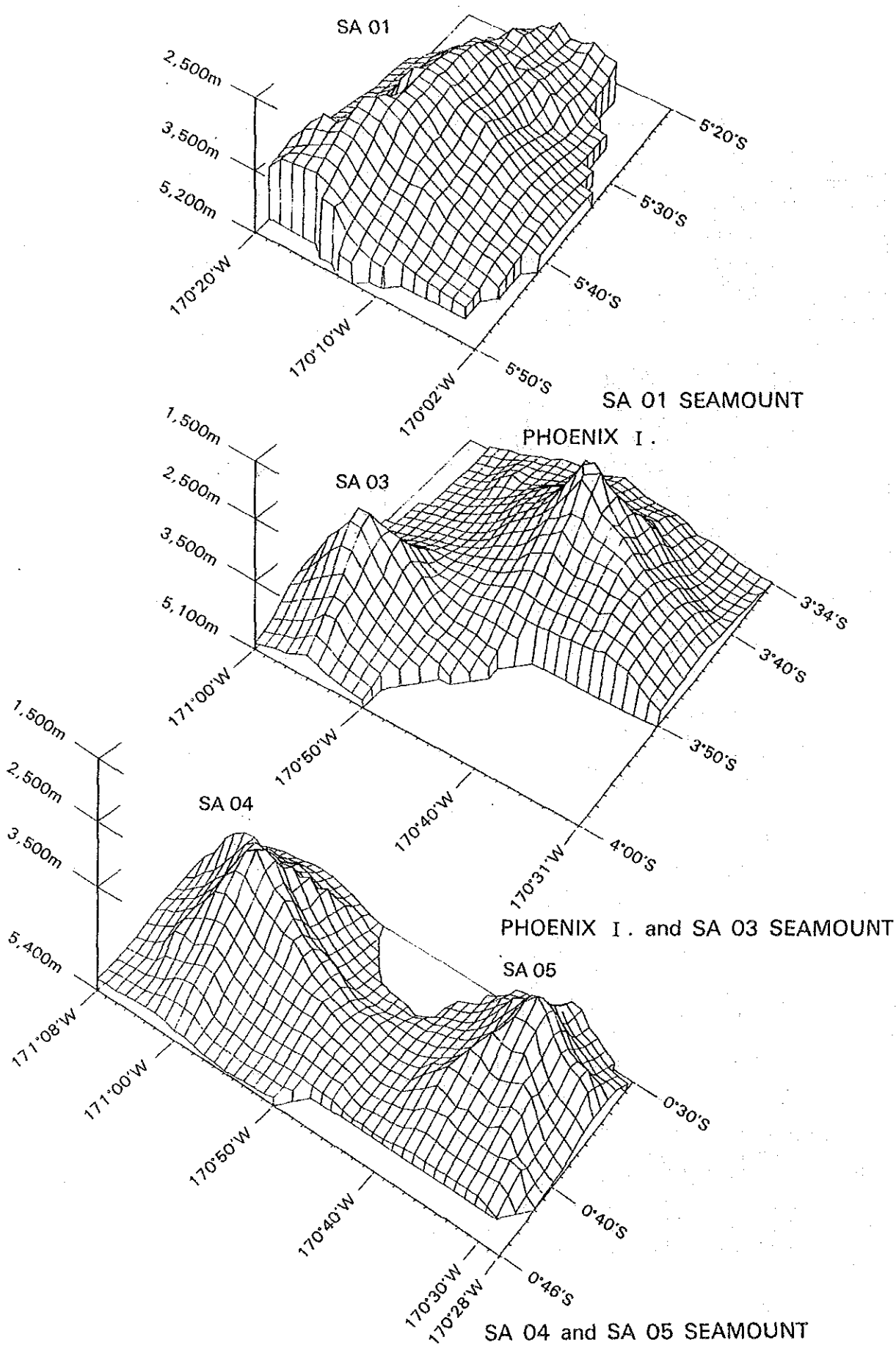


Fig. 4-1-1 Bird's-eye View of Seamounts

24° at the upper part of the slope and gentle at an angle of 10°-15° at the lower part of the slope. (Ref. Annexed Fig. 17(4))

4-2 Seamount Geology

1) General Geology of Seamounts

The geology of 5 seamounts is commonly composed of basalt lava and basaltic volcano clastic rocks, and there is difference in the growing speed of limestone whether it is the island of which summit is on the surface of the sea or under the surface of the sea. At the 2 islands (SA02 = Sydney Island and the eastern island = Phoenix Island) the ubiquitous reef coral limestone develops spreads over from their summit to the upper and middle part of the slope. The limestone is collected at 7 points of 8 dredge sampling points at the SA02 and it seems that the mix of the rocks other than limestone is extremely rare and the whole of the slope is covered with the limestone. However, judging from the fact that there is a place collected only basalt with certain crusts, there seems to be a place where the basaltic base exposes such as topographically convexed area. It seems that the almost whole of the slope is covered with limestone upto about 2,000m of water depth at the eastern island of SA03. On the other hand, basalt and phosphatized rocks become abundant in collected samples at the middle part of the slope, so that the part covered with limestone becomes a few. As mentioned above, there is a difference between the coverage of the limestone even in the same island, and this is presumed to result from the difference of the quantity of the creation of the reef coral limestone due to the distinction of the extent of the island. It is difficult to discriminate the native reef coral limestone from a collapse rock dropping from the upper part of the slope. The area which a native limestone grows up is considerably shallower than the zone of the above mentioned water depth because judging from the shape and size of the samples, the majority of samples seems to be a debris. On the other hand, judging from the collected ratio of the samples in the seamounts under the surface of the sea (the western seamount of SA01, SA03, SA04 and SA05), it seems that the limestone grows up quite partially. Except the limestone collected on the neighbourhood of the summit of SA01 and SA05 seamount, all samples of the 2 other seamounts were collected at the middle and lower part of the slope and were a collapse. It cannot judge wether the native limestone grows up at the neighbourhood of the summit of these seamounts or not. It is worth to notice that the coral limestone is left on some spots at these considerably washed out seamount. The development of the phosphatized rock is interesting. The rock was observed at all

limestone is left on some spots at these considerably washed out seamount. The development of the phosphatized rock is interesting. The rock was observed at all seamounts except SA02. There are a few examples as purely phosphatized rock was collected, and it almost constitutes the matrix of the basaltic volcano clastic rock or it is phosphatized at the surface of the limestone. The distribution area of this rock in every seamount ranges from the top to the middle or lower part of the slope. At the seamounts having less limestone and more basalt and the basaltic clastic rock, phosphatized rocks is more observed and sampling ratio is high. Judging from the whole mode of occurrence, this rock generally seems to be abundantly produced between the top and the upper part of the slope. Subject to the matter which may relate to the creation of the cobalt crusts, we mentions in the next paragraph. The basalt and the basaltic volcano clastic rock as base rock of all seamounts are massive lava, pillow breccia, hyaloclastite and talus debris etc as the mode of occurrence. There is partially a stratified rock considered as the marginal phase. The other characteristics are as follows.

- (1) The comparatively fine clastic rock such as the hyaloclastite etc. are generally developed on the topographically steep top.
- (2) The vesiculation degree is generally both in the lava and volcano clastic rocks. Generally it is 10-15%, but some of them reach to 70%.
- (3) Talus debris is observed everywhere.

Covering the above mentioned rocks, the foraminifera sand spreads over everywhere. These rocks lay thickly on the ridge of the topographically plain seamount and the concaved part of the slope and the gentle slope of the lower part of the slope, and also they lay even on the steep slope thinly, too. According to the SBP survey, the acoustic transparent layer is affirmed to reach about 70m on the ridge of SA01 seamount. It continuously distributes along the ridge at the interval of 3 miles north and south, and 0.5-1.0 mile west and east. Judging from the ripple mark spreading there, the direction of the bottom current is toward west. The outline of the geology in each seamount is shown in Tab. 4-2-1.

2) Description of Substrates of Cobalt crusts

The results of macroscopic characteristics and microscopic observation concerned with the kind of various rocks are shown in Tab. 4-2-2. The microscopic photos are shown in Fig. 4-2-2. The mineral composition is shown in Tab. 4-2-3. The principal chemical composition is shown in Tab. 4-2-4.

Table 4-2-1 Geology of Individual Seamount (1)

SA01	<p>(Type and Distribution of Rocks)</p> <p>Basalt : Whole area</p> <p>Pyroclastic rock : Whole area</p> <p>Limestone : Abundant on the eastern slope? (upper part - lower part)</p> <p>Phosphate rock : Abundant on the top and upper part of the slope. Occur as matrix of clastic rock on lower part of the slope. Other calcareous sand stone, etc.</p> <p>Foraminifera sands: Almost whole area, abundant on the ridge.</p>
	<p>(SBP Data)</p> <p>Acoustic transparent layer spreads on a part of top ridge. Maximum thickness 70m.</p> <p>(Other Data) By FDC observation</p> <p>The prominent foraminifera sand spreads on the top ridge. The direction of the bottom current is westward according to the ripple mark. The thin foraminifera sands spreads on crust in various places in the slope.</p>
	<p>(Characteristics)</p> <p>Basalts are massive type or pillow breccia type, and they are mostly vesicular (porosity: maximum 50%). Pyroclastic rocks are mainly hyaloclastite, changing into tuff with bedding in southern part. The lowest distribution limit of reef coral is approximately 2,200m in water depth.</p>
SA02	<p>(Type and Distribution of Rocks)</p> <p>Basalt : Almost whole area except top. Covered with clastic limestones in almost whole area. A few samples are obtained on middle and lower part of the eastern slope.</p> <p>Pyroclastic rock : Various places? Only a few samples are obtained on the middle part of the slope.</p> <p>Limestone : Cover the basement in almost whole area.</p> <p>Foraminifera sands: Various places.</p>
	<p>(SBP Data)</p> <p>Acoustic transparent layer is not observed.</p> <p>(Other Data) By Radar observation</p> <p>The atoll forms a lozenge shape in the exterior part and its each side is about 2 miles. The lagoon is independent of outer sea, so that the surface water is considered fresh water?</p>
	<p>(Characteristics)</p> <p>Limestones are block type or fragment type clastics of the reef corals. On the skirts of seamount, limestones are scarce? Coral limestones which are considered older occur on the same skirts.</p>

Table 4-2-1 Geology of Individual Seamount (2)

East-side Island of SA03	<p>(Type and Distribution of Rocks)</p> <p>Basalt : Whole area except top. Samples are obtained at only two points on the middle part of the slope.</p> <p>Pyroclastic rock : A sample is obtained at the middle part of the western slope.</p> <p>Limestone : Almost whole on the upper part of the slope. Various places on the middle part of the slope.</p> <p>Phosphate rock : The surface and matrix of basalt on the middle part of the slope.</p> <p>Foraminifera sands: Various places.</p>
	<p>(SBP Data)</p> <p>Acoustic transparent layer is not observed.</p> <p>(Other Data) By Radar observation</p> <p>The island forms an ellipse in the exterior part and its major axis is 0.8km. Its top is flat and there is no inner lake.</p> <p>(Characteristics)</p> <p>Reef limestone clastics are abundant on upper part of the slope. On middle and lower part, basalt basement crops out.</p> <p>Basalts are block type or pillow type, and their porosity indicates 20 -30%. The porosity decreases toward lower part of the slope.</p>
	<p>(Type and Distribution of Rocks)</p> <p>Basalt : Whole area.</p> <p>Limestone : A sample is obtained at 2,900m in water depth on the eastern side.</p> <p>Phosphate rock : Generally occur on the top and upper - middle part of the slope.</p> <p>Foraminifera sands: Various places.</p>
West-side Seamount of SA03	<p>(SBP Data)</p> <p>Acoustic transparent layer is not observed.</p> <p>(Other Data) By FDC observation</p> <p>Thin foraminifera sands spreads on steep slope between the top and upper part of the slope.</p>
	<p>(Characteristics)</p> <p>Basalts are all lava, and pyroclastic rock is not sampled. Phosphate rocks are prominent. Limestones are scarce.</p>

Table 4-2-1. Geology of Individual Seamount (3)

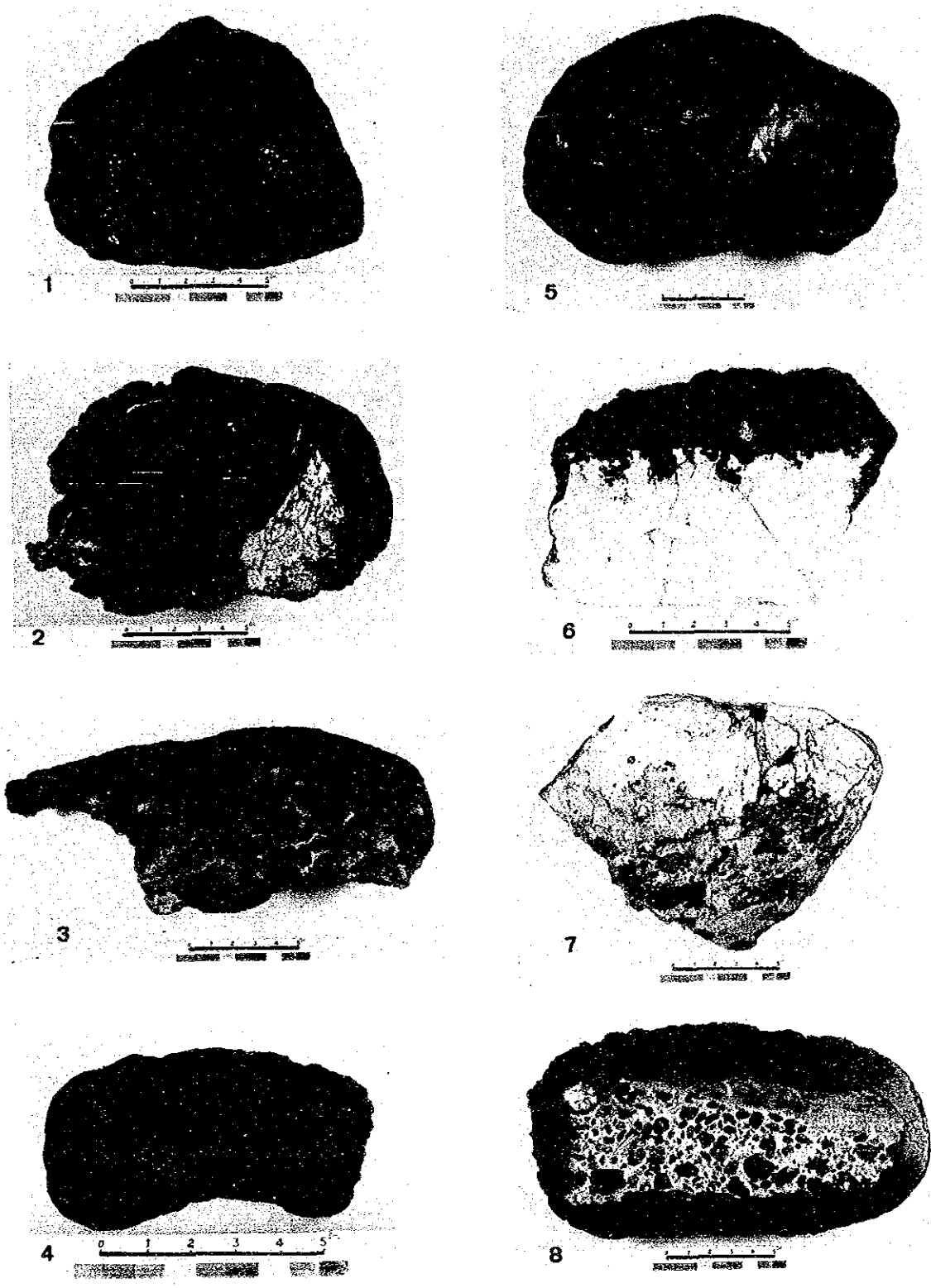
SA04	<p>(Type and Distribution of Rocks)</p> <p>Basalt : Whole area.</p> <p>Pyroclastic rock : Various places.</p> <p>Limestone : Little samples are obtained on middle of the slope.</p> <p>Phosphate rock : Occur on various places as matrix of pyroclastic rocks, the core of cobble crusts and the network in the crusts.</p> <p>Foraminifera sands: Various places.</p> <p>(SBP Data)</p> <p>Acoustic transparent layer is not observed.</p> <p>(Other Data)</p> <p>Nothing.</p> <p>(Characteristics)</p> <p>Basalts are lava, pillow and hyaloclastite. The porosity indicates high value, 70% at 1,700m in water depth, and 30% at 3,000m. The diameter of the vesicles are 1 - 5mm. The growth of phosphate is observed even at the deepest sampling point (3,200m in water depth).</p>
SA05	<p>(Type and Distribution of Rocks)</p> <p>Basalt : Whole area.</p> <p>Pyroclastic rock : Various places? (a few samples)</p> <p>Limestone : Phosphatized. Sampled on upper part of the slope.</p> <p>Phosphate rock : Above-mentioned. The others grow in the matrix of pyroclastic rocks, or the vesicles in basalts.</p> <p>Foraminifera sands: Various places</p> <p>(SBP Data)</p> <p>Acoustic transparent layer is not observed.</p> <p>(Other Data)</p> <p>Nothing.</p> <p>(Characteristics)</p> <p>Basalts are lava, pillow breccia and hyaroclastite.</p>

Table 4-2-2 Description of Substrates of Cobalt Crusts (1)

Basalt	<p>(Macroscopic Observation)</p> <p>Block lava, pillow lava, breccia, pillow breccia, hyaloclastite and fine-grained stratified rock like tuffite are observed; however, the rocks after breccia are classified into pyroclastic rock. Lava is mainly vesicular and partially compact. Generally, vesicles of 1mm - 5mm in diameter account for 10% - 50% and 70% at maximum. Most of samples are weathered at subaqueous condition and brownish.</p> <p>Watermelon-shaped rock fragments (SA05 AD03) and bulbous pillow buds (SA04AD10) are observed. The block of Pillow lava containing them has chilled margin. Weathered plagioclase is observed as a phenocryst at up to 20% in mode. Many vesicles are filled with calcite and phosphatic minerals. The variation of porosity by the water depth is observed (SA04).</p>
	<p>(Microscopic Observation)</p> <p>Lithologic character is the same as above-mentioned basalt; however, the porosity generally indicates high: 30 - 70%. The vesicles are filled with calcite and zeolite. Iron oxides occur remarkably. The matrix of rock fragments mostly consists of phosphatized (collophaned) foraminifera limestone, especially in the contact part with the crusts.</p>
Pyroclastic rock	<p>(Macroscopic Observation)</p> <p>The rocks classified into this type are close to above-mentioned lava. Hyaloclastite is mainly observed. Generally, they consist of basaltic and brecciated or irregular shaped fragments. The porosity of the fragments indicate high value (30% - 50%). The matrix is filled with basaltic fine-grained rocks and calcareous or phosphate rocks. The rock like tuffite consisting of only fine-grained glasses is observed (SA04CB09)</p>
	<p>(Microscopic Observation)</p> <p>Both olivine and clinopyroxene or each one occur as phenocrysts. Groundmass shows intersertal texture consisting of plagioclase, clinopyroxene, olivine, glass, ilmenite, etc. Orthopyroxene can not be observed in phenocrysts and groundmass. Chlorite, zeolite, calcite and iron oxide are observed as alteration minerals. Most of samples undergo alteration (submarine-weathered); however, very fresh rock fragments are observed barely. (87SA04-AS04, etc.)</p>

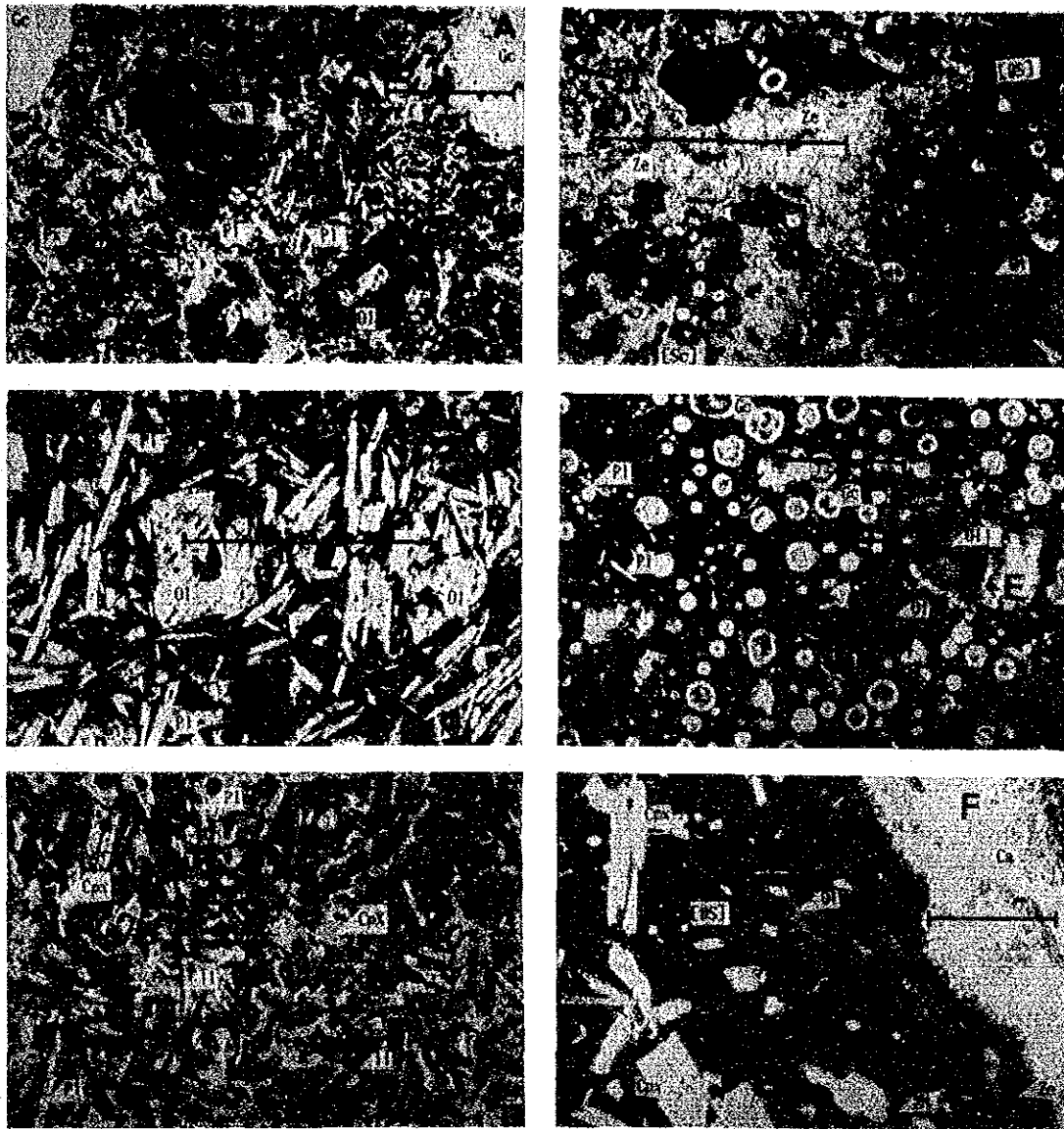
Table 4-2-2 Description of Substrates of Cobalt Crusts (2)

Limestone	<p>(Macroscopic Observation)</p> <p>Limestones are classified into two groups. One consists of coral fossils while the other consists of fine-grained fossils and is more compact. The former is the single or the mass of various shaped coral fossil. The latter, the texture of the fossil is neither clear nor vesicular. It is observed that the oxide coated one grows more conspicuously on the later even in the same sample group (SA02AD04).</p> <p>Therefore, the latter is considered older in a creation age than the former. Calcareous rocks are more whitish than phosphate rocks, and they grow foams by hydrochloric acid conspicuously.</p>
	<p>(Microscopic Observation)</p> <p>Most of the limestones contains numerous foraminifera of 0.05 - 0.5mm. All of the limestones are phosphatized (collophaned) more or less. The conspicuously phosphatized limestone is classified into the phosphate rock. The macroscopic lithofacies changes from whitish to creamy under collophaned effect. The type of collophaned effect is observed in various ways. In some case, collophane substitutes for foraminifera completely. Another case, only foraminifera is saved from collophaned effect.</p>
Phosphate rock	<p>(Macroscopic Observation)</p> <p>Phosphate rock is more creamy than limestone and is completely compact. The texture is not observed in it. Mainly, it occurs as follows: phosphated surface of limestone (SA04AD04), the matrix of pyroclastic rock (SA01AD11, SA03CB06, SA03AD08, SA04AD02), the network or vein in basalt and crust (SA05AD01, SA01AD11). On the other hand, the following types are observed, one shows the intricateness with crust that indicates the simultaneous creation of phosphate rock and crust (SA03AD09), the other shows the inclusion of older crust fragments in phosphate substrate (SA01AD11, SA05-AD04).</p>
	<p>(Microscopic Observation)</p> <p>As above-mentioned, the conspicuously phosphatized limestone is classified into the phosphate rock. In this type rock, the original texture such as foraminifera still remains; however, the boundary between collophaned part and calcareous part becomes obscure. The matrix of hyaloclastite in which cobalt crust grows at upper part, mainly consists of phosphate rock.</p>



- | | |
|---------------------------------------|--|
| 1) SA01AD08(B) Basalt | 5) SA04AD10 Pillow |
| 2) SA04AD10(A) Basalt and phosphorite | 6) SA01CB05(A) Lime stone |
| 3) SA04AD02(A) Hyaloclastite | 7) SA05AD04(A) Phosphorite |
| 4) SA01AD06(C) Hyaloclastite | 8) SA01AD11(D) Phosphorite with fragments of basalt and crust. |

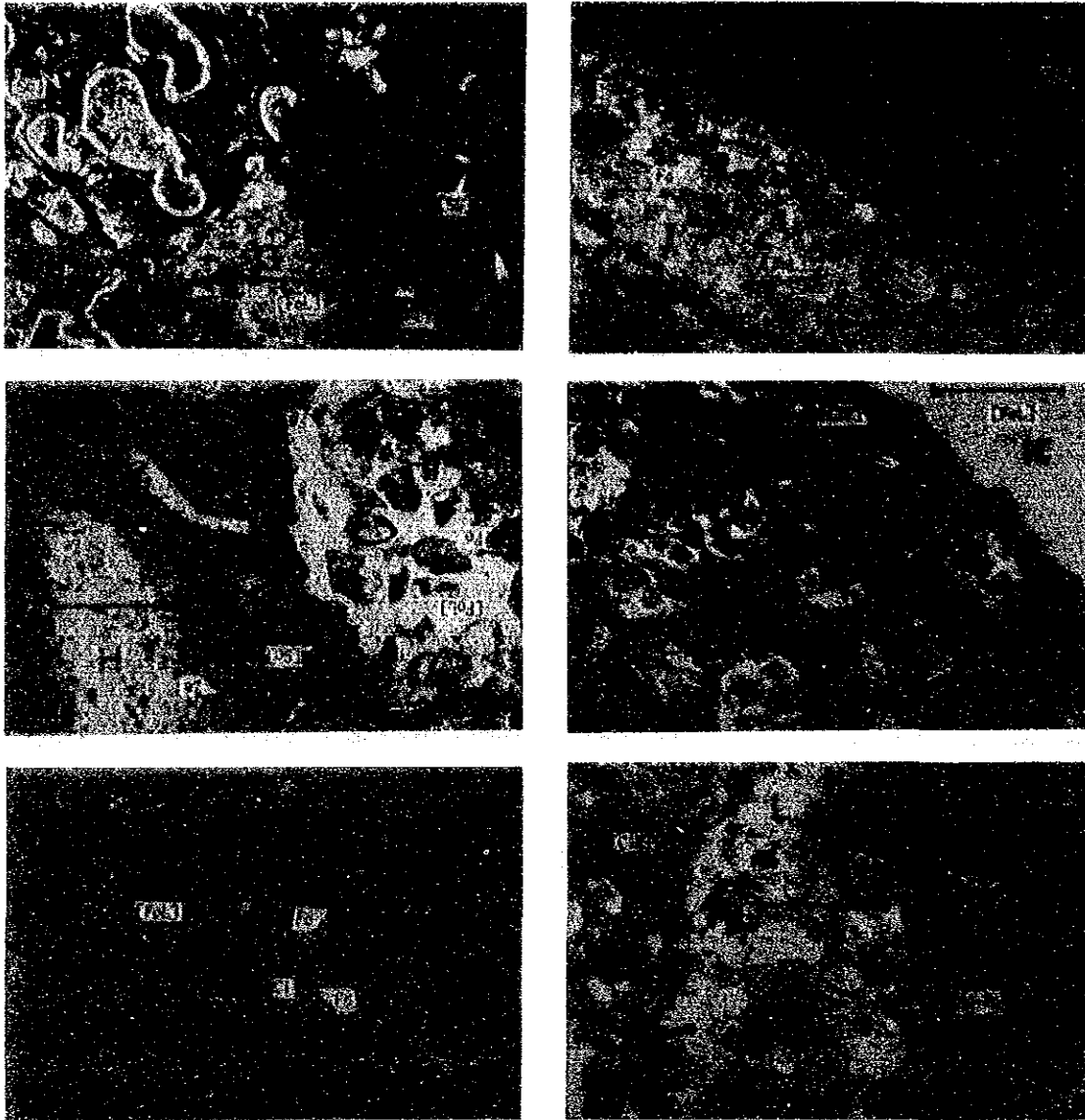
Fig. 4-2-1 Photos of Representative Rocks



Ca	: Calcite	Mn-Fe	: Mn-Fe Oxide minerals	[FoL]	: Foraminiferous Limestone
Chl	: Chlorite	Mt	: Magnetite		
Cl	: Collophane	Pl	: Plagioclase		
Fo	: Foraminifera	Px	: Pyroxene	[Sc]	: Scoria
Ge	: Gas cavity	Cpx	: Clinopyroxene		
Il	: Ilmenite	Ze	: Zeolite		
Ol	: Olivine				(Index scale : 0.5 mm)
Mf	: Mafic mineral	[Bs]	: Basalt		
Mn	: Oxidic manganese mineral	[CIR]	: Collophanitized rock		

A: 87SA01CB03, open nicol, 01-Px-basalt, Ze. and Chl. in vesicles.
 B: 87SA01AD06, open nicol, 01-basalt, Chl., Cal. in vesicles.
 C: 87SA05AD04, open nicol, Cpx-basalt, fresh, devitrified glass.
 D: 87SA04AD04, cross nicol, 01-Cpx-basalt, chilled facies, Cal., Ze. in vesicles.
 E: 87SA04AD09, cross nicol, basalt hyalocastite, many vesicles.
 F: 87SA04AD09, cross nicol, Same Sample with E, Ze. in pore.

Fig. 4-2-2 Microscopic Photos of Substrates of Cobalt Crusts (1)



Ca	: Calcite	Mn	: Oxidic manganese mineral	[Bs]	: Basalt
Chl	: Chlorite			[CIR]	: Collophanitized rock
Cl	: Collophane	Mn-Fe	: Mn-Fe Oxide minerals	[FoL]	: Foraminiferous Limestone
Fo	: Foraminifera	Mt	: Magnetite		
Gc	: Gas cavity	Pl	: Plagioclase	[Sc]	: Scoria
Il	: Ilmenite	Px	: Pyroxene		
Ol	: Olivine	Cpx	: Clinopyroxene		
Mf	: Mafic mineral	Ze	: Zeolite		

(Index scale : 0.5 mm)

- G: 87SA01AD06, cross nicol, hyaloclastite; collophenized FoL.-mix.
H: 87SA01AD08, cross nicol, hyaloclastite, collophenized, many-scoria fragments, Ze. in pore of scoria.
I: 87SA01AD09, open nicol, FoL, slight collophenization.
J: 87SA03AD08, cross nicol, FoL, collophenized, with Bs. fragments.
K: 87SA04AD01, open nicol, FoL, collophenized.
L: 87SA04AD06, open nicol, phosphorite, accompanying ferromanganese crust fragments and basalt scoria.

Fig. 4-2-2 Microscopic Photos of Substrates of Cobalt Crusts (2)

Table 4-2-3 Mineral Assemblage of Substrates

Sample No.	Rock Name	Texture	Pheno-cryst		Groundmass						Altered Minerals			
			Olivine	Pyroxene	Plagioclase	Pyroxene	Olivine	Glass	Ilumenite	Magnetite	Chlorite	Zeolite	Calcite	Fe-Mn-Oxide
87SA01CB03	Olivine pyrox. basalt	intersertal amygdaloidal	○	○	⊙	○	△		●		○	○		△
87SA01AD06	Olivine basalt	intersertal amygdaloidal			⊙			○	●	●	⊙		○	●
87SA05AD04	Pyroxene basalt	intersertal amygdaloidal	△	△	⊙	○		○	△		⊙			

Sample No.	Rock Name	Texture of Mn. crust	Rock Fragm			Matrix				Altered Minerals							
			Basalt	Scoria	Plagioclase	Trachite	Foraminif.	Colophane (Apatite)			Mn-Fe-Oxide	Fe-Mn-Min.	Calcite	Zeolite	Chlorite	Opal	
87SA01AD08	Limestone with hyaloclastic fragm.	Mn crust colloform	⊙								●	●					
87SA01AD09	Limestone						⊙	△				●					
87SA04AD06	Phosphorite	dendritic, colloform		⊙					⊙				△				
87SA03AD08	Hyaloclastite mixed limestone	colloform, banded, concentric	⊙	⊙	●		△	⊙	○				△				
87SA04AD01	Limestone with hyaloclastic fragm		⊙	⊙			△	⊙			●	●					
87SA04AD04	Olivine pyrox. basalt		⊙	⊙										⊙	○	●	●
87SA04AD09	Hyaloclastite		⊙	⊙										○	●		
87SA01AD06	Hyaloclastite	colloform, banded	△	⊙		○	●	⊙					△				

⊙ Abundant, ○ Common, △ Little, ● Minor

Table 4-2-4 Chemical Composition of Substrates

Sample No.	87SA05 AD04	87SA04 AD01	87SA01 AD08	87SA01 AD06	87SA04 AD07(C)	87SA04 CB09	87SA05 AD04(A)	87SA05 AD04(B)	
Rock Type	Limestone	Limestone	Basalt	Hyaloclastite	Phosphorite	Limestone	Phosphorite	Basalt	
Chemical Composition (%)	SiO ₂	5.76	0.33	41.92	42.06	2.35	1.61	1.19	41.36
	TiO ₂	0.01	<0.01	3.45	3.11	0.20	0.03	0.04	3.65
	Al ₂ O ₃	0.21	0.13	17.20	16.76	1.01	0.50	0.48	13.19
	Fe ₂ O ₃	1.64	0.07	7.43	8.44	1.13	0.09	0.39	4.95
	FeO	0.39	<0.01	1.56	1.36	0.19	0.19	0.06	3.89
	MnO ₂	0.04	0.04	0.13	0.16	0.47	0.02	0.01	0.10
	MgO	1.09	0.57	1.18	3.67	0.38	0.27	0.22	3.99
	CaO	48.20	56.79	10.25	10.19	49.96	55.68	52.74	14.92
	BaO	0.17	<0.01	0.04	0.04	1.03	0.40	<0.01	0.01
	Na ₂ O	1.27	0.08	3.14	3.28	1.12	0.41	0.71	2.64
	K ₂ O	0.15	0.04	2.48	1.43	0.24	0.18	0.18	1.40
	P ₂ O ₅	5.10	0.45	4.22	1.73	32.42	6.64	21.48	4.74
	Ig-loss	35.82	41.83	5.81	6.48	8.75	34.32	21.51	3.90
Total	99.85	100.36	98.81	98.71	99.25	100.34	99.02	98.74	

4-3 Bearing Situation of Cobalt Crusts

1) Classification of Types and Properties

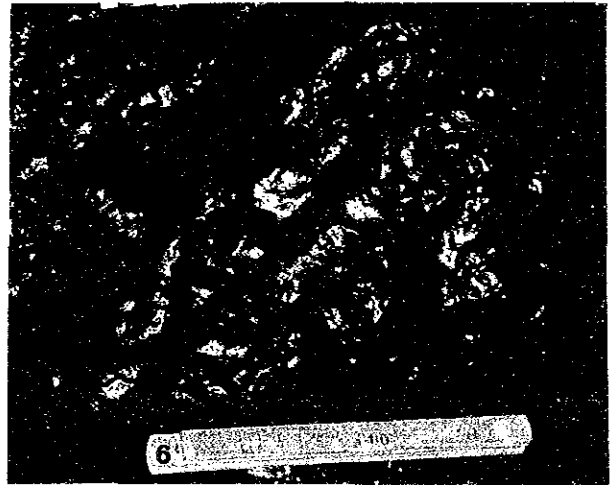
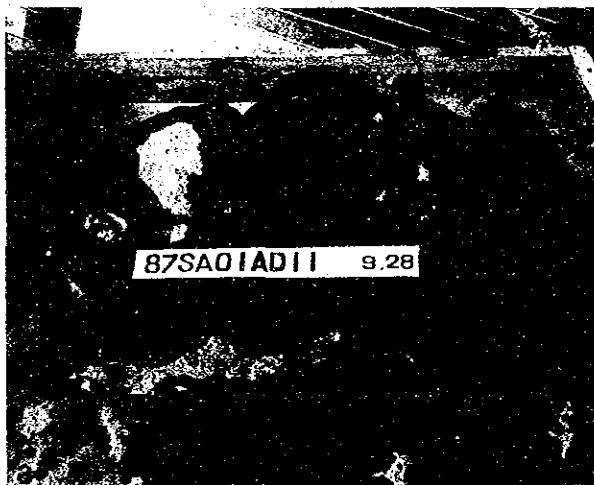
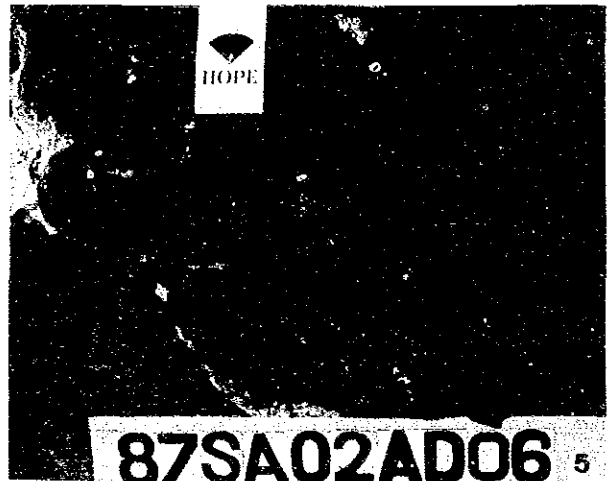
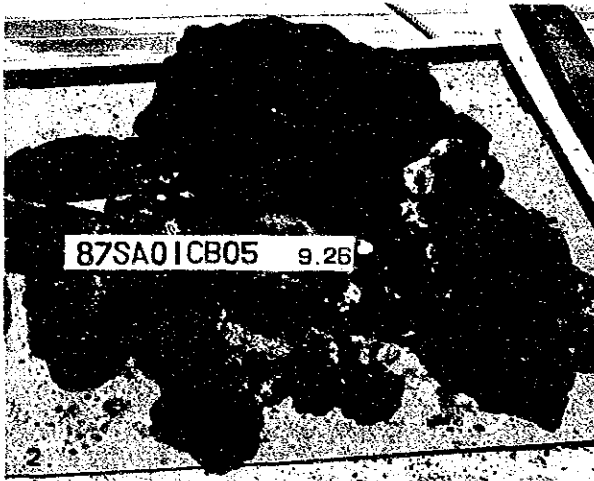
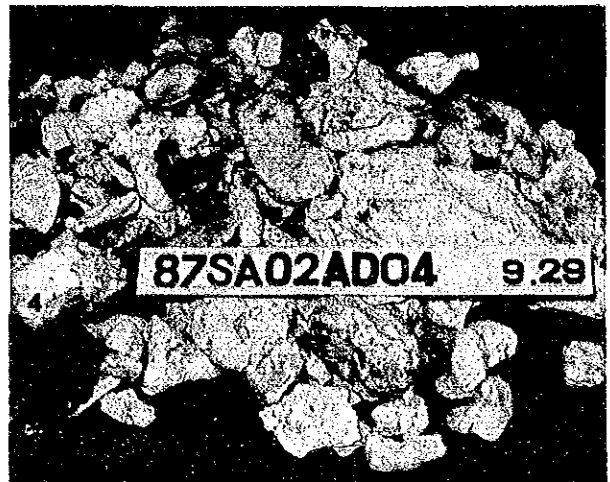
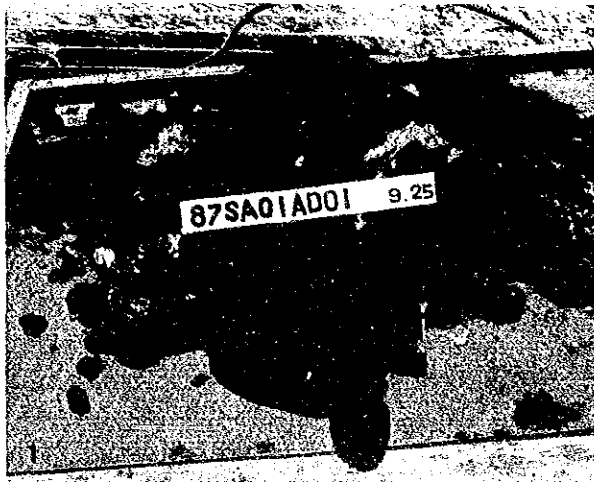
Covering the solid rock exposing on the surface of the seamount, the cobalt crust fundamentally grows up, and the mode of occurrence of the crust is different by the reason whether its rock is base rock or crushed and loose stone. In this report, the classification such as Tab. 4-3-1 is adopted. According to the shape of samples gathered by dredging and the FDC observation, the cobalt crust is classified into 7 types: crust type, slab type, pavement type, massive type, pebble type, nodule type and film type (coating type). As to the cobalt crust which is difficult to classify clearly into the above mentioned types, they are classified into the very near type as possible. The above mentioned 7 types are classified into 2 groups; one is a crust type group which grows up to cover the rock base and another is a massive type group which grows up to consider a loose rock as matrix. The slab type group contains two types. One is considered the plate pieces of rock as matrix and the

Table 4-3-1 Classification of Types of Cobalt Crusts (1)

	Name	Mark	Characteristics and Distribution
Crust type-group	Crust type	C	(Characteristics) The crust covers directly rocks such as a basalt, a volcano-clastic rocks and sedimentary rocks. The crust distributes continuously and present large scale mode of occurrence.
			(Distribution) Abundant at all seamounts. Universally from the top of seamount to the lower part of the slope. Maximum 8cm in thickness.
	Slub type	S	(Characteristics) The crust is flat shaped and grows at the whole surface. An exfoliated part of the crust shape is included.
			(Distribution) This type distributes at the transition zone between the crust shape zone and the cobble type zone at SA01 and SA03 seamounts.
	Pavement type	P	(Characteristics) This shape is a kind of crust shape. The crusts which are originally nodule shape or cobble shape are combined each other and form pavement like appearance.
			(Distribution) The shape which is close to this type is observed at SA01 seamount, but the typical one occurs rarely.

Table 4-3-1 Classification of Types of Cobalt Crusts (2)

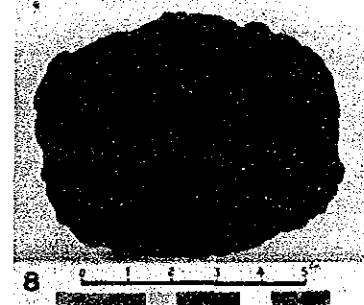
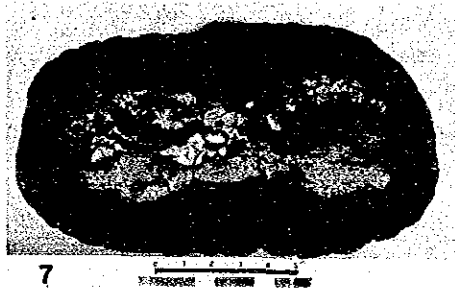
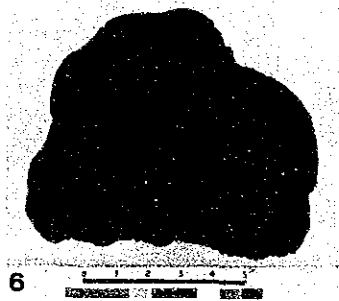
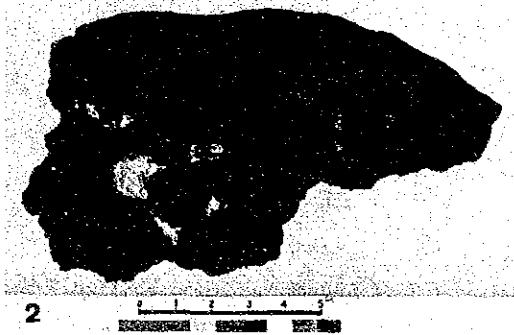
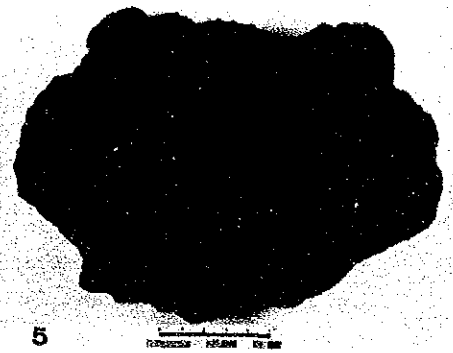
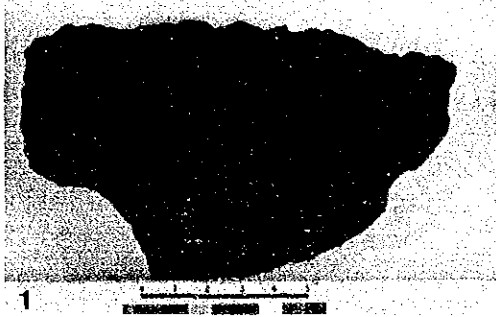
Nodule type- group	Massive type	M	(Characteristics) Covering the various pieces of rocks, the crusts grow up, and the external form is usually square. The size is not regarded.
			(Distribution) SA01, SA03 etc. The top of seamount and the outskirts of the slope. This type occurs mostly mixed with cobble type.
	Cobble type	B	(Characteristics) Covering the various pieces of rocks, the crusts grow up, and the external form is rounded. The diameter is more than 10cm±.
			(Distribution) SA01, SA03 and SA04 etc. This type is observed at the shoulder part of the top and at the gentle slope.
	Nodule type	N	The mode of occurrence of this shape is the same as that of manganese nodule. This size is between pebble and fist (10cm± in diameter).
			(Distribution) This type is observed every where at the flat area of the top of seamount. This type is barely observed at the other peaked seamount.
Others	Film type or coating type	F	The crust is covering the substrate as thin film whose thickness is less than about 1mm.
			(Distribution) SA02 and the eastern island of SA03. Substrate is collapsed rock of coral limestone.



- 1) Cobbles, crusts, slabs and nodules : Total weight 112kg.
- 2) Crusts, slabs and massive crusts : 107kg.
- 3) Cobbles, slabs, crusts and nodules : 116kg.

- 4) Coral limestone with partial crust coating : 28kg.
- 5) Crust coating on coral limestone.
- 6) Crust with smooth surface. SA05AD01. Scale : 20cm.

Fig. 4-3-1 Representative Cobalt Crust Types (On Board)



- 1) SA01AD01(B) Crust
- 2) SA01CB10(A) Crust
- 3) SA03CB06(A) Slub
- 4) SA01AD01(C) Slub

- 5) SA04AD10(A) Massive
- 6) SA01CB05(B) Massive
- 7) SA01AD01(A) Cobble
- 8) SA01AD01(D) Nodule

Fig. 4-3-2 Representative Cobalt Crust Types (Section)

Table 4-3-2 Occurrences of Cobalt Crusts at Individual Seamount (1)

Name of Seamount	Mode of occurrence
SA01	<p>Topographical characteristics: The summit is a ridge type lying from south to north, narrow flat and its water depth is 1,600m.</p> <p>Geological characteristics: The volcano clastic rock is abundant.</p> <p>Water depth of distribution: 1,600 - 3,250m</p> <p>Type: Crust type Slab type cobble type Massive type Nodule type Especially, massive type group is observed widely at the ridge.</p> <p>Matrix: Basalt, volcano clastic rock, limestone, collophatized rock</p> <p>Structure: Surface; botryoidal, fish-skin, coke type, smooth type etc. Single layer structure is abundant in all types. There are partially 2 - 3 layers at the summit.</p> <p>Thickness: 0.1 - 7.0cm, 1.7cm on average. There is a slightly thick type (about 2cm, maximum 7cm) as slab type and crust type, but there is even a thick type with limestone substrate.</p> <p>Coverage: Barren zone at the flat area of the summit. 10 - 100% at the slope.</p> <p>Number of sampling points: 12</p> <p>Grade analysis: 43</p>
SA02	<p>Topographical characteristics: Atoll, one side of the summit is about 2 miles long.</p> <p>Geological characteristics: The whole of the slope is covered with the coral limestone and its collapse.</p> <p>Water depth of distribution: 2,450 - 2,470m (only thin coating at the other points)</p> <p>Type: Crust type. The other types are thin coating less than 1mm thick.</p> <p>Matrix: Limestone/Basalt.</p> <p>Structure: Surface; rough.</p> <p>Thickness: 0.1 - 0.5mm, 0.2cm on average.</p> <p>Coverage: Nearly 0</p> <p>Number of sampling points: 1</p> <p>Grade analysis: 1</p>

Table 4-3-2 Occurrences of Cobalt Crusts at Individual Seamount (2)

Name of Seamount	Mode of occurrence
The Eastern Island of SA03	<p>Topographical characteristics: Atoll, Long axe is 0.8km, short axe is 0.5km.</p> <p>Geological characteristics: Coral limestone is abundant from the upper part to the middle part of the slope.</p> <p>Water depth of distribution: 1,500m - 2,830m (only coating type at the shallower part than 1,500m).</p> <p>Type: Crust type is abundant, and the other types are a slab type and pebble type.</p> <p>Matrix: Limestone, collophatized rock, volcanic blastic rock, basalt.</p> <p>Structure: Surface; More than 2 layers are abundant.</p> <p>Thickness: 0.1 - 0.5mm. 1.0cm on average. It is thinner than that of the western seamount.</p> <p>Coverage: Less than 10% at the upper part of the slope? About 10 - 70% at the lower part?</p> <p>Number of sampling points: 6</p> <p>Grade analysis: 17</p>
The Western Seamount of SA03	<p>Topographical characteristics: Peaked seamout, Water depth at the summit is 1,030m.</p> <p>Geological characteristics: Collophatized rock generally grows up. There is no volcano clastic rock.</p> <p>Water depth of distribution: 1,030m - 3,000m</p> <p>Type: Crust type is abundant, and the other types are slab type and cobble type.</p> <p>Matrix: Collophatized rock, basalt, limestone.</p> <p>Structure: Surface; 2 layers are abundant. Dense type is abundant. The boundary of collophatized rock and crust is intricated irregularly.</p> <p>Thickness: 0.1 - 7.0mm. 2.0cm on average. The thick crust is abundant.</p> <p>Coverage: 10 - 90%, average 40 - 50% (FDC data) at top of Seamount.</p> <p>Number of sampling point: 5</p> <p>Grade analysis: 20</p>

Table 4-3-2 Occurrences of Cobalt Crusts at Individual Seamount (3)

Name of Seamount	Mode of occurrence
SA04	<p>Topographical characteristics: Peaked seamount, Water depth at the summit is 1,040m.</p> <p>Geological characteristics: Basalt and volcano clastic rock are abundant. There is collophatized rock, too.</p> <p>Water depth of distribution: 1,170m - 3,400m</p> <p>Type: Crust type is abundant, and the other types are little.</p> <p>Matrix: Basaltic volcano clastic rock, collophatized rock, limestone.</p> <p>Structure: 1 - 4 layers Collophatized rock is mixed at the lower layer having an exfoliation characteristics as sheet.</p> <p>Thickness: 0.1 - 8.0mm. 1.8cm on average. 8.0cm at 3,000m water depth.</p> <p>Coverage: Judging from the situation, it is same as the western seamount.</p> <p>Number sampling points: 8</p> <p>Grade analysis: 32</p>
SA05	<p>Topographical characteristics: Peaked seamount, Water depth to the summit is 1,170m.</p> <p>Geological characteristics: Basalt, collophatized rock, limestone (collophatized) etc.</p> <p>Water depth of distribution: 1,170m - 3,000m</p> <p>Type: Only crust type collected.</p> <p>Matrix: Basalt, collophatized rock, limestone.</p> <p>Structure: 3 layers, exfoliation characteristics as sheet.</p> <p>Thickness: 0.1 - 6.0cm. 1.9cm on average. The thickness is uneven.</p> <p>Coverage: Topography is steep and it is low.</p> <p>Number of sampling points: 4</p> <p>Grade analysis: 10</p>

other is going to grow up on the surface after a part of crust is destroyed and is separated. And the former belongs to a massive type and the latter is a crust type, so that the latter is preferentially classified into the crust type. Although the cobalt crust is morphologically classified as mentioned above, as to the surficial and inner structure and the thickness, the group of crust seems to be generally similar. However, as to a massive type, the various matrix is mixed. It may be in question that there is the difference between the thickness and the chemical property. There are some cases where the group of samples gathered by dredging is consisted of only same type, but in the almost case, it is not easy to treat statistically the chemical composition and the thickness of the group of samples.

2) Distribution and Mode of Occurrence

The 5 seamounts (strictly 6 seamounts) are topographically divided into 2 atolls and 4 peaked seamounts. The cobalt crust grows up at all seamounts except atoll SA02. At the atoll SA02, the cobalt crust develops quite partially. The crust generally grows up from the summit of every seamount to the middle and lower part of the slope where is the lowest limit in this survey at the 4 seamounts. The water depth of the summit is about 1,000m to 1,600m and the lowest limit of water depth in this survey is 3,000m to 3,400m. It seems that the crust grow up until the deeper part than the lowest limit of water depth as mentioned above at all peaked seamounts. Comparing the transformation of water depth and the distribution of the crust, there is a tendency that the crust becomes inferior at the lower part of the slope. On the other hand, subject to the atoll, the crust grows up from the water depth of 1,500m to 2,830m at the eastern island (Phoenix Island) SA03 which is one of the above mentioned barren atoll (SA02). The thin coating of crust on the surface of the limestone is observed at the shallower point. As mentioned above, the great difference of the bearing of the crust between the atoll and the seamount is observed. The difference is observed in the crust type between the seamount SA01 which has flat plain on the summit and the western seamounts of SA03, the other seamounts SA04, and SA05 which do not have the flat plain. Generally speaking, nodule type, pebble type massive type, and slab type etc. are abundant at the plain on the summit or the convex part of the slope. The outline of the mode of occurrence at each seamounts is shown in Tab. 4-3-2. The substrates of the cobalt crusts are basaltic lava, basaltic clastic rock, limestone and phosphatized rock etc. The all kinds of these rocks are observed at all seamounts except the atoll SA02.

The basalt lava and the basaltic clastic rocks are abundant, and the total of them reaches 70% of all. (Tab. 4-3-3) The hyaloclastite is abundantly contained in the clastic rocks and is observed, too. In the most cases, the limestone of which crust grows up comparatively thick, has more obscure structure and denser type than the limestone of which crust is barren and has the coral structure, is obvious as the atoll located at the east of SA02 and SA03. As to the limestone which the crust grows up, its surfacial layer is partially phosphatized. The rock contains a piece of crust and the crust attached rock chips, boundary of the crust and the collaphotized rock is irregularly complicated. The phosphatized rocks observed in almost all crust types and especially abundant in the pebble type. As to the surfacial structure of the crust, the botryoidal type is the most abundant and in addition, there are irregular concave-convex type, rough type and smooth type etc. As to the botryoidal structure, the surface of crust is covered with a hemispheroidal aggregate of which diameter is about 5-15mm. This type is abundant in all seamounts except SA02, and it is accounted 60% of analyzed samples. The rest is about 20% as smooth type and about 20% as another type. The inner structure of the crust of which thickness is generally less than 1cm is homogeneous and its transformation is

Table 4-3-3 Bearing Rates of Different Rock Types in Each Crust Types

(Based on analyzed samples)

Crust Type	Rock Type					Total
	Basalt	Clastic * rocks	Limestone	Phospho-rite	No substrate	
Crust	32	5	12	5	7	61
Slab	3	7	0	0	5	15
Massive	7	0	0	0	0	7
Cobble	6	6	1	1	0	14
Nodule	1	1	0	1	0	3
Total	49	19	13	7	12	100

(*include hyaloclastite)

a little, and the porous layer would be observed at the boundary of matrix. On the other hand, the comparatively thick crust (more than 2cm) is classified into 2 layers which are the outer core and the inner core and the thicker crust (more than 3cm) is

Table 4-3-4 Average Thickness of Cobalt Crust at Each Seamount

Seamount	Survey Stations	Thickness of Crust	
		Average	Standard deviation
SA01	10	17.4	10.4
02	—	—	—
03	10	15.3	11.1
04	8	17.8	15.5
05	4	19.0	21.0
Total	32	17.0	12.9

(mm)

able to be classified into 3 layers having an outer core, a middle core and an inner core, and more than 3 layers. (Cf. 4 layers at SA04AD03(A)). Generally speaking, the outer core is like metallic black brown lustrous and the inner core is black metallic lustrous. There also exists a striped structure as leaf type in the types of core which is possible to be classified into layers. The boundary between crust and substrate is generally clear, but there is also an irregular and mixed type in the case of phosphatized rocks as matrix and of volcaniclastic rocks. The average of thickness as to the crust of every seamount is shown in Tab. 4-3-4. The example of the individual measured samples is shown in Tab. 4-3-5. The frequency distribution of every sample is shown in Fig. 4-3-3. The maximum thickness at every measuring point is 5.0cm at SA04ADad03(A). The maximum thickness of individual sample is 8cm in the crust type at SA04ADad03(A). Comparing 5 seamounts (strictly 6 seamounts), the atoll SA02 and the eastern atoll of SA03 are about 1.0cm. On the other hand, it is between 1.7cm (SA01 seamount) and about 2.0cm (western seamount of SA03) at the peaked seamounts and all of them are thicker than the eastern atoll. There is not a significant difference among the peaked seamounts. As to the relation between the thickness and the water depth, the decrease of the thickness is observed at the lower part of the middle slope and lower slope (less than 2,500m - 3,000m) compared with the summit (about 1,700m and about 1,000m at every seamount) at the seamount SA01 and the western seamount of SA03. However, it does not always follow that it evenly changes at shallower part than 2,500m. At the eastern atoll of SA03, the crust of the middle part of the slope where the other kinds of rocks distributes is thicker than upper part of the slope

Table 4-3-5 Thickness Examples of Cobalt Crusts

Sample No.	Sea-mount	Zone of Seamount	Water Depth	Crust Type	Substrate Structure	Thickness of Crust (mm)
SA01AD01	SA01	Top	2,060	B	Ph 1	15~20 (17)
CB03	"	M-slope	2,700	C	Bs 1	20~35 (25)
"	"	"	"	M	Bs 1	5~10 (7)
CB04	"	L-slope	3,380	C	Br 1	3~4 (3)
CB05	"	"	3,380	S	Bs 1	5~25 (17)
"	"	"	"	M	Bs 1	7~35 (20)
CB06	"	Top	1,980	S	1	20~30 (25)
AD07	"	L-slope	3,150	C	Bs 1	10
AD08	"	M-slope	2,870	S	Br 1	1~8 (5)
AD09	"	Top	2,210	S	1	10~15 (12)
CB10	"	M-slope	3,100	C	Br 1	20~30 (25)
AD11	"	Top	1,910	B	Bs, Ph 2	20~30 (25)
"	"	"	"	N	Bs, Ph 1	10~20 (15)
AD12	"	"	1,970	S	Br 2	25~35 (30)
SA02AD03	SA02	U-slope	1,140	F	Ls -	Coating (below 1mm)
AD08	"	M-slope	2,450	C	Bs -	1~5 (3)
SA03AD01	SA03	U-slope	1,790	C	Bs 2	20~25 (15)
AD02	"	Top	1,310	C	Ls, Ph 2	20~30 (25)
AD04	"	M-slope	2,450	B	Bs 1	1~3 (2)
CB05	"	"	3,000	C	Bs 1	1~5 (3)
CB06	"	"	2,620	S	Ls 1	10 (10)
AD08	"	"	2,500	C	Bs, Ph 1	3~10 (5)
JD10	"	"	2,020	C	Ls 1	10~30 (20)
CB12	"	"	2,600	B	Bs 3	35~60 (40)
"	"	"	"	C	Ph 1	25~30 (27)
SA04AD02	SA04	U-slope	1,760	C	Bs 2	10
AD03	"	M-slope	2,950	C	Bs 4	45~80 (50)
AD06	"	Top	1,290	C	Bs 2	20~30 (25)
AD07	"	M-slope	2,160	B	Bs 2	20~40 (30)
AD10	"	L-slope	3,190	B	Bs 1	15~20 (17)
SA05AD01	SA05	Top	1,195	C	Bs 1	5~10 (7)
AD02	"	U-slope	2,110	C	Bs 3	45~55 (50)

Water Depth; On bottom depth.

Zone of Seamount; U: Upper, M: Middle, L: Lower.

Substrate; Bs: Basalt, Br: Clastic rocks, Ls: Limestone, Ph: Phosphorite.

where coral limestone is abundant. At the seamount SA04, the crust type samples of which thickness is 5cm and its maximum is 8cm thick is gathered at the point of 3,000m deep. At SA05 seamount, the crust seems to be thin at the deeper point than 2,500m, but the details are unknown for the short of sampling. As to the relation between the thickness and type of the crust, there was not a significant difference between the crust type and the massive type at the seamount SA01 where

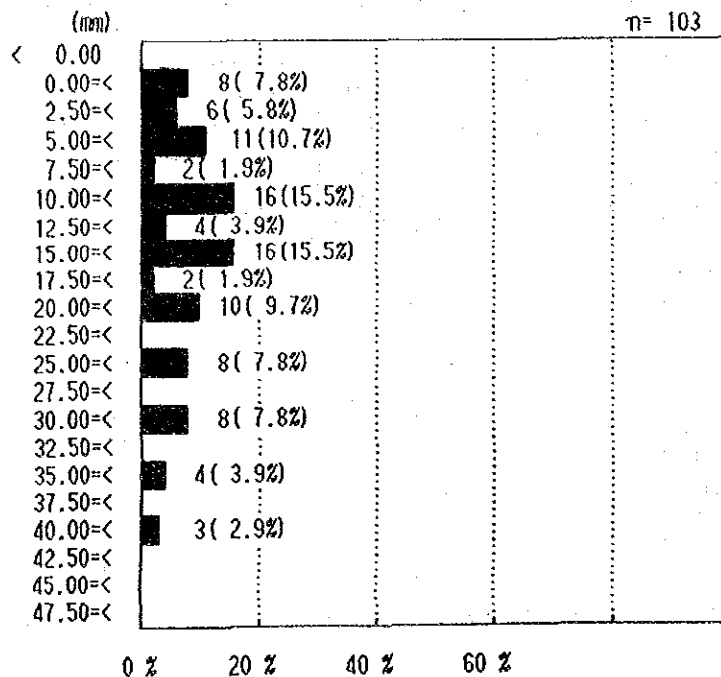


Fig. 4-3-3 Frequency Distribution of Thickness of Cobalt Crusts

the various type was gathered. In the case classified by the substrate, the crust with limestone substrate grow up slowly and average of crust is thin, but the significant difference is not always observed at the other seamounts. The crust on the basaltic lava, the basaltic clastic rock and the phosphatized rock grows up in the same value. The value of thickness in this survey is indicated by simplified average. It is added that it has certain standard deviation. As to the thickness of massive type and slab type, which has crusts on both sides of substrate, the average thickness of those both sides was taken into calculation. At last, the coverage is calculated by the only limited data, but, by means of FDC observation, the considerably exact value could be observed. Its outline is mentioned as the following paragraph.

3) Survey Results of FDC Survey

Sea bottom observation by FDC was performed at the summit of 2 seamounts of SA01 and SA03. The survey distance is 9.5 miles for the former case and 3.5 miles for the latter. The survey route and the summary of the results are given in Annexed Fig. 18, a detail description of the results is given in Fig. 4-3-4 (1) and (2).

Some of the sea bottom photos are shown in Fig. 4-3-5. The number of the sea bottom photos taken in the course of this survey totaled 147 for SA01, 65 for SA03, and 212 in total. The coverage of the crust was calculated, based on these photos, whose results are given in Fig. 4-3-4 (1) and (2). Results of VTR pictures observation were also taken into consideration to compensate some discontinuity of photographing used in the calculation. From the figure for the summit of SA01, a remarkable contrast between the development of barren zone in the flat plain and that of crust-type crust in the inclined part, as well as the development of nodule-type crust in the transitional zone between the above two topographic zones. On the other hand, almost general development of various types of crust is observed for the SA03 seamount having sharp summits. As for the coverage, an excellent correspondence with topography and bearing situation of the crust is observed in SA01, although the scattering is big as for the SA03 values.

These results are schematically summarized as follows.

(Topography)	(Mode of occurrence)	(Coverage)
Steep slope with inclination around 20°	Crust-type only	90 - 100%
Gentle slope with inclination around 10°	Crust-type Pavement-type Slub-type Partly massive type	50 - 80%
Foot of slope	Slub-type Massive-type Pebble-type Nodule-type	20 - 50%
Flat Plain	Foraminifera sand only Barren	

In the case of the coverage around 50%, thin layer of foraminifera sand covers slightly the upper side of the crust, for the most part. Therefore, there should be almost continuous development of crust beneath the foraminifera sand. The maximum thickness of the foraminifera sand layer is 70m at the plain zone of the seamount SA01. In this foraminifera sand belt, development of ripple marks is remarkable, signifying general east to west direction of bottom current.

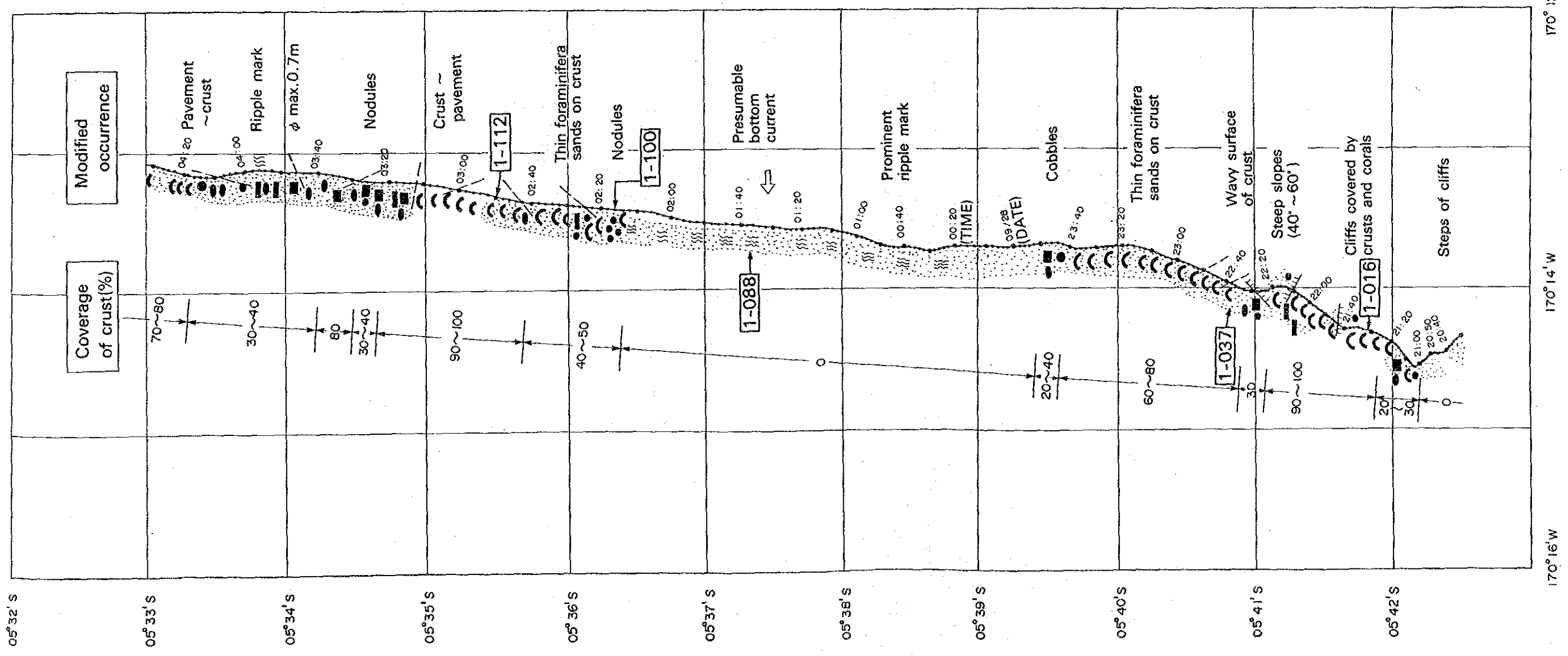
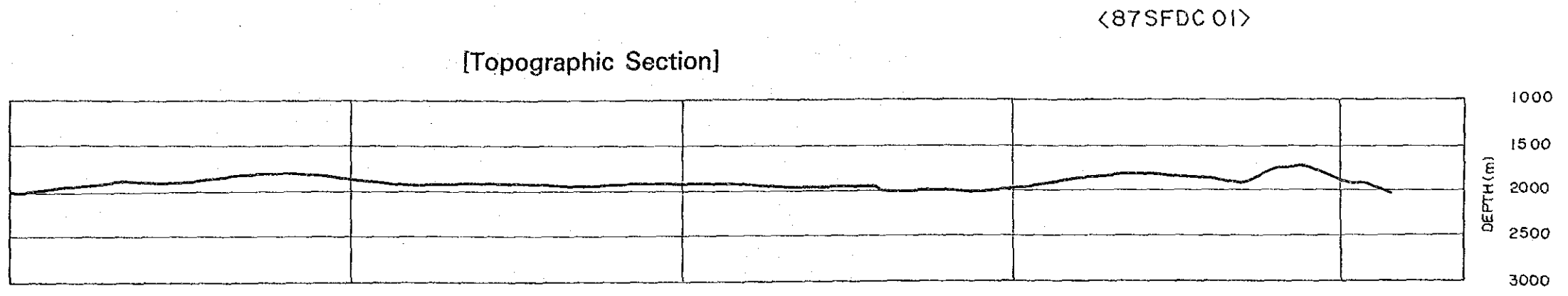
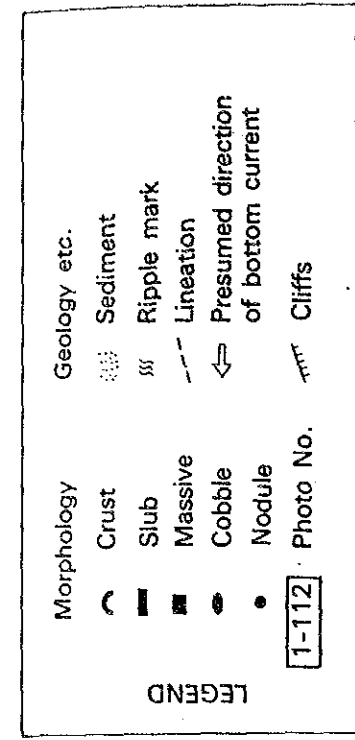


Fig. 4-3-4 Modified Distribution of Cobalt Crusts along FDC-Survey Line (1)

<87SFDC02>

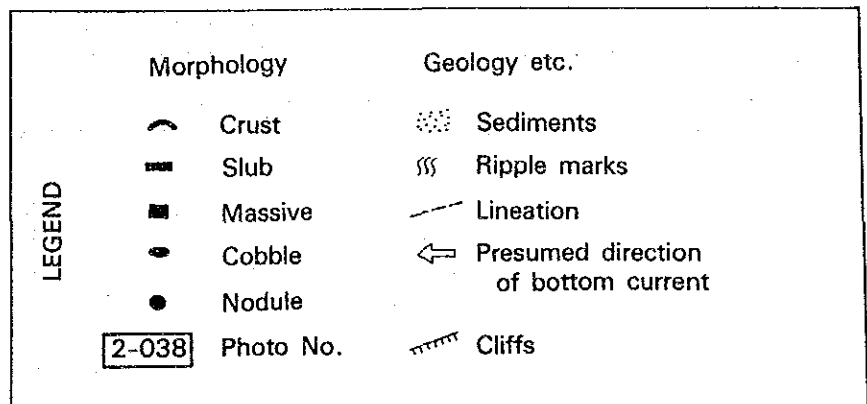
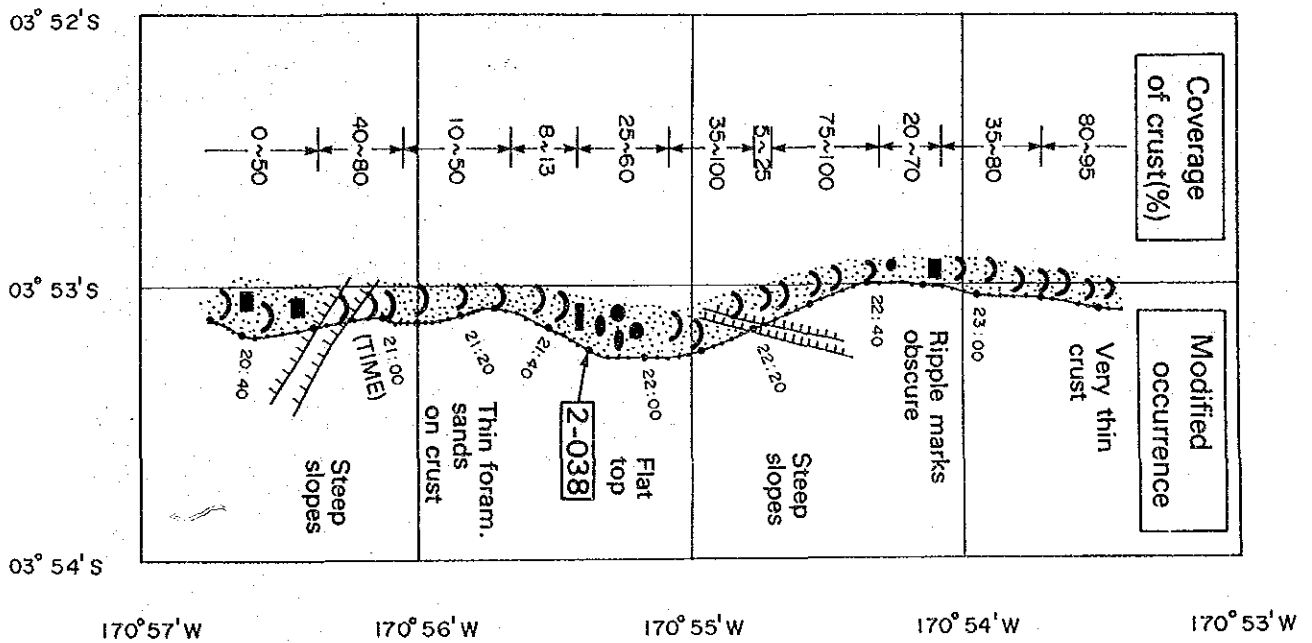
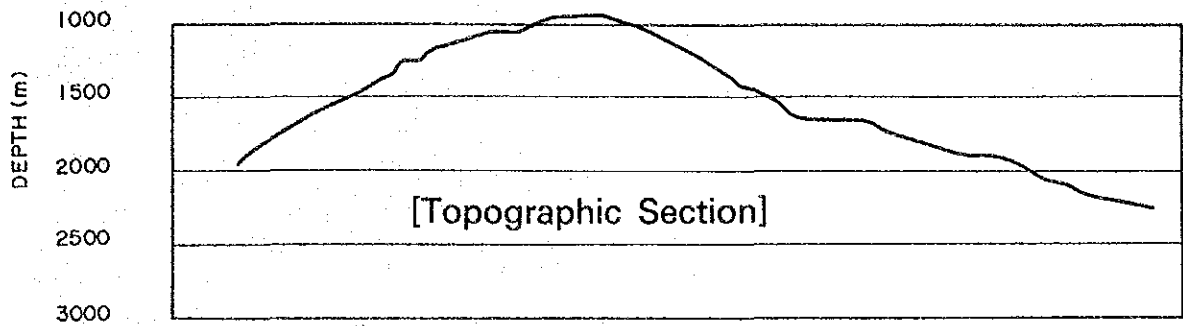
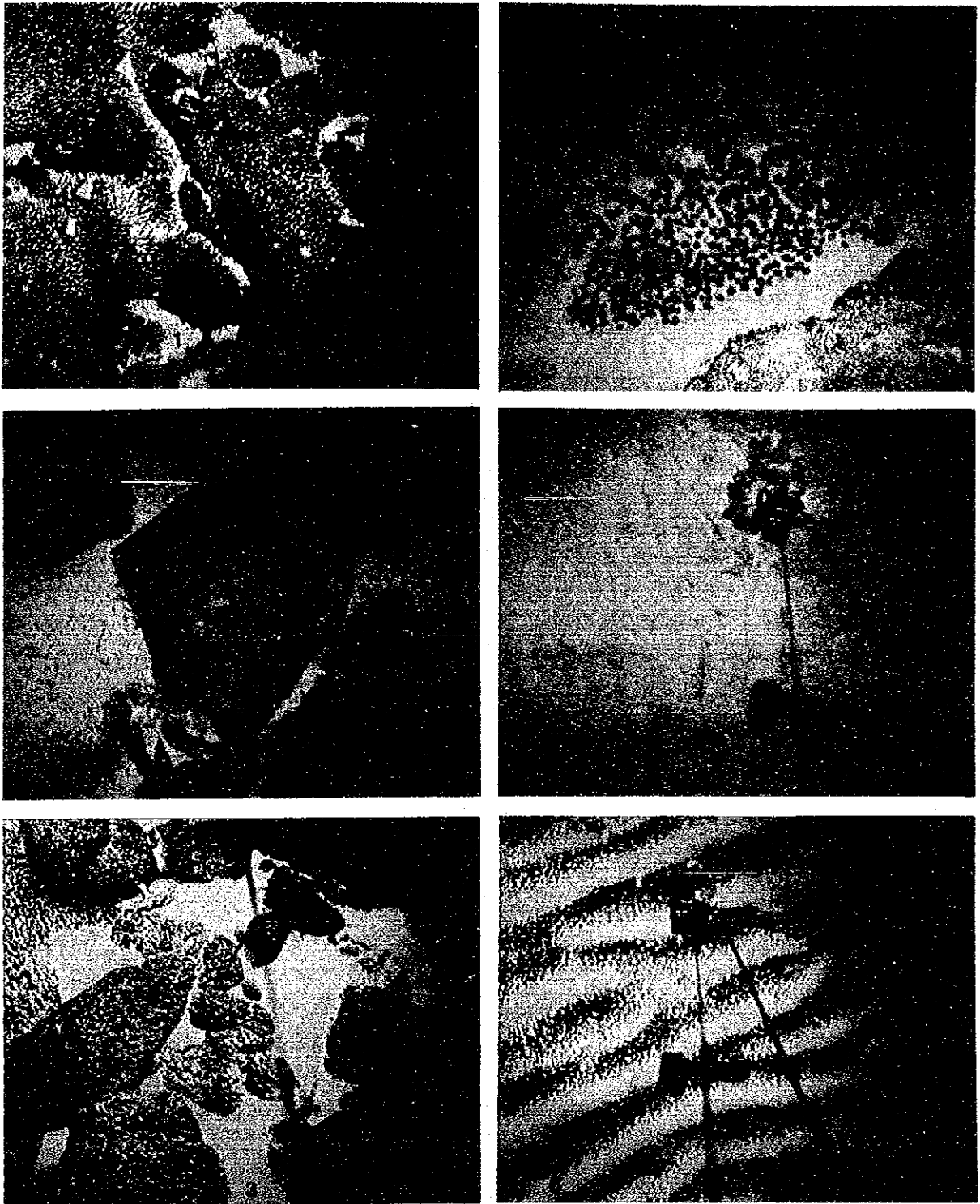


Fig. 4-3-4 Modified Distribution of Cobalt Crusts along FDC-Survey Line (2)



- 1) Crust with botryoidal surface (1-016). 4) Nodules (1-100).
 2) Blocky massive crust (2-038). 5) Ripple marks indicating water
 flowage from left to right (1-088).
 3) Slabs and cobbles (1-112). 6) Wavy surface structure on crusts (1-037).

*White sediments are foraminifera sands. Locations of each figures are shown in Fig. 4-3-4

Fig. 4-3-5 Sea Bottom Pictures by FDC Survey

